UNIVERSITÀ
DI PAVIA

Dipartimento di Biologia e Biotecnologie

The role of inflammation in the development of adenomas in individuals with *APC* gene-associated Familial Adenomatous Polyposis

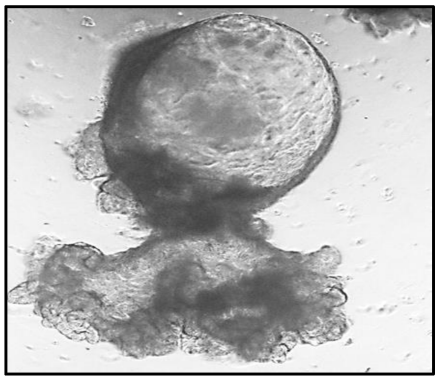

Antonino Belfiore

Dottorato di Ricerca in
Genetica, Biologia Molecolare e Cellulare
Ciclo XXXIII – A.A. 2017-2020

Supervisors:

Prof. Guglielmina Nadia Ranzani
Department of Biology and Biotechnology
Laboratory of Human Genetics-Cancer Genetics

Dr. Manuela Gariboldi
Istituto Nazionale Tumori Milano
Department of Experimental Oncology and Molecular Medicine

TABLE OF CONTENTS

1 ABSTRACT

Background

APC-associated Adenomatous Polyposis (AAP) is an autosomal dominant hereditary colorectal cancer (CRC) syndrome associated with germline mutations in the *APC* tumor suppressor gene with nearly complete penetrance. AAP is characterized by the development in the colon of hundreds to thousands of adenomatous polyps starting from the teen years. Currently, there are no approved chemo-preventive agents for AAP individuals. Several clinical studies using Non-Steroidal Anti-Inflammatory Drugs (NSAIDs), have shown a notable reduction in the size and number of polyps. Indeed, inflammation is directly related to adenoma formation and CRC development. Celecoxib, a NSAID specifically directed against the enzyme Cyclooxygenase 2 (COX-2), has been shown to significantly reduce burden and size of polyps in the colon of AAP patients, but its approval has been revoked by the Food and Drug Administration (FDA) due to cardiovascular and cerebrovascular safety concerns. Therefore, alternative strategies to mimic anti-inflammatory effects are needed. Recently, a low inflammatory dietary pilot study was conducted at the Fondazione IRCCS Istituto Nazionale dei Tumori of Milan (INT) on a group of 34 patients with AAP, with the aim to reduce the high local inflammation on the rectal mucosa.

Patients Derived Organoids (PDOs) from AAP adenomas have been developed to study the effects produced by inflammatory microenvironment on epithelial cells. AAP PDOs are an innovative *in vitro* model that reproduces most of the characteristics of the adenomas.

Material and Methods

34 patients, diagnosed with AAP, under surveillance at INT were enrolled in the pilot dietary intervention study. Participants accepted to follow a six months low inflammatory diet, providing fecal and blood samples at three different times: baseline (T0), three months of diet (T1), end of dietary intervention (T2). Local and systemic inflammation markers such as fecal and serum Calprotectin, Insulin and Insulin Growth Factor-1, were evaluated. Formalin Fixed and Paraffin Embedded (FFPE) biopsies were collected from 16 patients at T0 and T2 for immunohistochemistry (IHC) evaluation of COX-2 and 15-PGDH.

Four 3D-Patients Derived Organoids (PDOs) cultures from colorectal adenomas of AAP patients were generated, immunophenotypically and molecularly characterized.

Gene expression profiles of FAP PDOs maintained under lymphoid and myeloid pro-inflammatory conditions were carried out with the Nanostring PanCancer Immune Profile panel.

Results

Changes in the expression of stool and serum Calprotectin were observed on 24 patients at different samplings (p-values: 0.012 and 0.002 respectively). All the tissue samples showed high COX-2 immunoreactivity and no significant differences in COX-2 expression were observed between T0 and T2 in normal colonic crypts, adenomatous crypts, stromal infiltrating immune cells and adenoma infiltrating immune cells. Coherently, 15-PGDH expression was almost null in most of healthy crypts at T0. After the dietary intervention, a significant increase in 15-PGDH IHC expression was observed in the normal colonic crypts of the matched T0-T2 biopsies (Wilcoxon Signed Rank: 0.02).

All FAP PDOs, showed spheroidal and well-differentiated components with a solid core. Next Generation Sequencing analysis of FAP PDOs and their matched AAP tissue showed high concordance for all samples.

Cell Cycle analyses of FAP PDOs cultured under pro-inflammatory conditions (grown in presence of a cocktail of interleukins - IL, including IL-17a, IL-22 and IL-6) were similar for FAP1, FAP2 and FAP3 PDOs, while FAP4 presented a higher percentage of cells in G2/M phase. Differential gene expression (DGE) analysis of FAP PDOs cultured under ILs vs Standard conditions using an Immune Profile panel highlighted that 28 genes were significantly increased ($log_2FC > 2$ and FDR cut off 0.05). *DMBT1* was the most differentially expressed gene and showed more than 3-fold increase in FAP3, 9-fold in FAP2, and 7.5-fold in FAP1 PDOs, no changes were observed in FAP4 PDOs. Conversely, FAP4 PDOs grown under ILs condition presented several Human Leukocyte Antigen genes upregulated.

Conclusions

After 3 months of diet AAP subjects reduced their local (fecal Calprotectin) and systemic (serum Calprotectin) inflammation, as also confirmed by the increase of 15-PGDH observed on rectal AAP biopsies collected from patients at the end of the dietary intervention.

PDOs obtained from AAP polyps proved to be suitable *in vitro* models to study AAP. The reconstruction of a lymphoid pro-inflammatory condition for AAP PDO growth highlighted that IL-17a, IL-22 and IL-6 cocktail could have a protective role for epithelial cells composing the AAP colonic mucosa at the very early steps of CRC progression through the activation of the tumor suppressor gene *DMBT1*. Overall, this study provides evidence that inflammatory mechanisms regulate the progression of AAP adenomas at different levels. Further investigations, on a larger number of PDO models originated from different AAP subjects in order to cover the large variety of *APC* mutations, are needed to support the proposed hypothesis.

2 ABBREVIATIONS

Colorectal Cancer (CRC)
Lynch Syndrome (LS)
Hereditary non-polyposis colorectal cancer (HNPCC)
Mismatch Repair (MMR)
microsatellite instability (MSI)
APC associated Adenomatous Polyposis (AAP, formerly FAP)
Adenomatous Polyposis Coli (*APC*)
Attenuated form *APC* associated Polyposis (AFAP)
MUTYH associated polyposis (MAP)
mutY DNA glycosylase (MUTYH)
nth like DNA *glycosilase* 1 (*NTHL1*)
phospatase and tensin homolog (*PTEN*)
Mutation Cluster Region (MCR)
T-cell factor (TCF)/lymphoid enhancing factor (LEF)
Desmoid Tumor (DT)
Proctocolectomy with ileal-pouch-anal-anastomosis (IPAA)
Ileorectal anastomosis (IRA)
Non-Steroidal Anti-Inflammatory Drugs (NSAID)
Cyclooxygenase 2 (COX-2)
Fondazione IRCCS Istituto Nazionale dei Tumori di Milano (INT)
Phosphatase 2A (PP2A)
Glycogen synthase kinase 3β (GSK-3β)
Inflammatory Bowel Disease (IBD)
Tumor Necrosis Factor-α (TNF-α)
Prostaglandin E2 (PGE2)
Toll Like Receptor (TLR)
Interleukin (IL)
CD4+ helper T cells (Th)
Major histocompatibility complex (MHC)
15-Hydroxyprostaglandin dehydrogenase (15-PGDH
Phospholipase A2 (PLA2)
Arachidonic Acid (AA)
Prostaglandins H2 (PGH2)
Extracellular matrix (ECM)
Intestinal stem cells (ISCs)
3D-Patients Derived Organoids (PDOs)
Immunohistochemistry (IHC)
Human Acute Monocytic Leukemia (THP1)
Insulin Growth Factor 1-Receptor (IGF1-R)
Empirical Analysis of Digital Gene Expression Data in R (EdgeR)
Formalin Fixed and Paraffin Embedded (FFPE)

Caudal Type Homeobox 2 (CDX2)
Leucine Rich Repeat Containing G Protein-Coupled Receptor 5 (LGR5)
C-Reactive Protein (CRP)
Log_2 Fold Change (log_2FC)
Chemokine Ligand (CCL)
False Discovery Rate (FDR)
Differential Gene Expression (DGE)
Deleted In Malignant Brain Tumors 1 (*DMBT1*)

3 INTRODUCTION

3.1 Colorectal Cancer

According to GLOBOCAN 2018, colon cancer is the fourth most incident cancer in the world, while rectal cancer is the eight; collectively, ColoRectal Cancers (CRCs) are the third most commonly diagnosed form of cancer globally, accounting for 11 % of all cancers [1]. The incidence of CRC is constantly increasing worldwide, especially in developed countries that are adopting a “Western” lifestyle. In fact, environmental risk factors typical of this habit, such as obesity, sedentary lifestyle, and consumption of red meat, alcohol and tobacco are considered among the driving causes of CRC development [2]. The most common age of onset is after 50 years. Sporadic disease accounts around 70% of all CRC, the remaining 30% are familial or inherited. Familial CRC accounts up to 25% of cases. Patients display a family history of CRC, but the pattern is not consistent with an inherited syndrome. Individuals with a single first-degree relative affected have 1.7-fold increased risk of developing CRC compared to the general population. Finally, fewer than 10% of patients have a true inherited predisposition to CRC. These conditions are referred to heterozygous germline pathogenic variants in genes involved in different processes such as DNA surveillance and repair or prevention of uncontrolled cell growth [3].

3.2 Inherited predisposition to CRC

3.2.1 Lynch Syndrome

Among the CRC inherited predispositions, Lynch Syndrome (LS), also known as hereditary non-polyposis colorectal cancer (HNPCC), is the most frequent. Estimates suggest that as many as 1 in every 300-400 people may carry an alteration in a gene predisposing to the disease. LS is caused by the presence of mutations in the Mismatch Repair (MMR) genes *MLH1*, *MSH2*, *MSH6*, *PMS2* or *EPCAM.* The role of the DNA MMR system is to maintain genomic integrity by correcting base substitutions and small insertion-deletion mismatches that are generated by errors in base pairing during DNA replication. Normal MMR requires the coordinated function of several different gene products. Inactivation of both alleles of one of the MMR genes leads to defective MMR [4]. Cells carrying mutations in MMR genes can accumulate errors during the replication of short repeated sequences of DNA referred to as "microsatellites", whose length varies from person to person. As a result, microsatellites can be lengthened or shortened.

Two different methodologies are used for genetic testing in families with suspected HNPCC: one is to proceed directly to mutational analysis of the *MSH2*, *MLH1*, and possibly *MSH6* genes (testing a blood sample for germline mutations in these MMR genes); the other consists in the analysis of the length of microsatellite regions through capillary electrophoresis directly on tumor tissue. If the tumor displays microsatellite instability (MSI), patients will undergo mutational analysis.

3.2.2 *APC*-Associated Polyposis

APC-associated Adenomatous Polyposis (AAP, formerly FAP) is the second more common hereditary CRC syndrome: it is an autosomal dominant condition associated with germline mutations in the *APC* tumor suppressor gene. AAP is characterized by the development in the colon of hundreds to thousands of adenomatous polyps starting from the teenage years. Unless the colon is removed, these polyps will become malignant (cancerous). The average age at which an individual develops CRC in classic familial adenomatous polyposis is 39 years. By age of 35 years, 95% of individuals have polyps and carriers of these alterations have 70-100% of lifetime risk to develop CRC [5]. The diagnosis of an *APC*-associated polyposis is established by molecular genetic testing. It is suspected in individuals with suggestive personal or family history features and confirmed by identification of heterozygous germline pathogenic variants in the Adenomatous Polyposis Coli (*APC*) gene. About 25-30% of AAP cases are due to *de novo* mutations of *APC* occurring in subjects without family history for the disease.
AAP can also present an Attenuated form (AFAP) characterized by fewer colonic polyps (average of 30), more frequently in the colon region than in classic AAP. The cumulative risk for CRC by age of 80 years in AFAP is estimated at 70%. The average age of CRC diagnosis in individuals with attenuated AAP is 52 years from 10 to 15 years later than in those with AAP, but earlier than in those with sporadically occurring colon cancer [6].

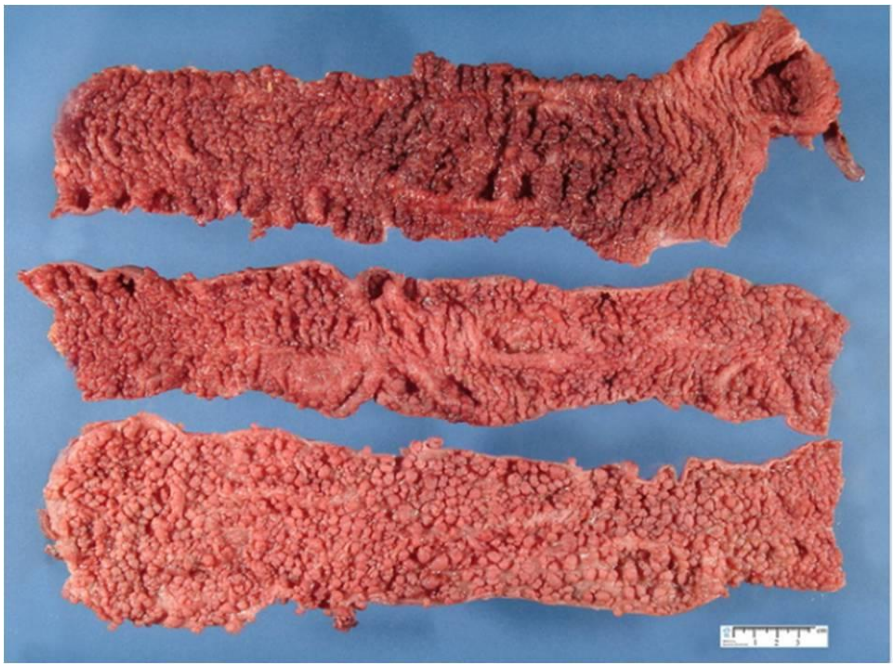

Figure 1: Colectomy specimen of a profuse AAP**.**
Credits: Dr. Jean-Christophe Fournet, Paris, France.

3.2.3 *MUTYH*-associated polyposis

Less common is MAP (*MUTYH*-associated polyposis), a recessive disease caused by biallelic pathogenic variants in the *mutY DNA glycosylase (MUTYH)* gene involved in the Base Excision Repair pathway. While AAP is frequently characterized by the presence of hundreds to thousands adenomatous polyps throughout the colorectal mucosa, MAP is characterized by a milder phenotype (ten to hundred colonic adenomatous polyps that are evident at the mean age of about 50 years). The risk of CRC is highly increased during lifetime and goes from 43 to almost 100% in the absence of timely surveillance [7]. MAP molecular testing can include single-gene testing and/or the use of multigene panels. Sequence analysis of *MUTYH* is performed first and followed by gene-targeted deletion/duplication analysis if only one pathogenic or no pathogenic variant is found. The multigene panel approach usually includes *MUTYH* and other genes of interest such as *APC*, *nth* like DNA *glycosilase* 1 (*NTHL1*), phospatase and tensin homolog (*PTEN*), where the second hit frequently occurs.

3.3 Genetic Features of AAP

AAP is caused by germline mutations in the *APC* tumor suppressor gene located on chromosome 5q21-q22. This condition follows an autosomal dominant pattern of inheritance with nearly complete penetrance of colonic polyposis development but variable penetrance of the extracolonic manifestations of the disease. Mutations in *APC* gene are often frameshifts, insertions or small deletions and introduce premature stop codons, leading to the production of a truncated APC protein. However, large deletions may account for up to 15% of cases. To date up to 1000 different mutations of the *APC* gene have been described [8, 9, 10]. Most *APC* mutations in colorectal tumors are clustered in a crucial region of the gene, called mutation cluster region (MCR) [11]. Moreover, specific location of mutations within the *APC* gene has been associated with the severity of colonic polyposis, as well as with the degree of cancer risk. Generally, mutations between codons 169 and 1393 are associated with classic AAP, while AFAP displays mutations that are typically in the 5' (5' to codon 158) and 3' (3' to codon 1596) ends of the *APC* gene. (Figure 2).
Inactivation of both *APC* alleles is necessary for the development of adenomas in AAP [12]. This typically results from an inherited mutation of one *APC* allele and a somatic mutation or deletion of the other allele and leads to the absence of functional APC protein.

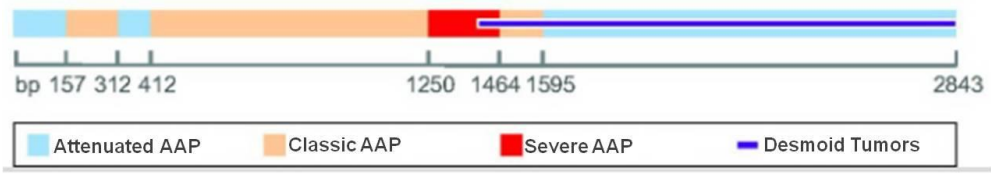

Figure 2: *APC* gene: most frequently mutated regions and codons associated to different forms of AAP and to Desmoid Tumors. Credits: Disease Models & Mechanisms 2014.

3.3.1 Functions and pathways of APC protein

APC is a 312-kDa protein that performs different cellular functions and localizes to multiple subcellular compartments. The best-known function of APC is the ability to interact with Beta-catenin in the cytoplasm and promote its phosphorylation, ubiquitination and subsequent proteolytic degradation. In normal conditions, Beta-catenin is a dual-function protein involved in cell adhesion and in the regulation of gene transcription. However, high levels of Beta-catenin, due to its accumulation in the cytoplasm, lead to

transcriptional activation of the Wnt (Wingless-Type) signaling pathway and of its target genes which control cell growth. The Wnt signaling pathway is an ancient and evolutionarily conserved pathway that regulates crucial aspects of cell fate determination, cell migration, cell polarity, neural patterning and organogenesis during embryonic development. The positive loop derived from the aberrant activation of the Wnt pathway increases Beta-catenin stabilization and accumulation in the cytoplasm, allowing its translocation in the nucleus where it acts as a transcriptional co-activator of the members of the T-cell factor (TCF)/lymphoid enhancing factor (LEF). It is known that the Beta-catenin/TCF-LEF complex induces the transcription of genes involved in carcinogenesis including c-myc, matrix metalloproteinase-7 (MMP-7) and the vascular endothelial growth factor (VEGF) [13]. APC is part of a multi-protein complex together with protein phosphatase 2A (PP2A), Axin, glycogen synthase kinase 3β (GSK-3β), and casein kinase I (CK1) and turns off the Beta-catenin signaling pathway. When this complex is active, GSK-3β and CK1 phosphorylate the amino terminal serine and threonine residues of Beta-catenin, the first step for degradation by the proteasomal machinery (Figure 3).

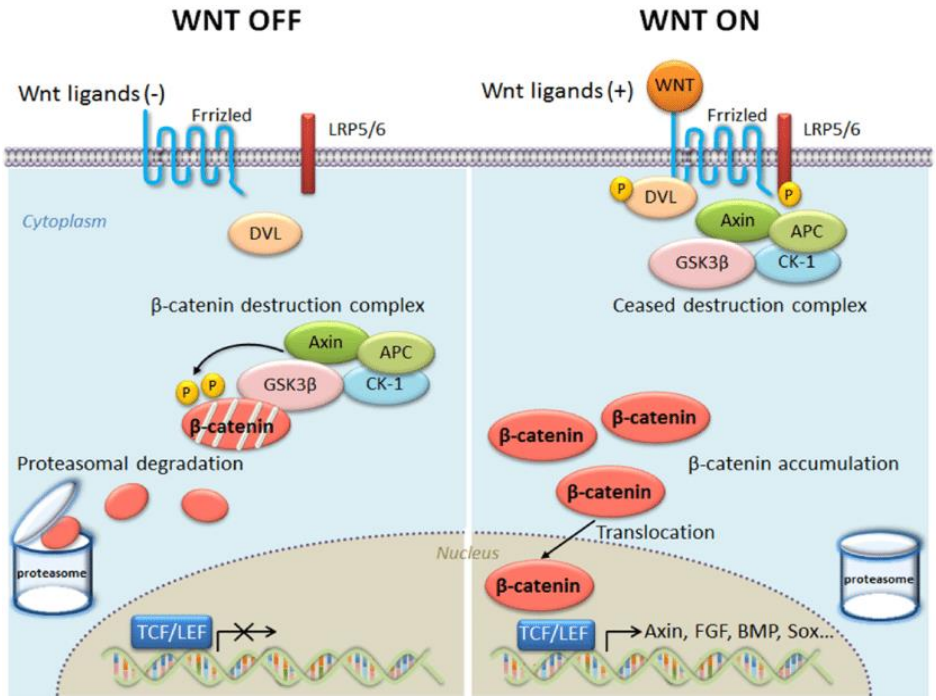

Figure 3: (LEFT) The *APC* (adenomatous polyposis coli) gene modulates β-catenin, Tcf transcriptional activation, and Wnt signal transduction. In the presence of wildtype *APC* or in the absence of Wnt ligand, Beta-catenin is

associated with GSK3β, β-catenin and Axin family members, and Beta-catenin is rapidly degraded by ubiquination at the proteosome. (RIGHT) When *APC* is mutated, or in presence of Wnt ligand, Beta-catenin accumulates in the cytoplasm and in the nucleus. Beta-catenin is associated with members of the Tcf family of transcription factors and modulates the transcription of target genes with Tcf recognition sequences. Credits:Chiharu Ota et al. Molecular and Cellular Pediatric, 2016.

Most of *APC* gene mutations (both germline and somatic) lead to premature truncation of the APC protein and loss of its Beta-catenin regulatory domains, resulting in nuclear accumulation of Beta-catenin. Recent studies have proposed that beta-catenin/TCF LEF acts as a switch controlling the proliferation process with respect to the differentiation of intestinal crypt cells. Activation of this pathway prevents cells from entering the G1 arrest phase; on the contrary, its dysregulation allows cells to continue towards terminal differentiation leading to resistance to apoptosis [14, 15, 16]. Loss of *APC* gene activity is a common event in sporadic colorectal tumorigenesis, occurring in about 80% of cases. *APC* alterations are involved in the neoplastic transformation of patients' earliest malignant lesions, encompassing the formation of dysplastic aberrant crypt foci and small adenomatous polyps. These findings suggest that loss of *APC* expression is a very early event in CRC tumorigenesis. Since *APC* carries out its functions within the Wnt/Beta-catenin arm of the Wnt signalling pathway, changes in this pathway and in their action associated with tumorigenesis can be similar in both genetic and sporadic diseases [17, 18, 19].

3.4 Features of the adenomatous polyps

Adenomatous polyps are histologically classified as villous, tubular or a mixture of the two:

• Villous – Villous adenomas are characterized by more than 75% villous features, where villous refers to finger-like or leaf-like epithelial projections. They account from 5 to 15% of adenomas. Villous adenomas are characterized by long and extended glands crossing from the surface to the center of the polyp. Adenomas with villous features may be associated with a slight increase in development of more advanced neoplasia or dysplasia compared to other types of adenomas.

• Tubular – Tubular adenomas account for the more than 80 % of colonic adenomas. They are characterized by a network of branching adenomatous epithelium. Tubular adenomas display less than 25% villous features.

• Tubulovillous – Adenomas with 25 to 75% villous features are considered to be tubulovillous. They account for 5 to 15 % of colonic adenomas.
All adenomas present some levels of dysplasia. Based on their dysplasia level polyps are classified as: Low-grade dysplasia and High-grade dysplasia.
High-grade dysplasia (also called intraepithelial carcinoma) represents an intermediate step in the progression from a low-grade dysplasia to cancer. This term is applied to lesions of the epithelial layer of colonic crypts with no invasion through the basement membrane into the lamina propria. In carcinoma in situ (Tis), or intramucosal adenocarcinoma, cancer cells invade into the lamina propria and may involve but not penetrate the muscularis mucosa. Cancer instead extends through the muscularis mucosa into the submucosa and beyond. (Figure 4)
AAP carriers develop hundreds to thousand adenomatous polyps on the colonic mucosa surface. Adenomas are generally asymptomatic, do not typically bleed and are mostly detected by screening tests. Within the healthy population only a small minority of adenomas progress to cancer (around 5%) over 7 to 10 years. The risk of progression is higher for advanced adenomas (adenoma with high-grade dysplasia and >10mm in size) [20]. The high number of polyps in AAP patients, strongly increases the risk of cancer development up to 100% during life.
The growth rate of adenomatous polyps in AAP subject is related to *APC* germline variants. In addition, increasing age in AAP patients is associated with development of high-grade dysplasia within the adenomas, independently from size and histology [20].
Most small polyps exhibit minimal growth with an average of 0.5 mm/year, although their growth rate remains variable and does not follow a consistent linear trend [21].

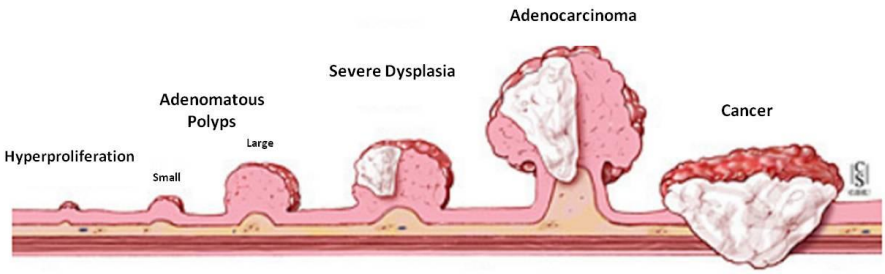

Figure 4: Histological features leading the formation and progression of adenomas from normal colorectal mucosa. High grade dysplasia is the first characteristic observed under microscope and is known as a discrimination factor between benign adenomas and early colorectal cancer.

3.4.1 Extra colonic conditions related to *APC* inactivation

Individuals carrying AAP syndrome develop also extra colonic conditions due to *APC* mutations:

• Adenomatous polyps of the duodenum, observed from 50 to 90% of individuals with AAP, are commonly found in the second and third portion of the duodenum [22] and less frequently in the distal small bowel [21].

• Adenomatous polyps of the periampullary region (including the duodenal papilla and ampulla of Vater) are seen in at least 50% of individuals with AAP. Polyps in this area can cause obstruction of the pancreatic ducts resulting in pancreatitis or biliary obstruction.

The lifetime risk for small bowel malignancy is from 4 to 12%, with the large majority occurring in the duodenum. Duodenal adenocarcinoma occurs most commonly in the periampullary area and can be observed in patients from 17 to 81 years [21].

• Pancreatic Cancer is rarely observed. Few data are available for AAP individuals; however, a study performed on 197 AAP families showed that the relative risk for pancreatic cancer was of 4.5 higher when compared to the general population risk [23].

• Thyroid cancer and benign thyroid disease display a high degree of variability in the frequency in AAP individuals. Retrospective studies have found prevalence from 2.6 to 11.8% with a striking female to male ratio of 80 to 1 in AAP subject. Also, the age at diagnosis displays great variability for more than 80% of individuals, going from 18 to 35 years [24].

• Desmoid Tumors (DTs) develop in approximately 10 to 30% of individuals with AAP. The risk within the AAP population is more than 800 times the risk in the general population [25]. DTs are locally invasive benign fibrous tumors that do not metastasize derived from clonal proliferations of myofibroblasts. The incidence of DTs in AAP is higher in the second and third decades of life, with 80% occurring by age of 40. Approximately 65% of DTs in AAP subjects occur within the abdomen or in the abdominal wall [26]. Five percent of AAP individuals experience death for DTs, with the highest mortality rate reported for intra-abdominal tumors.

3.4.2 Prophylactic Treatment

For individuals with AAP, colectomy is recommended after adenomas appearance. Colectomy can be delayed depending on adenoma size, presence of advanced histology (villous architecture, high-grade dysplasia), and overall number of adenoma polyps. Absolute indications for colectomy include documented or suspected CRC or other significant symptoms, such as obstruction or bleeding, although these symptoms are uncommon in the

absence of cancer. Relative indication for colectomy includes presence of multiple adenomas larger than 6 mm, which cannot be handled by endoscopy. Moreover, the increasing number of adenomas between surveillance examinations is a driver for the prophylactic intervention, as well as presence of adenomas with high-grade dysplasia [3]. Surgery consists either in restorative proctocolectomy with ileal-pouch-anal-anastomosis (IPAA) or colectomy with ileorectal anastomosis (IRA). The choice of procedure depends on the clinical circumstances.

• IPAA is generally performed in AAP where the rectal polyps burden is high or as a second procedure after IRA, in case of the rectal disease cannot be resolved endoscopically. This procedure nearly eliminates the risk of rectal cancer preserving relatively the bowel function.

• IRA is generally considered when the rectal polyp burden is low and endoscopically manageable. It is a technically straightforward procedure with low complication rates, associated with good functional outcome. It is not recommended when patients display rectal severe disease or when the individual cannot perform periodic endoscopic surveillance of the remaining rectum post-operatively.

3.4.3 Chemoprevention

Currently there are no approved chemo preventive agents for AAP. The first observational studies were performed using Non-Steroidal Anti-Inflammatory Drugs (NSAID), such as Sulindac. The results were initially promising, showing remarkable reduction in the size and number of polyps, and were confirmed after several controlled trials in which patients experienced a reduction of polyp burden during treatment [27]. However, after ending Sulindac administration, a rapid increase in the number of polyps was observed. Celecoxib, a NSAID specifically directed against the enzyme Cyclooxygenase 2 (COX-2), has been shown to significantly reduce burden and size of polyps in the colon of AAP patients, as well as in the duodenum. Unfortunately, due to cardiovascular and cerebrovascular safety concerns, FDA approval for celecoxib in AAP treatment has been revoked. These results have led researchers to test alternative methods to limit the inflammatory conditions of the mucosa. Numerous epidemiological studies have evaluated the relationship between diet and inflammation, focusing on diet components and patterns, in an attempt to reduce the inflammatory state of the colorectal district through an adequate balance of dietary compounds. In the colonoscopy-based Tennessee Colorectal Polyp Study, a high body mass index and high red meat consumption emerged as clear-cut risk factors for adenomas and cancer, while high dietary fiber and dietary calcium intake were associated with decreased risk. Other studies

reported the promising results of an “ad hoc” low-inflammatory diet used in patients with Inflammatory Bowel Disease (IBD) [28, 29]. A similar study was recently conducted at the Fondazione IRCCS Istituto Nazionale dei Tumori di Milano (INT) on a group of patients with AAP undergoing IRA surgery. These patients were enrolled in a pilot low-inflammatory dietary intervention aimed at reducing the high local inflammation on the rectal mucosa. Early results showed that levels of both fecal and systemic calprotectin were reduced in the stool and blood of patients, three months after the start of the diet. Calprotectin is a calcium- and zinc-binding protein highly released by neutrophils of the intestinal tract in inflammatory conditions and is used as a marker for the level of intestinal inflammation.

3.5 The Role of Inflammation on Colorectal mucosa

Pro-inflammatory stimuli, derived from various factors such as lifestyle, diet and environment, are normally present in the colorectal mucosa of healthy individuals.
The intestinal epithelium is composed of a single layer of cells with different functions including the absorption of nutrients and liquids, the preservation of intestinal homeostasis and the creation of a physical boundary capable, among all, of coordinating immune cells against pathogens. In healthy conditions, a thick layer of mucus is produced from specific epithelial cells (Goblet cells) that reside on the surface of the colorectal mucosa. Alterations of the peculiar populations of epithelial and immune cells composing the colorectal mucosa, as well as impairments of the mucus layer located between the epithelial cells and the bacteria that form the intestinal microbiota, result into a continuous stimulation of the immune system. Chronic intestinal inflammation promotes the formation and growth of adenomas and CRCs [30].
IBD and AAP are two different examples of Chronic intestinal inflammation. In fact, both diseases, despite showing many differences, are related to inflammation and increase the risk of developing CRC.
Chronic inflammation is also assumed to lead to genomic changes. Animal models suggest that both onset and progression of colon cancer can be accelerated by an inflammatory insult. In sporadic CRC, activation of the WNT pathway, particularly through mutational inactivation of *APC*, is often the initiating event [31]. Furthermore, the effects of proinflammatory factors of the innate and adaptive immune systems are widely reported to contribute to the development and growth of CRC [32]. Some proinflammatory cytokines, such as Tumor Necrosis Factor-α (TNF-α), which is released by activated Macrophages and T cells, have been reported to promote inflammation and colitis associated cancer. TNF-α can

initiate carcinogenesis by promoting DNA damage; moreover, it can stimulate angiogenesis and also influence the expression of COX-2, which promotes angiogenesis and supports uncontrolled proliferation of the colon mucosa. Aberrant expression of COX-2 is reported along the entire colorectal mucosa of AAP individuals; this upregulation leads to an increase of abundance of its main metabolic product, Prostaglandin E2 (PGE2). The pleiotropic effects of PGE2 appear to affect most, if not all, of the hallmarks of cancer (Figure 5) [32].

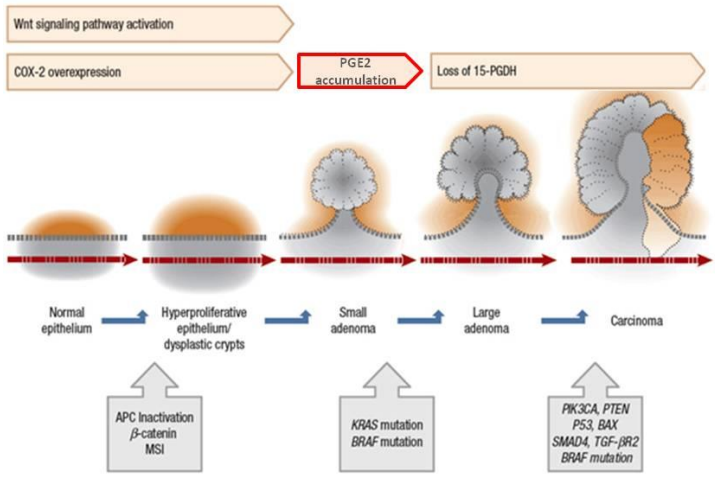

Figure 5: Role of COX-2 in CRC development: increase of COX-2 expression in normal mucosa of AAP and *APC* wt individuals activates the Wnt pathway and promotes cellular proliferation through accumulation of PGE2 and inactivation of 15-PGDH.
Arranged from www.basicmedicalkey.com

3.6 Cell populations of the colorectal mucosa

Cell composing the intestinal mucosa can be divided in three categories: epithelial, stromal and immune.

3.6.1 Epithelial cells of the intestinal crypts

The structural complexity of colorectal epithelial cells limits the potential damage inflicted by semi-solid stools that pass through the large bowel and consist of invaginations called “Crypts of Lieberkühn” (Figure 6). Intestinal

stem cells reside at the base of these crypts and generate transient proliferative cells that differentiate and mature along the transition crypt area, shedding into the intestinal lumen at the apex of the crypts [33]. Intestinal Epithelial cells (IECs) undergo constant cycles to replenish and renew the walls of the crypts. Under homeostasis conditions, the entire intestinal epithelium is estimated to be replaced every 4-5 days [34]. Inside the gut epithelium there are different types of differentiated cells that perform unique and specialized functions:

•Enterocytes: the most prominent cell type of the epithelium that is responsible for nutrient and water absorption;
•Goblet cells: secretory cells that secrete mucins;
•Entero-endocrines: cells involved in hormones secretion;
•Paneth Cells: cells releasing antimicrobial factors which protect the stem cells at the base of the crypts;
•Tuft cells: chemosensory cells which play a key role in defense against helminthes;
•M cells: integral in the uptake and luminal presentation of antigens to the immune system;

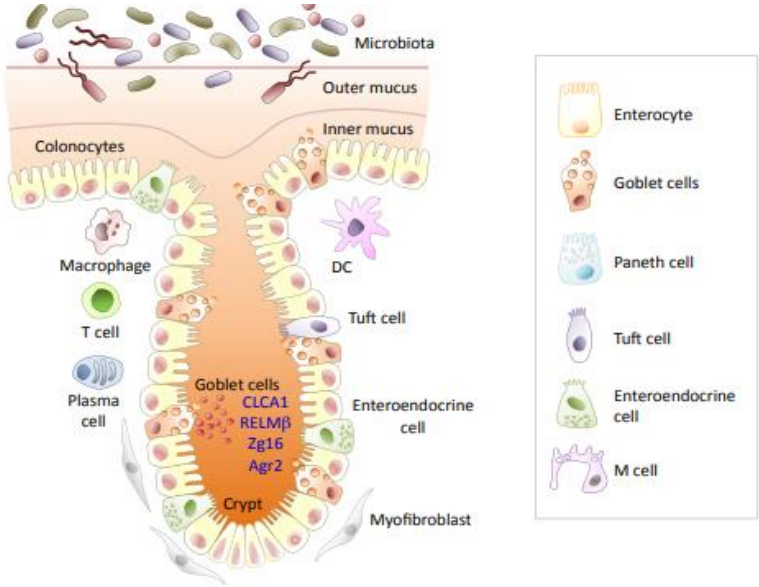

Figure 6: Representation of a single colonic Lieberkühn crypt and of the immune and stromal cells composing the lamina propria that surrounds it. The different epithelial cells composing the colonic crypt are listed on the left.
Credits: Gan Quan Fu, ResearchGate 2014

The fine mechanism that regulates homeostasis inside the colon crypts is supported by the proliferation index of stem cells and by the subsequent differentiation of daughter cells. The balance between stem cell renewal and fate is disrupted by mutations in the *APC* gene. Studies in *APC* Mutant -/+ mice have highlighted that the loss of the wild-type (WT) allele triggers the formation of microadenomas [35]. At the same time, *in vitro* studies on cultured cells, have shown how *APC* mutations induce a series of mitotic defects [36,37,38]. The appearance of normal crypts *in vivo* in *APC* Min/+ mice shows alterations in the orientation of the spindle and in the cytokinesis of transit-amplifying cells. These features are believed to be responsible for the loss of lamina propria ploidy [39, 40], and loss of vertical spindle reorientation of stem cells [41] expressing the Leucine-rich repeat-containing G-protein coupled receptor 5 (LGR5), an enhancer of the canonical Wnt signaling pathway. These mitotic defects are considered among the first detectable alterations that predispose to adenomas and, subsequently, cancer initiation [42]. The uncontrolled proliferation of stem cells affects the structure of the crypt and its ability to maintain the retention of single-layer cells. After breaking of crypt symmetry, the resulting structural deficit opens the way for disordered cell proliferation. Adenomatous crypts reduce the portion of the lamina propria between the adjacent crypts, deregulating the stromal and immune cells population of the lamina propria. Furthermore, this structural alteration affects the absorption of nutrients and liquids. The alteration of tissue permeability and the decrease of mucus production expose the surface of the colonic crypts to the microorganisms populating the colon lumen. Mechanistic studies have shown that commensal-Toll Like Receptor (TLR) interaction is required to preserve epithelial barrier function by maintaining a normal distribution of junctional proteins in intestinal epithelial cells [43]. The metabolites produced by commensal bacteria or introduced with the diet play an important role in the regulation of intestinal epithelial cells. Studies showed that butyrate, a short chain fatty acid converted through the fermentation of dietary fiber, is largely consumed by the differentiated colonocytes located at the top of the crypts [44]. Similarly, microbe-derived lactate has been observed to be a potent inducer of colonic hyperproliferation in mice models [45]. The uncontrolled profileration of epithelial cells in AAP patients leads to changes in the architecture of the crypts and the consequent loss of colonic barrier function, which protects the integrity of the stem cells at the base of the crypt. Furthermore, exposure to microbial-derived compounds may affect epithelial stem cells and increase their proliferative rate.

3.6.2 Stromal cells

Mesenchymal stromal cells participate in the regulation of acute and chronic inflammation in peripheral organs, including secondary lymphoid organs. Apart from their role as structural elements, stromal cells act as resident sentinels that produce chemokines upon activation, starting the recruitment of leukocytes at the site of tissue injury and inflammation [46,47]. Stromal cells have the ability to play either an immunosuppressive or an immunostimulatory role, depending on the microenvironmental milieu of cytokines, chemokines, growth factors and TLR ligands. The understanding of their immune function is far from complete. However, recent data acquired from intestinal stromal cells and from those in other parenchymal organs suggest that they are adequately licensed to actively participate in the regulation of professional immune cells during immunity and tolerance. Moreover, considering the physical connection between stromal and immune cells inside the Lamina Propria region of the mucosa, they are part of a sophisticated immune lymphatic network throughout the mammalian body [48].

3.6.3 Immune cells

Immune cells of the gut play a fundamental role in the maintenance of the normal homeostasis.
In the process of absorbing essential nutrients, the human intestine must discriminate between harmless food antigens and infectious or toxic agents. In order to protect the host from microbial infection, the intestine, in addition to an effective barrier, has an innate and acquired immune system.
• The innate immune system is formed by myeloid-derived cells (neutrophils, monocytes, dendritic cells, and macrophages), natural killer cells, and innate lymphoid cells. These cells, in addition to epithelial cells, endothelial cells, and stromal cells, express the so-called pattern recognition receptors, which bind microbial products.
Macrophages resident in the normal gut wall play essential housekeeping functions, such as the clearance of apoptotic or senescent cells [49, 50]. Furthermore, intestinal macrophages are known to produce a variety of cytokines and other soluble factors that help to maintain tissue homeostasis. One of all is PGE2 which allows local macrophages to stimulate the proliferation of epithelial progenitors in intestinal crypts [51], thus regulating the integrity of the epithelial barrier. One of the characteristics that distinguish healthy macrophages in the intestine to those in other areas of the body is the absence of pro-inflammatory responses following exposure to bacteria or to their products [52].
Within normal condition macrophages do not enhance production of TNF-α,

Interleukin 1 (IL-1), Interleukin 6 (IL-6), or other inflammatory cytokines and chemokines in response to ligation of TLR [53]. However, recent studies in mice indicate that intestinal macrophages are not completely anergic in terms of cytokine production, as they show constitutive production of substantial amounts of Interleukin 10 (IL-10), as well as low levels of TNF-α [54]. This finding opened a new scenario of inflammatory macrophages that constitutively produce prototypical pro-inflammatory cytokines. TNF-α, in fact, may have much wider effects, such as the regulation of the growth of enterocytes and the altered permeability of the epithelial barrier [55] as well as the production of matrix metalloproteinases and other tissue remodeling enzymes in the intestinal mesenchymal cells that are involved in the regulation of epithelial cell function [56].
The composition of the human intestinal macrophage pool changes considerably when there is perturbation of homeostasis. For example, in the mucosa of patients with inflammatory conditions, there is an accumulation of pro-inflammatory macrophages. The ability of these cells to produce large amounts of mediators such as IL-1, IL-6, TNF-α, COX-2, reactive oxygen intermediaries and nitric oxide makes them quite distinct from the macrophages present in the healthy intestine and has led to an interest in the idea of targeting the monocyte-macrophage lineage for therapeutic purposes. AAP syndrome displays altered homeostasis of the intestinal mucosa and it may be reasonable that macrophages take part in the alteration of the mucosa of these patients, unfortunately data supporting this hypothesis are still lacking.
• The acquired immune system is designed to respond to foreign antigens displayed by "professional" antigen-presenting cells (APCs) (mostly dendritic cells and macrophages) in association with molecules of the major histocompatibility complex (MHC).
Cellular immunity is mediated by T lymphocytes, which can be functionally divided into CD4+ helper T cells (Th), CD8+ T cells (cytotoxic), and regulatory T cells. CD4+ T cells respond to processed antigen on professional APCs in association with MHC class II molecules. CD8+ T cells respond to processed antigen on all cell types in association with MHC class I molecules.
Within Th lymphocyte family, Th17 plays a critical role in regulating the inflammatory process and carry out their task at mucosal surface. Th17 cells secrete predominantly Interleukin 17a (IL-17a), Interleukin 21 (IL-21), Interleukin 22 (IL-22), and granulocyte-colony stimulating factor (G-CSF) [57]. Studies on colonic stromal cells interacting with Th17 cells showed that IL-22 induces antimicrobial proteins, defensins, acute-phase proteins, inflammatory cytokines, chemokines and hyperplasia [58, 59, 60]. The repertoire of combined cytokines determines the behavior of Th17 cells at

the mucosal surface, enhancing inflammation or limiting tissue damage induced by IL-17. Biopsies performed on inflamed colonic tissue from patients with IBD expressed IL-17 at the mRNA level and CD4+ Th17 cells were found clustered in the lamina propria [61]. Other studies confirmed that IL-22 was found to be overexpressed by colonic CD4+ T cells of IBD patients compared with healthy controls [62], suggesting that the lamina propria is an inductive site for human Th17 cells during IBD. Despite AAP patients display high inflammation level along the colonic mucosa, no data on Th17 cells are available at present.

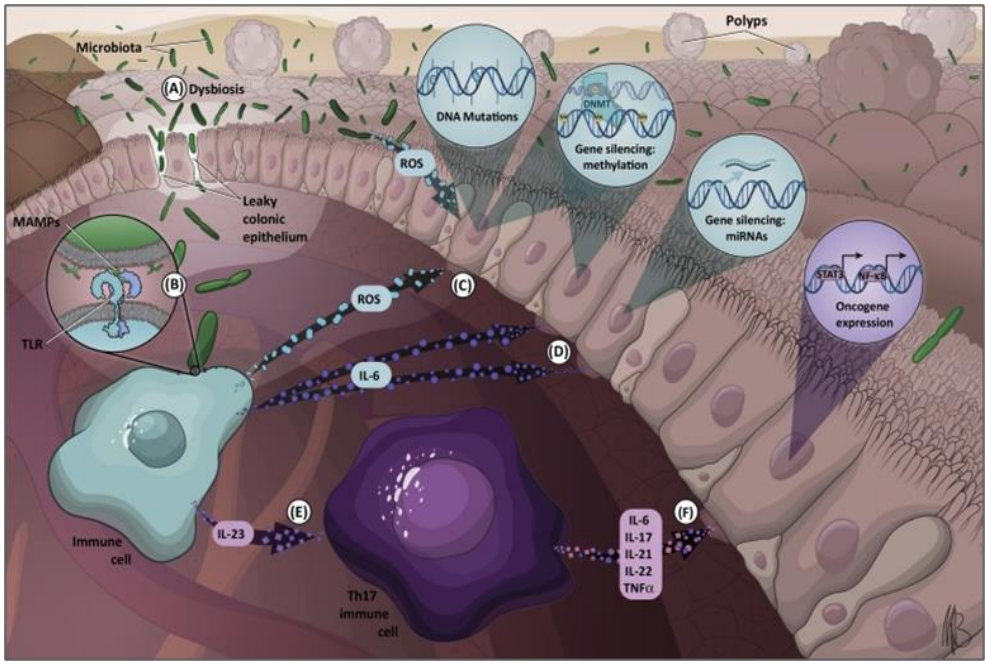

Figure 7: Role of innate and acquired immune system during homeostasis perturbation of the colonic mucosa. Pro inflammatory stimuli, derived from microbial dysbiosis, or DNA mutations amplify the immune response via specific ILs production. ILs interacts with epithelial cells and alters cellular mechanisms such as gene silencing and oncogenes expression that lead to uncontrolled proliferation and polyp's development.

3.6.4 COX-2/PGE2/15-PGDH Axis

COX-2 is involved in the progression of large adenomatous polyps, both in healthy and AAP subjects, and in the formation of the overall number of

polyps. Increased expression of *COX-2* contributes to the genesis of up to 85% of all CRCs [63]. PGE2, the product of *COX-2*, is a small molecule derived from arachidonic acid (AA). Its accumulation at local levels, mainly due to its production by myeloid and stromal cell, is regulated by a local balance between its synthesis, driven by *COX-2* and its degradation, operated by 15-Hydroxyprostaglandin dehydrogenase (15-PGDH) the enzyme primarily responsible for the enzymatic metabolism of PGE2. The receptors for PGE2 (EP1-EP4) are present on multiple cell types, reflecting the ubiquitous function performed by this small molecule. Some of the most important roles of PGE2 and its receptors are the regulation of different stages of immune responses and different effector mechanisms of immunity [64]. PGE2 was generally recognized as a mediator of active inflammation, promoting local vasodilatation, local attraction and activation of neutrophils, macrophages and mast cells at early stages of inflammation [65]. During the past years a second role has been attributed to PGE2: the ability to promote the induction of suppressive IL-10 and directly suppress the production of multiple proinflammatory cytokines, limiting no specific inflammation and promoting immune suppression associated with chronic inflammation and cancer [66]. PGE2 can be produced by different cells such as epithelial, fibroblasts, and infiltrating inflammatory cells. PGE2 synthesis involves members of the phospholipase A2 (PLA2), who mobilize arachidonic acid from cellular membranes. COX-2 converts arachidonic acid into prostaglandins H2 (PGH2) and prostaglandin E synthase performs the final formulation of PGE2 (Figure 7) [67].

The suppression of 15-PGDH activity is observed in many forms of cancer. Studies on premalignant colon lesions showed that 15-PGDH deactivation was responsible for resistance to pharmacological inhibition of the COX-2 activity via celecoxib [68].

The COX-2/15-PGDH pathway plays an important role in the maintenance of the colonic mucosa homeostasis. Apoptotic cells on top of the colonic crypts can modulate the production of different prostanoids, a subclass of eicosanoids which includes prostaglandins. Prostanoids act enhancing the macrophages expression of both COX-2 and microsomal prostaglandin E synthase-1 (mPGES-1), the enzyme involved in PGE2 production, resulting in an increase of PGE2 extracellular levels.

On the other hand, the same cells that undergo apoptosis can suppress 15-PGDH activity, enhancing intracellular PGE2 accumulation.

These observations suggest that in addition to the PGE2 synthesis, also PGE2 decay may contribute to immune related pathologies and constitute a potential target of immune modulation. In normal colon mucosa 15-PGDH is highly expressed by colonic epithelial cells located in the luminal regions of colonic crypts; on the contrary, the transcription of 15-PGDH mRNA is

ubiquitously reduced in colorectal adenomas and lost in colon cancers. Interestingly, 15-PGDH mRNA contains several regulatory sites within its 3′ untranslated region (UTR), including AU-rich elements and putative microRNA (miRNAs)-binding sites, highlighting a possible control of 15-PGDH expression at post-transcriptional level [69, 70, 71].
Based on these data 15-PGDH can be considered a tumor suppressor gene which acts in the normal colon to antagonize the prostaglandin generating activity of the COX-2 oncogene. *In vivo* studies on C57BL/6J mice carrying *15-PGDH* -/- genotype displayed high susceptibility to the development of colon adenomas and cancer caused by treatment with pro inflammatory agents. This result was observed also in C57BL/6J *15-PGDH* +/- mice which were partially sensitive to colon adenomas and tumor development under pro inflammatory conditions [72]. Loss of 15-PGDH in normal colonic mucosa, adenomas and colorectal cancer is nowadays recognized as a factor contributing to the increase of PGE2 levels. These changes in expression can result from various regulatory mechanisms, including the differential expression of miRNAs which have been observed in colorectal tumors. Monteleone and collaborators demonstrated that levels of miR-21 are inversely correlated to 15-PGDH expression in both colorectal cancer tissue and cell lines. Therefore, miR-21 can directly regulate 15-PGDH binding to different sites in its 3' untranslated region (3'UTR) as shown in figure 8 [73].

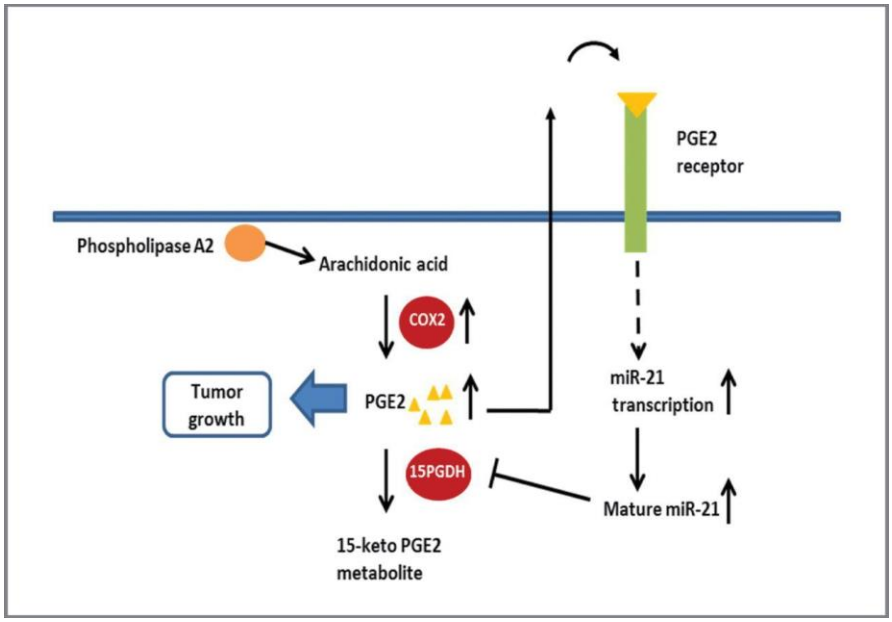

Figure 8: COX-2/15-PGDH pathway regulates PGE2 production and accumulation. High levels of COX-2 interact with PLA2 which mobilize AA from the cellular membrane and result to high levels of PGE2. On the other side PGE2 interacts with its specific receptor on the cellular membrane and increases miR-21 expression. Mature miR-21 performs its inhibitory function on 15-PGDH contributing to PGE2 accumulation.
Credits: L. Lu et al. Molecular Cancer Research, 2014.

3.6.5 miRNAs and colonic mucosa inflammation

miRNAs are a highly conserved class of tissue specific, small non-protein coding RNAs involved in the maintainance of cell homeostasis by negative gene regulation. Deregulation in miRNAs expression correlates with various cancers, such as CRC, by acting as tumor suppressors and oncogenes. Different studies have demonstrated that miRNAs are essential for mucosal integrity and barrier function [74, 75]. miRNAs screenings performed on IBD patients demonstrated that they are critically involved in the development and progression of Chron's disease and Ulcerative Colitis [76, 77]. In addition, altered levels of specific miRNAs can modulate the adaptive and innate immune response. For example, overexpression of miR-193a-3p was found to dampen mucosal inflammation by negatively regulating the Peptide transporter 1 a protein involved in the absorption of small peptides produced by the colonic microbiota [78]. Low expression of miR-146a in the colonic mucosa were found to be critical in regulating the expansion of certain intestinal T cell subtypes, including Th17 cells [79]. Few studies correlateded changes in miRNA expression and adenoma formation in AAP subjects and only two miRNAs, miR-126 and miR-20b were found downregulated in AAP adenomas and CRC (in 100% of adenomas and 85.7% of CRCs and 64% of adenomas and 50% of CRCs respectively[80]).

3.6.6 PGE2 and innate immune cells

PGE2 can promote tissue influx and affect the functions of different innate effector cells such as Natural Killer (NK), Granulocytes and Macrophages. Focusing on colorectal mucosa, PGE2 acts on its specific receptor (via EP2-dependent manner), limiting the phagocytosis activity of macrophages which reside in the lamina propria of the colonic crypts and their pathogen-killing function. The effect of PGE2 on Macrophages affects the scavenger receptor mediated phagocytosis and the Toll-Like Receptors-dependent activation of TNF-α [81]. Modulatory effects of PGE2 affects also antigen specific Immune Response.
High doses of PGE2 suppress Interleukin 2 (IL-2) production and

responsiveness of T cells, affecting in a no specific manner T cell activation and proliferation. On the contrary, when present at lower concentrations PGE2 shows profound modulatory effects switching the pattern of CD4+ T cells from the aggressive Th1 (players of inflammatory / cytotoxic form of immunity) towards Th2 and Th17 cells, which mediate less tissue-destructive forms of immunity [82].
Moreover, acting on EP2 and EP4 receptors, PGE2 has also been shown to promote the development of IL-17a producing T cells in multiple models of infections and diseases displaying homeostasis unbalance. The Th17 promoting activity of PGE2 is related to interleukins production. Some studies underlined how PGE2 enhances synthesis of Interleukin 23 (IL-23) which stimulates cellular proliferation acting on different pathways [83].

3.6.7 PGE2 and suppressive immune cells

PGE2 has been shown to promote the development of T regulatory lymphocytes (Treg) in human and in mouse models. COX-2 and PGE2 have been shown to be essential for the EP2- and EP4- dependent induction of Treg in cancer [84].
In addition to promoting *de novo* Treg proliferation and differentiation from naïve precursors, PGE2 also promotes the interaction of Dendritic Cells (DCs) with Treg, suggesting that it may also promote the expansion of pre-existing Treg cells, as observed in cancer patients vaccinated with PGE2-matured DCs [85]. PGE2 is needed for the development of tumor-associated suppressive macrophages and myeloid-derived suppressor cells (MDSC). Interestingly, in addition to be the recipients of PGE2-mediated signals, MDSCs express high levels of COX-2 and are the major source of PGE2 secretion in human cancer [86, 87, 88]. The resulting positive feedback loop between PGE2 and COX-2 is essential for the functional stability of myeloid derived suppressor cells. Moreover, the COX-2 pathway attends to the production of suppressive mediators of CD8+ T cells [88].

3.7 Organoid generation

Advances in stem cell culture have made possible to derive *in vitro* 3D structures, named “Organoids”, which capture some of the key multicellular, anatomical and even functional hallmarks of real organs at the micrometre to millimetre scale [89]. Traditional mammalian cell cultures preclude the study of behaviors that are intrinsically linked to the 3D organization of cells into tissues and organs. In addition, one of the main advantages of using

organoids is the greater ease of use in the laboratory compared to animal models.

The establishment of 3D culture systems resulted, among all, from the better understanding of extracellular matrix (ECM) biology [90, 91] and from the development of methods for culturing cells in suspension. However, only in the last ten years, the establishment of organoids has become a reproducible and highly successful laboratory practice [92]. Clevers H. and co-workers demonstrated that organoids could be derived from intestinal adult stem cells [93]. Their work promoted the idea that stem cells have the intrinsic ability to self-organize into 3D structures that resemble *in vivo* organs, which remains one of the cardinal concepts underlying organoid biology. Self-organization can be defined as the capacity of a cellular system that initially lacks an ordered structure to spatially rearrange under the guidance of system-autonomous mechanisms, even if exposed to a uniform signaling environment [94].

The most common way to grow organoids in a three-dimensional structure is to use solid ECMs that support cell growth and function as a scaffold during Organoid formation. Matrigel, a natural ECM purified from Engelbreth-Holm-Swarm mouse sarcoma [92], is the most widely used matrix for 3D organoid derivation. The main advantage of these natural matrices is the presence of a complex mix of ECM components and growth factors, which makes cell growth and differentiation very efficient. However, considering its origin, the variability in composition makes it more difficult to control the culture environment and may affect reproducibility.

Different studies performed on mouse intestinal stem cells (ISCs) expressing the staminal *Lgr5* gene showed that the self-renewing colonies formation is dependent by Paneth cells, a neighboring cell type of ISCs in the colonic crypt [95]. Indeed, Paneth cells express high levels of WNT ligands, and Wnt signaling is essential for ISCs maintenance [96].

Another primary advantage of organoid cultures is their use in disease modeling, where they recapitulate specific human features that are relevant for translational studies. A wide range of organoid-based disease models that reproduce genetic diseases [97, 98], host–pathogen interactions [99, 100, 101, 102] have already been developed and provide proof of principle that organoids can reproduce well-known pathological features. The fact that organoids can shape human pathologies has paved the way for studies on the feasibility of drug testing and screening. For example, drugs for the treatment of Zika virus infections have recently been screened in human-derived cortical progenitor neuronal stem cells (hPSC) and validated in parallel in Organoid and mouse models, confirming that Organoids are a valid alternative model for testing drugs against this disease [103]. Organoids have also been used in drug testing for cystic fibrosis (CF), a

genetic disorder caused by defects in the *CFTR* gene [104]. Patient derived intestinal organoids carrying *CTFR* mutations possibly represent the only example of Organoids that have already been applied to personalized medicine. In the study performed by Saini and collaborators, Organoids derived by one patient with a very rare *CTFR* mutation associated with no known treatments were used to screen several existing CF drugs. The results showed the reactivity of the Organoids to a drug already used for the treatment of other CF mutations, thus allowing the identification of an effective cure for this patient.

As for cancer, Organoid culture protocols developed by Clevers's and Sato's groups for several tumor types (breast [105], pancreas [106], liver [107]) and by other groups (kidney [108], brain [109]) allowed researchers to reproduce the conditions for both normal and tumor tissues with an elevated successful rate [110], especially for CRC. Despite this is a "hot topic" in the field of CRC research, most of the studies are focused on Organoids generated from sporadic CRC, while only few of them consider patients carrying hereditary CRC syndromes like AAP [111]. The establishment of normal and adenomatous Organoids from the colorectal mucosa of patients with AAP could help clarify the mechanisms underlying the rapid and continuous development of polyps typical of AAP.

4 AIM of the study and novelty

The mechanisms underlying the formation and development of adenomas in the colon and rectum have been investigated for several years. Most of the studies have been conducted on patients who developed sporadic CRC and have clarified which alterations drive the neoplastic transformation of the healthy colorectal mucosa. In recent years, the intestinal microenvironment, dietary and lifestyle habits have emerged as important player in maintaining the right balance between cell proliferation, protection from dysbiosis and homeostasis; alterations of this balance can favor the development of CRC. Chronic inflammation of the colonic mucosa is the main event involved in the alteration of homeostasis and it has been shown to be closely related to adenoma formation and CRC development. Inflammation also has a role in AAP and drives the formation and growth of intestinal adenomas.
The goal of this study was to explore the inflammatory processes that lead to the development of adenomas along the colorectal mucosa of AAP subjects. To achieve this goal, different specific aims were assayed:
1- evaluation of the possible changes in COX-2/15-PGDH axis in a cohort of adenomas and normal mucosa biopsies collected during a pilot dietary intervention study conducted on AAP subjects and designed to test whether a low-inflammatory diet can reduce intestinal markers of inflammation.
2- development of 3D organoids models derived from AAP adenomas to use as innovative *in vitro* model closer to the tissue of origin.
3- characterization of AAP organoids maintained under different inflammatory environments in order to evaluate the effects of inflammatory conditions on the proliferation of the epithelial cells composing the organoids.

5 MATERIAL AND METHODS

5.1 Study design

AAP subjects were enrolled in a non-randomized dietary intervention pilot study that started in September 2017 at the Fondazione IRCCS Istituto Nazionale dei Tumori of Milan (INT). This study enrolled 34 patients diagnosed with AAP, selected from the Hereditary Digestive Tumor Registry of INT. All registered patients signed an informed consent to be recalled for future studies. Subjects enrolled were older than 18, were tested for *APC* gene mutations, underwent prophylactic total colectomy/IRA and are currently involved in the surveillance program of INT. Participants accepted to adhere to the study and to follow a six months low-inflammatory dietary program that provided accurate information about healthy status and clinical problems. Briefly, AAP participants were invited to take part in dietary intervention activities that included 12 days of training, cookery, supportive educational content about the diet and common meals. The participants received the nutritional content and recipes of the menus provided during cooking classes and common meals. The intervention lasted 3 months and patients were assisted with lifestyle changes. At the beginning of the study (T0, baseline), at the end of the dietary intervention (T1), and 6 months after T0 (T2), participants were asked to give blood samples for the determination of insulin, IGF-1, C-Reactive Protein (CRP), glucose and circulating calprotectin. Stool samples were also collected at T0, T1 and T2 and were used for the determination of fecal calprotectin. Samples of Normal and Adenomatous Rectal Mucosa were collected for all the patients enrolled in the study during the endoscopy procedure at T0 and T2. Patients were asked to complete a 14-item Mediterranean Diet Adherence Screener (MEDAS) [112] questionnaires and 24-hour dietary recalls throughout the 3-month dietary intervention. Study design is shown in Figure 9.

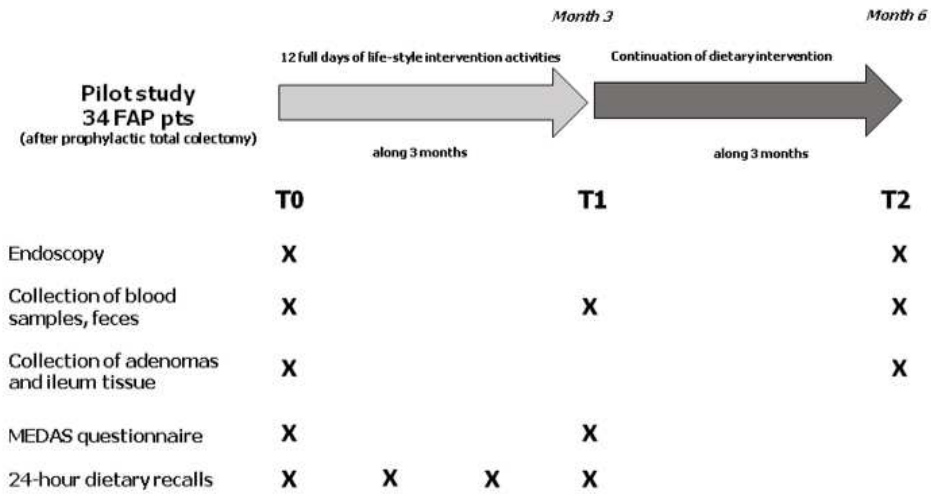

Figure 9: Timetable of the pilot dietary intervention study in patients with AAP, including collection of biological samples at set intervals.

5.2 Dietary Intervention

The proposed diet had 5 main objectives [113]:
1) to strongly reduce the introduction of certain carbohydrates. High plasma levels of glucose increase inflammation, it is therefore useful to avoid foods that quickly raise glycaemia (sugary drinks, flour 00, white bread, potatoes and sweets);
2) to promote the ingestion of pre- and pro-biotics. These components included in the diet help to restore the balance of the intestinal flora;
3) to distinguish between saturate, trans-, mono-, and poly-unsaturated fatty acids. Processed red meat (rich in saturated fats) and some foods of vegetal origin, such as margarine (with trans- fatty acids) promote inflammation and should be avoided or strongly reduced. Omega 3 and poly- unsaturated fatty acid have, instead, an anti-inflammatory function;
4) to modify the texture of the food. Whole grain has anti-inflammatory properties. Since the fibers of whole grain cereals may be problematic for patients, they were reduced in cream;
5) to encourage a review of the overall dietary pattern. AAP patients progressively expand their diet as their tolerance and absorption increase.

5.3 Generation of AAP Organoid models

In order to test, and eventually confirm, the hypothesis observed on AAP subjects enrolled in the low inflammatory pilot dietary intervention, four 3D-Patients Derived Organoids (PDOs) cultures were generated from colorectal adenomas of AAP patients (here and after named FAP1, FAP2, FAP3 and FAP4), not enrolled in the dietary intervention and who underwent to prophylactic IRA surgery. *APC* germline mutations of the selected patients are listed in Table 1.

Primary Sample ID	Gene Mutated	Genomic alteration	Protein alteration
FAP 1	*APC*	c.2369_2372 DEL GACA	p.Arg790ThrFS*2p
FAP 2	*APC*	c.3927_3931 DEL AAAGA	p.Glu1309ASPFS*4
FAP 3	*APC*	c.3927_3931 DEL AAAGA	p.Glu1309ASPFS*
FAP4	*APC*	c.3919_3937 DUP AATAAAAGAAAAGATTG	p.Thr1313ASNFS*Ter8

Table 1: Genetic alterations of the adenomatous colon tissue of patients with AAP used for the generation of 3D PDOs.

Briefly, following the protocol published by Sato and collaborators [110] 2-3 adenomas were collected from total colectomy of patients who underwent surgery at INT. Samples were identified by a gastrointestinal tract expert pathologist. Each adenoma was cut in two part: one was processed for histological analysis, the other was used for organoids generation. AAP Adenomas were mechanically homogenized, using two sterile scalpels, washed ten times using cold, sterile Dulbecco Phosphate Saline Buffer (DPBS) (Life Technologies), to avoid possible contaminations by bacteria which normally colonize the intestinal tract. Once cleaned, tissue fragments were enzymatically digested for 2 hours at 37°C in humidified incubator, using 1X Type II Collagenase obtained from Clostridium Histolyticum (Sigma Aldrich). After collagen digestion the remaining fragments were further treated with 0.05% of Trypsin EDTA (Life Technologies) diluted in sterile DPBS for 20 minutes at 37°C in humified incubator. The obtained cells were washed twice in DPBS and resuspended in growth factor reduced Matrigel (Corning). Cells were seeded at a concentration of 200 cells/well in a 24 multi-well plate.
The aim of this phase was to reproduce an *in vitro* culture condition suitable for the growth of AAP PDO. To achieve that a combinatorial strategy was set and PDOs were seeded in 14 different media supplemented with specific growth factors and/or inhibitor molecules. Most of the selected molecules are produced *in vivo* by cells present in the microenvironment

surrounding the colonic crypts, with greater consideration of those involved in the processes linked to stem cell proliferation, as well as differentiation of daughter's cells along the colonic crypt. All details of the different media tested are shown in Table 2.

The combinatorial strategy is based on the preliminary results obtained in the generation of PDOs from cells derived from the left-over material of patients with sporadic CRC undergoing surgery at the INT. All patients signed acceptance consent for the use of the left-over for research purposes. During this setup phase several CRCs at different tumor stages were cultured. Stage 3 and 4 tumor-derived cells required few factors for their growth, whereas early-stage tumor-derived cells (T1-T2) required a culture media richer in stem and epithelial factors. Despite AAP adenomas and early stage CRCs being two distinct entities, they are both well differentiated, and they display similar requirements in terms of culture conditions. With these experiments two media that favoured the growth of organoids derived from AAP adenomas were identified: medium #2, suitable for the cell passage procedure and #4 for maintaining cultured organoids. Briefly, for both media, DMEM F12 was supplemented with 50 ng/mL mouse recombinant EGF, 1X GS21, 10 nM Gastrin 1, 1 mM N-Acetylcysteine, 10 µM α-P38, 500 nM α-ALK, 100 ng/mL mouse recombinant Noggin 1 and 10 µM PGE2. Media details are shown in Table 2. To avoid apoptosis, after every passage, 10 µM α-ROCK was added to medium #2 and was maintained for a maximum of two days. After one week, Matrigel was digested adding 250 µl of Cell Recovery (Corning) solution to each well for 1 hour at 4°C. Released Organoids were washed and centrifuged twice in cold sterile D-PBS, supplemented with antibiotics. After these passages Organoids were resuspended in Matrigel and split 1:3 in order to expand their total number. Once obtained, cultures were frozen in liquid nitrogen following standardized procedures until they were used.

Medium	GS21	NAC	PGE2	Gastrin	αALK	α-P38	EGF	Noggin	WNT3A	α-Rock
1	+	+	+	+	+	+	-	-	-	+
1+	+	+	+	+	+	+	-	-	+	+
1-	+	+	+	+	+	-	-	-	-	+
2	**+**	**+**	**+**	**+**	**+**	**+**	**+**	**+**	**-**	**+**
2+	+	+	+	+	+	+	+	-	+	+
2-	+	+	+	+	+	-	+	+	-	+
3	+	+	+	+	+	+	-	-	-	-
3+	+	+	+	+	+	+	-	-	+	-
3-	+	+	+	+	+	-	-	-	-	-
4	**+**	**+**	**+**	**+**	**+**	**+**	**+**	**+**	**-**	**-**
4+	+	+	+	+	+	+	+	-	+	-
4-	+	+	+	+	+	-	+	+	-	-
5	+	+	+	+	+	+	+	-	-	-
6	+	+	+	+	+	+	+	+	+	-

Table 2: Culture media developed after the combinatorial strategy. Media #2 and #4 gave the best results than the others for the growth and maintenance of AAP 3D PDOs.

5.4 *In vitro* pro-inflammatory culture of AAP Organoids

In order to recreate a proinflammatory environment enriched with specific CD4+ inflammatory immune cells factors, medium #4 was modified adding a cocktail of interleukins (ILs) which are reported in literature as specifically produced by Th17, Th22 and CD4+ immune cells. Briefly, medium #4 was deprived of PGE2, which is physiologically produced by epithelial colorectal cells under inflammatory conditions, and supplemented with recombinant human IL-6, recombinant human IL-17a and recombinant human IL-22 (25 ng/mL each) as described by De Simone V. and collaborators [114] Organoids were maintained under this condition for 24 and 36 hours while medium #4 without ILs was used as blank control, then Matrigel was digested and PDOs were used for subsequent analysis.

5.5 Cell cycle analysis

To examine whether the CD4+ pro-inflammatory environment influenced FAP1-FAP4 Organoids cell cultures proliferation a cell cycle analysis was performed on both standard and ILs conditioned Organoids Culture. Briefly, after 24 and 36 hours of growth Organoids were disrupted using 0.05% Trypsin EDTA at 37°C for 15 minutes. Once at single cell both standard and ILs cells were washed with D-PBS and fixed using cold 70% ethanol for 1 hour. Cells were washed twice with DPBS before the staining, and then incubated for 40 min with 400µL of 50 µg/ml Propidium Iodine plus 0.5mg/ml RNase A solution at 37°C without direct light exposure. All the stained samples were analyzed within 1 hour on a FACS Calibur (Becton-Dickinson) flow cytometer, equipped with 2 lasers (488 nm, 635 nm) and 6 parameters (FSC, SSC, FL1–FL4). At least 10,000 cells/condition were acquired and used for analysis which was performed through FlowJo software. Percentage of G1, S and G2/M cells was calculated on cells distribution considering FL4-H, FL2-A gates. G1, S, G2/M ratios were build using both ILs 24 and 36h compared to the Standard culture condition which was used as blank.

5.6 AAP Organoids and THP1 co-culture

For the co-culture condition, AAP organoids were resuspended in Matrigel and seeded on 24 mm diameter, 0.4 µm pore size inserts (Corning Transwell®) at a concentration of 200 PDOs per insert. After Matrigel polymerization 2 mL of medium #2 were added for the first two days of culture. From third day medium #2 was replaced with medium #4 for the maintenance until PDOs reached exponential growth phase. At the same time Human Acute Monocytic Leukemia (THP1) cell line was seeded on a six well plate at the concentration of 0.5 million/mL in RPMI 1640 (Life Technologies) supplemented with L-glutamine, 10% Fetal Bovine Serum (FBS) (Corning) and 50µg/mL Gentamicin (Life Technologies). After one-week THP1 cells were stimulated using Lipopolysaccharides (LPS) at the final concentration of 10 ng/mL for 8 hours as described by Bosshart H and collaborators [115]. At the end of 8 hours THP1 stimulation, inserts containing AAP Organoids covered with medium #4 were put into THP1 stimulated well, resulting in a double communicating cell cultures as better shown in Figure 11. Cells were maintained in these co-culture conditions for 36 hours. At the end of the 36 hours inserts were removed by THP1 stimulated well. The base of each strainer, on which the Matrigel drop was polymerized, was cut with a sterile scalpel and put inside a 15 mL sterile tube. A total of 2 mL of Cell recovery solution was added to the tube in order to release the Organoids within the Matrigel drop following the procedure previously described.

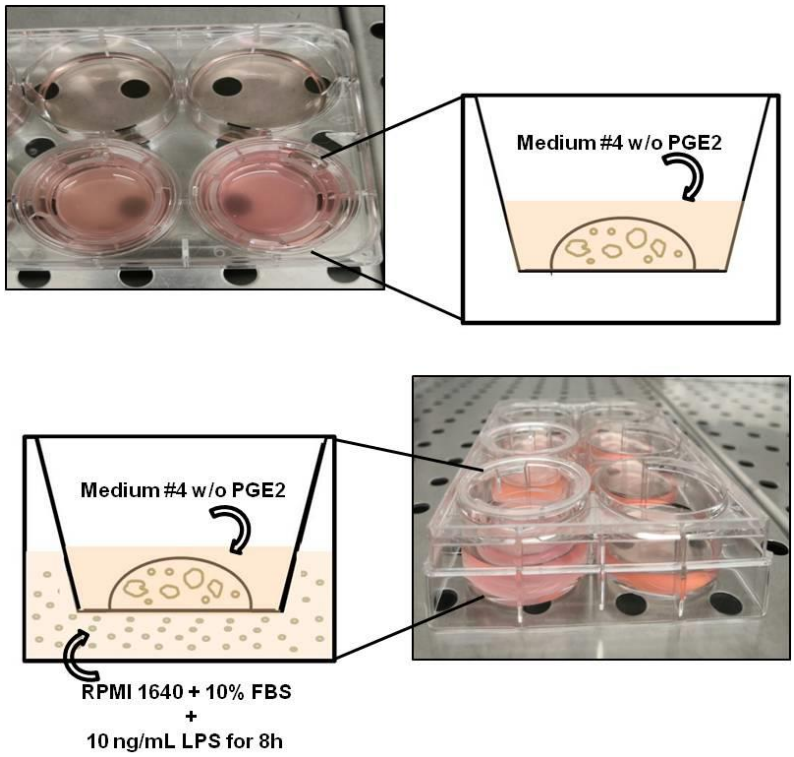

Figure 11: Schematic representation of the co-culture strategy used for AAP PDOs and THP1 cells that have been pre-stimulated for 8 hours with LPS. RPMI 1640 supplemented with 10% of FBS was used to maintain the THP1 stimulated cells for the following 36 hours.

5.7 Tissue samples and Organoids immunohistochemistry (IHC)

Patients enrolled in the pilot low-inflammatory dietary intervention study underwent endoscopy at both T0 and T2 times, at which adenoma and normal mucosa specimens were collected, formalin-fixed and paraffin-embedded (FFPE) for morphological and immunophenotypical characterization.
Five additional normal mucosa samples, obtained from *APC*-wt subjects with sporadic CRC who underwent surgery at INT, were used as control for comparison of the IHC results of *APC*-wt mucosa with those of AAP patients. Sectioning and staining were carried out following standard procedures. Briefly, slices of 3 μM were cut at the microtome, dried, pre-treated and stained using an automatic Agilent Dako Autostainer Link 48 with the following primary antibodies: anti-COX2 (Cayman 1:300) and anti-15-PGDH (Sigma Aldrich 1:500).

AAP-derived Organoids in exponential growth phase were released from Matrigel and fixed in 4% buffered formaldehyde for 30 minutes. After fixation Organoids were resuspended in Bio-Agar, processed and paraffin embedded. In order to perform the immunophenotypical characterization of FAP1-FAP4 Organoids IHC was performed using the following primary antibodies: anti-CK AE1/AE3 (Dako 1:100), anti-CK20 (Dako 1:500), anti-CK19 (Sigma 1:1000), anti-CDX2 (Dako 1:50), anti-Mib1 (Dako 1:400), anti-LGR5 (Origene 1:200), anti-COX2 (Cayman 1:300) and anti-15-PGDH (Sigma Aldrich 1:500). Images were captured using Aperio Leica ScanScope XT.

5.8 COX2/15PGDH IHC evaluation

To investigate whether the dietary intervention changed the local inflammatory state of the rectal mucosa of patients with AAP, 16 FFPE biopsies of the 34 patients enrolled in the pilot study were selected, focusing on those patients who had both Normal and Adenomatous mucosal specimens (details are showed in Table 3). Biopsies were collected at T0 and T2 of the dietary intervention, stained for COX-2 and histologically evaluated together with and expert pathologist. The percentage of COX-2 immunoreactive normal crypts was obtained relatively to the total number of normal crypts within the biopsy; the same approach was used to determine the COX-2 immunoreactivity of the adenomatous crypts compared to the total number of adenomatous crypts. COX-2 immunoreactive lamina propria stromal cells and adenoma infiltrating immune cells was assessed calculating the percentage of stained cells within the two regions relatively to the unstained ones, at both T0 and T2.

ID	T0 Biopsies	Normal Mucosa	Adenoma	T2 Biopsies	Normal Mucosa	Adenoma
FAP_2	1	A	A	1	A	NA
	2	A	A	2	A	A
FAP_6	1	A	A	1	A	A
	2	A	A	2	A	A
	NA	NA	NA	3	A	A
FAP_7	1	A	A	1	A	NA
	NA	NA	NA	2	A	NA
FAP_8	1	A	A	1	A	A
	2	A	A	2	A	A
FAP_9	1	A	A	1	A	NA
	2	A	A	2	A	NA
	NA	NA	NA	3	A	A
FAP_10	1	A	A	1	A	NA
	2	A	A	2	A	A
	3	A	A	NA	NA	NA
FAP_11	1	A	A	1	A	A
	2	A	A	2	NA	A
	NA	NA	NA	3	A	NA
FAP_12	1	A	A	1	A	A
	2	A	A	2	A	A
	3	A	A	NA	NA	NA
FAP_13	1	A	NA	1	A	NA
FAP_14	1	A	NA	1	A	NA
	2	A	NA	2	A	NA
FAP_15	1	A	A	1	A	NA
	2	A	A	2	A	NA
FAP_19	1	A	NA	1	A	NA
	2	A	NA	NA	NA	NA
FAP_21	1	NA	A	1	A	A
	NA	NA	NA	2	A	A
	NA	NA	NA	3	A	A
FAP_23	1	A	NA	1	A	NA
	NA	NA	NA	2	A	NA
FAP_24	1	NA	A	1	A	NA
	2	NA	A	2	A	NA
FAP_26	1	A	A	1	A	NA
	2	A	A	2	A	NA
	NA	NA	NA	3	A	NA
FAP_28	1	A	NA	1	A	NA
	2	A	A	2	A	A
FAP_29	1	A	NA	1	NA	A
	2	A	A	2	NA	A
FAP_30	1	A	A	1	A	A
	2	A	A	NA	NA	NA
	3	A	A	NA	NA	NA
FAP_31	1	A	A	1	A	A
	2	A	A	NA	NA	NA

Table 3: Biopsies collected from AAP patients enrolled in the pilot dietary intervention study at both T0 and T2, availability and unavailability of the sample are indicated by (A) and (NA) respectively.

Similarly, the same FFPE T0 and T2 biopsies obtained from the 16 patients were stained for 15-PGDH and evaluated following the same procedure used for COX-2.

5.9 DNA extraction

FFPE specimens from the four AAP patients from whom 3D-organoids had been generated, were referred by an exert pathologist at INT. Ten 5µM thick sections were cut for DNA extraction; DNA was purified with commercially available kits (QIAmp DNA FFPE Tissue Kit, QIAGEN,) following the manufacturer's instructions. At the same time, DNA was extracted from the corresponding 3D Organoids (at passage 8) with commercially available kits (DNeasy Blood & Tissue Kit, QIAGEN). DNA quantification was performed with the Invitrogen Qubit 4 Fluorometer (Thermo Fisher Scientific, US), following manufacturer's instructions.

5.10 Next Generation Sequencing

Targeted next-generation sequencing (T-NGS) was performed using the Ion AmpliSeq™ Cancer Hotspot Panel (Thermo Fisher Scientific, US); this panel is designed to amplify 207 amplicons covering about 2800 COSMIC mutations from 50 oncogenes and tumor suppressor genes frequently mutated in most of the human cancers (*ABL1, AKT1, ALK, APC, ATM, BRAF, CDH1, CDKN2A, CSF1R, CTNNB1, EGFR, ERBB2, ERBB4, EZH2, FBXW7, FGFR1, FGFR2, FGFR3, FLT3, GNA11, GNAS, GNAQ, HNF1A, HRAS, IDH1, IDH2, JAK2, JAK3, KDR/ VEGFR2, KIT, KRAS, MET, MLH1, MPL, NOTCH1, NPM1, NRAS, PDGFRA, PIK3CA, PTEN, PTPN11, RB1, RET, SMAD4, SMARCB1, SMO, SRC, STK11, TP53, VHL*).
Briefly, 10 ng of genomic DNA were used to amplify the regions of the 50 genes included in the "hotspot panel" using the Ion AmpliSeq Library Kit2.0 (Thermo Fisher Scientifics) according to the manufacturer's instructions (MAN0006735 rev 5.0). Emulsion PCR and chip loading were performed on the IonChef System (Thermo Fisher Scientifics), according to the manufacturer's instructions. Sequencing was carried out on the ION PGM System (Thermo Fisher Scientifics) using Ion 318 v2 Chip and ION PGM HI-Q View Chef Kit according to the manufacturer's instructions. Data from the PGM sequencing were initially processed using the Ion Torrent platform-specific software Torrent Suite Software™ (version 5.10.0) to generate sequence reads, align the reads on the reference genome Hg19, trim adapter sequences, filter and remove poor signal-profile reads. The variant calling from the sequencing data was generated using the Variant Caller plug-in. Some filters were applied to eliminate erroneous base calling: 1) average coverage depth >100; 2) each variant coverage >20; 3) variant

frequency on each sample >5; 4) quality value >30. Filtered variants were visually inspected using the Integrative Genomic Viewer (IGV) tool to assay their level of quality and to confirm the presence of each variant on both strands. The resulting variants were annotated using COSMIC database and dbSNP database. Variants with Minimum Allele Frequencing (MAF) value greater than 0.01 in 1000 genomes combined population were considered as SNPs and thus excluded.

5.11 AAP Organoids RNA extraction

To assess changes in gene expression of Organoids cultured under CD4+ pro-inflammatory condition and THP1 co-culture condition, total RNA was extracted from the four AAP Organoid cell cultures after respectively 36 hours of IL-6, IL-17a, IL-22 conditioned medium and THP1 co-culture condition. Organoids grown under standard conditions were used as blank control. AAP Organoids were released from Matrigel and washed as previously described. Total RNA extraction was performed using the Masterpure Total DNA-RNA purification Kit, following manufactures conditions. Briefly, 0.5 - 1 x 10^6 Organoid-disrupted cells were lysed using Tissue and Cell Lysing buffer additioned with 50 µg/µL of Proteinase K. After that, 150 µL of Protein Precipitation buffer was added to the lysate of each sample in order to remove ribosomal proteins. Endogenous DNA was removed through 1X DNase solution performed at 37°C for 30 minutes. Total RNA was quantified with the Invitrogen Qubit 4 Fluorometer (Thermo Fisher Scientific), following manufacturer's instructions, while RNA integrity was assessed via the 260/280 ratio. Total RNA was stored at -80°C until use.

5.12 Nanostring PanCancer Immune gene expression profiling

To investigate whether the *in vitro* pro-inflammatory culture conditions affect PDO gene expression, Nanostring PanCancer Immune Profile was performed. This Gene expression assay was developed by NanoString Technologies (Seattle, WA) and has several potential benefits relatively to microarray- and PCR-based technologies: the possibility to run several samples together with the small manual manipulation generate data faster than many PCR-based methods; the hybridization method directly interrogates target sequences, avoiding the need for bias prone amplification steps, even for low abundant transcripts; measurement is achieved using digital detection of uniquely bar-coded probes, providing absolute quantification. The RNA hybridization reaction consists of color-coded molecular bar-codes representing 770 immune profile genes, including 40 housekeeping genes (details regarding genes category and annotation are summarized in Supplementary Table 1 and 2). These genes

sum up 14 different immune cell types, common checkpoint inhibitors, CT antigens, and genes covering both the adaptive and innate immune response (Figure 11).
Specific mRNA targets are represented by 100-base region recognized by a 3′ biotinylated capture probe and a 5′ reporter probe tagged with a specific fluorescent barcode designed by NanoString. For this experiment, probes were hybridized to 250 ng of total RNA for 20 hours at 65 °C, leading to the creation of two sequence-specific probes for each target transcript. After hybridization sample were transferred to the nCounter preparation station which removed automatedly probes excess by immobilization of probe-transcript complexes on a streptavidin-coated cartridge.
Raw counts were collected using the nCounter Digital Analyzer by counting each single barcode.
Spiked-in external RNA positive and negative controls included in the specific codeset were used to determine the background hybridization.
All signals below mean background plus 2 standard deviations were considered below the limits of detection and set to mean background. A normalization factor was calculated from the spiked-in exogenous positive controls in each sample and applied to the raw counts from the nCounter output data.

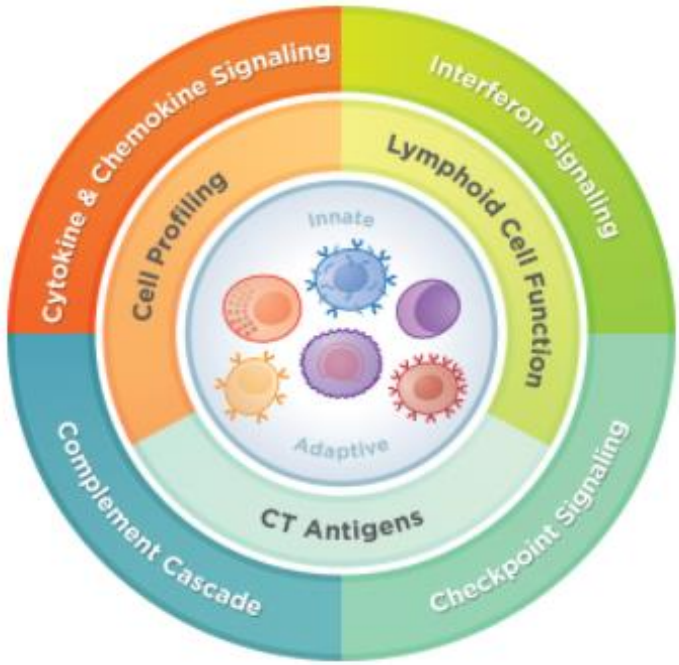

Figure 11: PanCancer Immune Profile is a multiplex gene expression analysis of 770 genes from 14 different immune cell types, common

checkpoint inhibitors, CT antigens and gene covering both the adaptive and innate immune response.
Image arranged from Nanostring website: https://www.nanostring.com

5.13 Nanostring miRNA profiling

The role of microRNAs in the regulation of gene expression is deeply documented in literature, also for inflammatory processes. For this reason, possible changes in miRNA espression of FAP1-FAP4 organoids were evaluated through the NanoString nCounter Human v3 miRNA Expression Assay (Seattle, WA). This panel contains tags for 800 of the 2588 mature miRNAs described so far, sequenced with high confidence and/or found clinically relevant in the cumulative sequencing analyzes of all mature human miRNAs inserted into the v21 version of miRBase. The assay provides a method for detecting miRNAs without the reverse transcription or amplification steps by using molecular barcodes called nCounter Reporter Probes. The assay can be run on total RNA isolated from any source. Sample preparation involves a multiplexed annealing of the specific tags to their target miRNAs, a ligation reaction, and an enzymatic purification to remove the unligated tags. Sequence specificity between each miRNA and its appropriate tag is ensured by stepwise controls of annealing and ligation temperatures (Figure 12). Control RNA included in the nCounter miRNA Sample Preparation Kit allows the user to monitor the ligation efficiency and specificity through each step of the reaction. After hybridization, excess probes are washed away using a two-step magnetic bead-based purification. Magnetic beads derivatized with short nucleic acid sequences that are complementary to the Capture Probe and the Reporter Probes are used sequentially. First, the hybridization mixture containing target/probe complexes binds to magnetic beads complementary to sequences on the Capture Probe. Wash steps are performed to remove excess Reporter Probes and non-target cellular transcripts. After washing, the Capture Probes and target/probe complexes are eluted off the beads and are hybridized to magnetic beads complementary to sequences on the Reporter Probe. An additional wash is performed to remove excess Capture Probes. Finally, the purified target/probe complexes are eluted off the beads and immobilized on the cartridge for data collection.

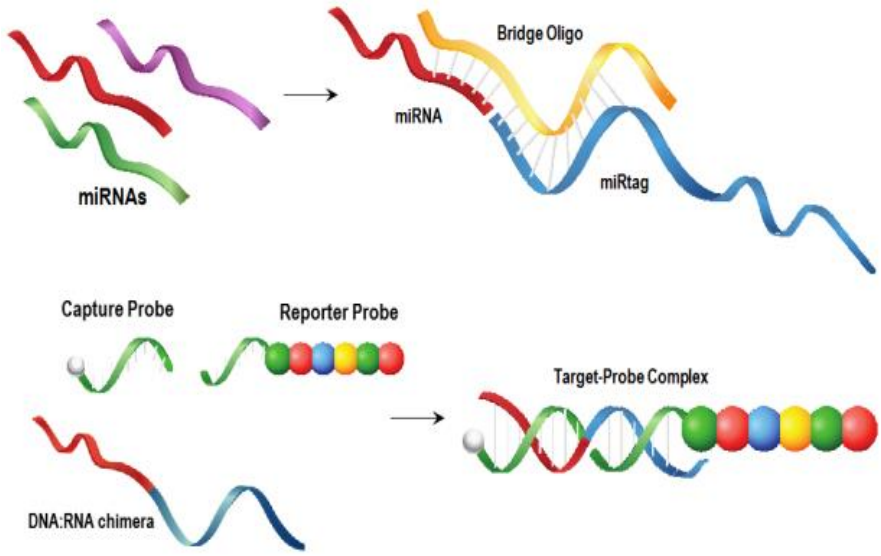

Figure 12: Example of construction of the Target-Probe Complex for miRNA detection on NanoString nCounter platform. The process is made by three steps: the first is the ligation step between sample miRNAs and the miRtag through an Oligo Bridge. Second step involves the interaction between the chimera obtained in the first step and Capture and Reporter probes. Image arranged from Nanostring website: https://www.nanostring.com

5.14 NanoString Immune Profile analysis and quality control

RCC raw data generated by the nCounter platform were processed using the nSolver 4.0 software released by NanoString Technologies (Seattle, WA). The current normalization procedure recommended by NanoString involves a set of simple aggregation and adjustment steps using control genes. In order to minimize the impact of outlier values, after the experiment creation on the nSolver software, the NanoStringNorm package for R software [116] was used to verify the hybridization and counting quality. The geometric mean was used to summarize the CodeCount (positive) and the SampleContent (housekeeping) controls. Moreover, a stringent background correction was applied (mean +2 standard deviation), to remove a large portion of false positives and therefore increase specificity at the expense of some sensitivity (Figure 13).

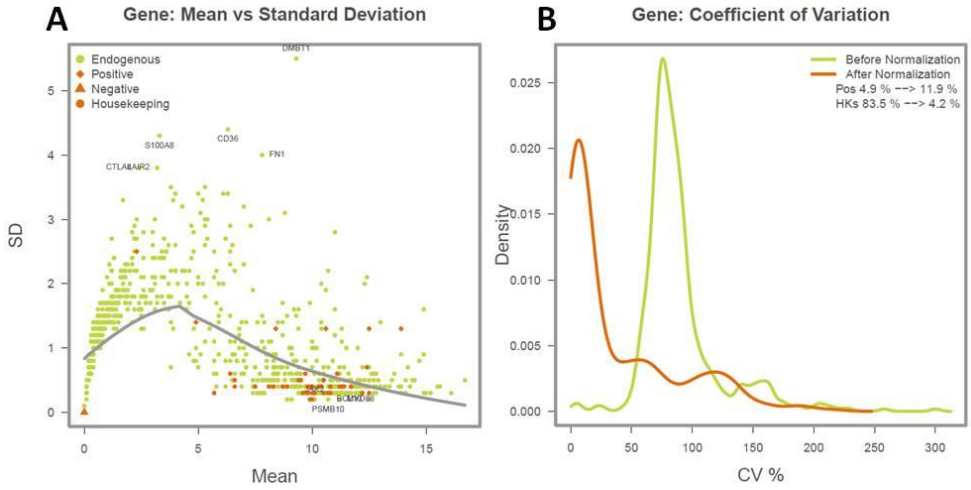

Figure 13: Panel A) Mean distribution and Standard Deviation of the gene counts composing the immune profile panel; Panel B) Coefficient of Variation of the gene counts before and after normalization.

The expression counts of the most recurrent housekeeping genes and quantile normalization was used to account for inter sample variations (Figure 14).

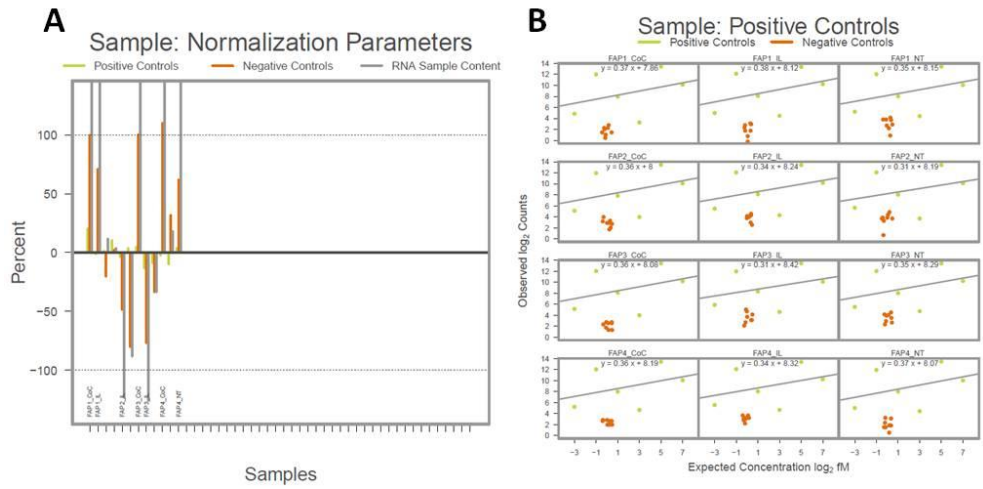

Figure 14: Panel A) Relative RNA content, calculated for each sample and based on the positive and negative control values; Panel B) distribution of the Positive and Negative controls for each sample.

Gene expression analysis was performed on normalized data using the Degust [117] software as described by Cheasley D. and collaborators [118] Empirical Analysis of Digital Gene Expression Data in R (EdgeR) tool was used to calculate differentially expressed genes, accordingly to what described by Chen Y. and collaborators [119].

5.15 NanoString human v3 miRNA analysis and quality control

Using an analysis pipeline based on recommendations by NanoString, raw data RCC files produced by the nCounter were initially processed using the NanoString nSolver 4.0 software (Seattle, WA). Before analysis, each sample was run through several QC checks, examining the quality of imaging, binding density, positive control linearity and positive control limit of detection. Considering that some samples displayed the ligation flag, a preliminary step not discussed by NanoString was applied before normalization in order to correct flagged samples. The miRNA counts were firstly normalized to account for technology-associated sources of variation using the geometric mean of the ligation control probe POS_A. This step accounts for lane-by lane variation of the nCounter platform (Figure 15).

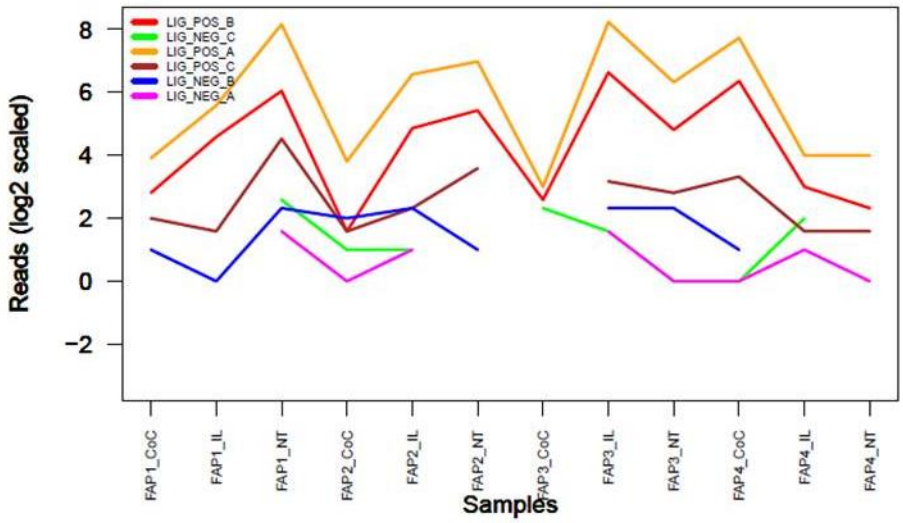

Figure 15: Logarithmic distribution of the Ligation Positive and Negative Controls for each sample of the panel.

The raw data were normalized using the *NanoStringNorm* function for the homonymous package in R software. Specifically, technical biases were limited by adjusting each sample on its relative value to all sample (cartridge correction on the geometric mean of the values); background correction was applied on the threshold of the mean +2 standard deviation of the negative control signals; and the normalized signal was generated on the geometric mean of the housekeeping transcripts.
Probes normalization was performed on a series of exogenous probes (Positive control probes POS_A, POS_B, POS_C) of known concentration, allowing observed variation to be attributed specifically to the assay (Figure 16). Normalization occurs by summarizing (geometric mean) the positive control counts and adjusting samples by a factor relative to other samples.

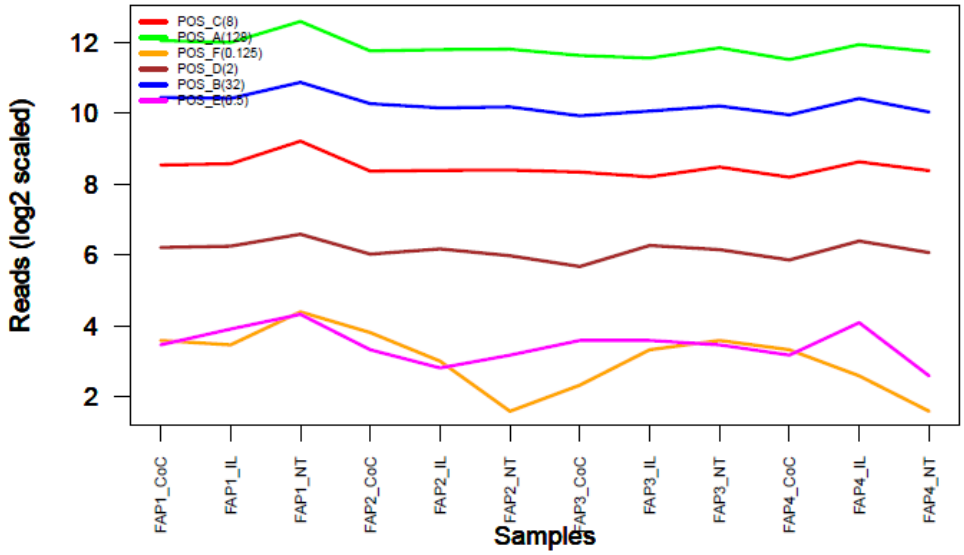

Figure 16: Logarithmic distribution of the Positive Controls for each sample of the panel.

After normalization, the data was imported into the R Language and Environment for Statistical Computing. The counts for a specific probe were considered background if they were not found to be significantly different than the negative controls ($P > 0.05$). *NanostringNorm* package for R was used on resulting miRNAs in order to compare the distribution of mean vs standard deviation, as previously described for Immune Profile mRNA (Figure 17 A). Finally, Coefficient of Variation of miRNAs before and after Normalization was calculated as shown in Figure 17 B.

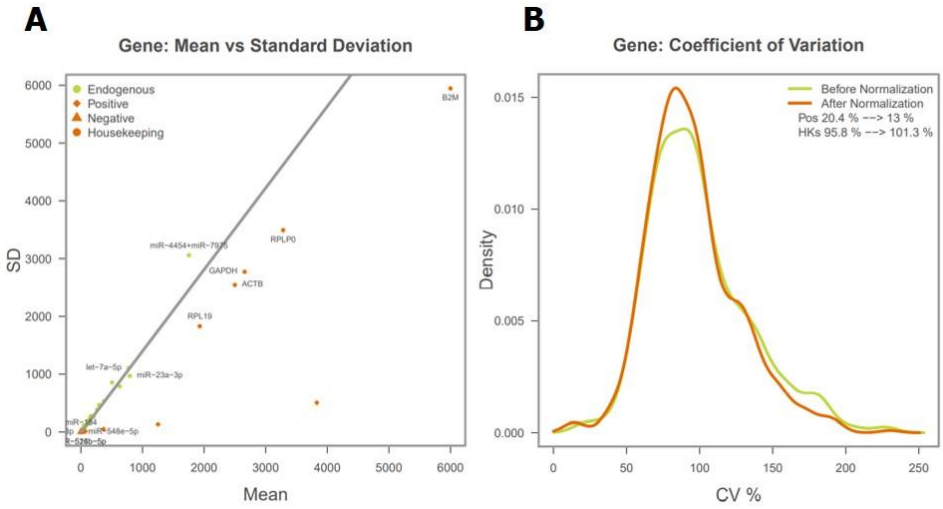

Figure 17: Panel A) Mean distribution and Standard Deviation of the miRNA counts composing the immune profile panel; Panel B) Coefficient of Variation of the miRNA counts before and after normalization.

6 RESULTS

6.1 Effects of the dietary intervention of the dietary intervention on inflammation in AAP subjects

6.1.1 Fecal and serum calprotectin evaluation

Among the 34 patients who participated to the study, 24 provided stool samples for all the three time points. For the stool calprotectin biomarker (on logarithmic scale), a significant change of quantity was observed during time (p-value: 0.012). Figure 17 depicts the stool and serum calprotectin distribution at baseline (T0), after three and six months (T1 and T2). Specifically, a borderline significant reduction was observed between T0 and T1 (p-value 0.072) and a significant increase between T1 and T2 (p-value 0.006) (Panel A). Interestingly, reduction in the stool calprotectin variability was observed at T1 (end of active dietary intervention), compared to that observed at both T0 and T2. A similar trend was observed for the 24 patients with all the three serum calprotectin measurements (p value 0.002), with a significant decrease between T0 and T1 (p-value 0.005), followed by an increase between T1 and T2 (p-value 0.003) (Panel B).

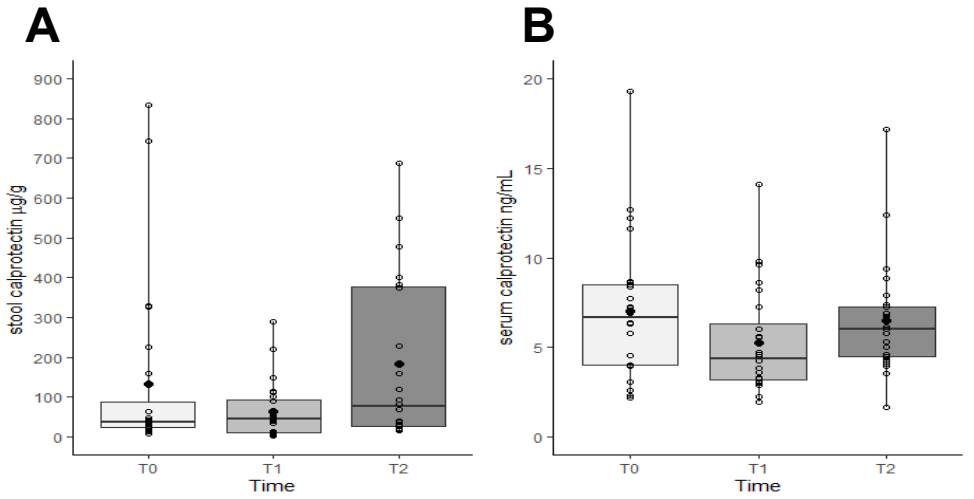

Figure 17: Distribution of stool and serum calprotectin at baseline (T0), after three (T1) and six months (T2). Boxplot reflecting the distribution of the stool calprotectin (A) and serum calprotectin (B) at the different time points. Each box indicates the 25th and 75th centiles of the distribution. The horizontal line inside the box indicates the median, and the whiskers indicate the

extreme measured values. Each individual value is represented by a circle, whereas the mean value is represented by a black circle.

6.1.2 Inflammation and dysmetabolism markers

Descriptive statistics of the considered markers at baseline (T0) at T1 and T2 are reported in Table 4, while Figure 18 depicts the corresponding boxplots. Statistically significant time trends were observed for insulin (Panel A) and IGF-1 (Panel B) factors (p-value: 0.046 and < 0.001, respectively). Interestingly, we observed no significant changes between T0 and T1 (dietary intervention effect) for both the markers, followed by a significant decrease between T1 and T2 time points. No statistically significant time trends were observed for the CRP, glycemia and glycated hemoglobin.

	n	min	25th centile	Median	75th centile	Max value	IQR*
Stool Calprotectin (µg/g)							
T0	24	9.00	23.00	37.50	112.60	835.00	89.00
T1	24	4.00	9.50	45.00	96.00	290.00	86.50
T2	24	15.00	25.00	76.00	378.50	689.00	353.50
Serum Calprotectin (µg/g)							
T0	24	2.21	4.00	6.65	8.54	19.30	4.54
T1	24	1.95	3.16	4.35	6.64	14.10	3.48
T2	24	1.65	4.41	6.02	7.30	17.20	2.89
Insulin (µU/mL)							
T0	27	1.90	5.20	8.20	12.90	19.20	7.70
T1	27	4.00	6.50	8.60	12.40	39.70	5.90
T2	27	1.40	5.00	6.60	10.70	27.10	5.70
IGF-1 (ng/mL)							
T0	27	84.80	135.00	176.90	249.00	431.50	114.00
T1	27	97.20	129.80	162.50	244.10	351.60	114.30
T2	27	52.40	88.70	123.10	164.90	259.10	76.20

*IQR: 75th centile - 25th centile

Table 4: Descriptive statistics of Stool and Serum Calprotectin, Insulin and IGF-1 measurements.

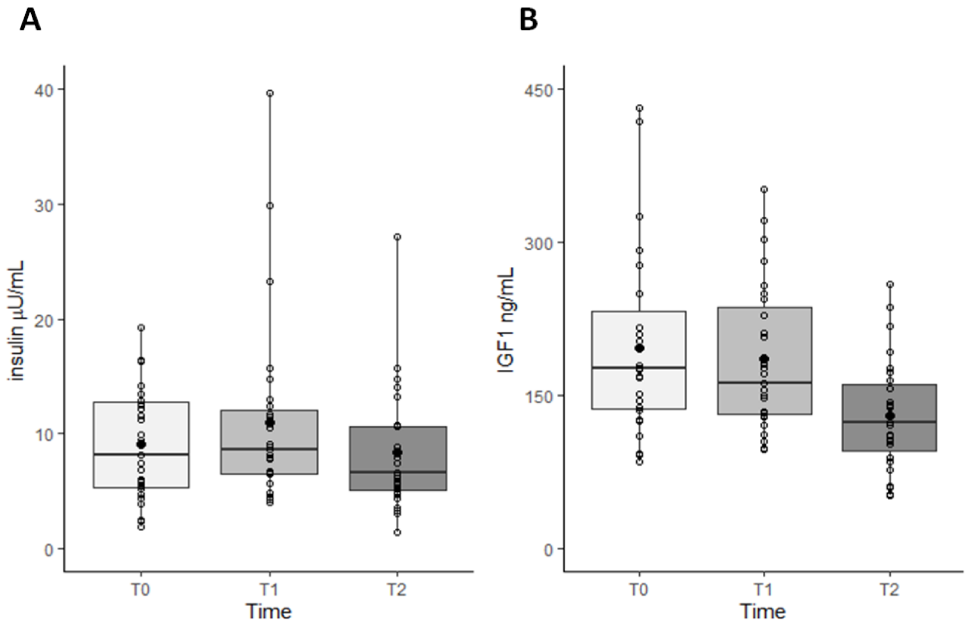

Figure 18: Distribution of insulin and IGF-1 at baseline (T0), after three (T1) and six months (T2).
Boxplot reflecting the distribution of insulin (A) and IGF-1 (B) at the different time points. Each box indicates the 25th and 75th centiles of the distribution. The horizontal line inside the box indicates the median, and the whiskers indicate the extreme measured values. Each individual value is represented by a circle, whereas the mean value is represented by a black circle.

6.1.3 COX-2 IHC expression

FFPE colorectal biopsies of 16 of the 34 patients enrolled in the pilot study, collected at T0 and T2 of the dietary intervention, were stained for COX-2 and histologically evaluated under the supervision of an expert pathologist. The percentage of immunoreactive normal crypts, lamina propria stromal cells, adenomatous crypts and adenoma infiltrating immune cells was assessed (Figure 19). As a control, the expression of COX-2 was also analysed in five FFPE normal colon mucosa samples of subjects not affected by AAP: indeed, increased COX-2 expression has been found in approximately 50% of adenomas but not in the normal mucosa of healthy individuals [120]. Normal colonic mucosa of the control samples presented more intensive immunoreactivity in glandular cells facing the intestinal lumen, while enterocytes in the bottom of the crypts showed less intensive positivity. This was likely due to poorer stimuli originating from antigens present on the surface of colon lumen (e.g. food and bacteria antigens)

(Figure 19 A). On the contrary, immunoreactive cells of AAP subjects enrolled in the dietary study collected at T0 were visible all along the crypts facing the colon lumen, but also on those turned towards the colon submucosa. This finding supports the diffuse inflammation status of the colonic mucosa in polyposis patients. Also, T2 evaluation showed the same COX-2 immunoreactive pattern of T0, although some patients (5/16) presented less COX-2 immunoreactivity (Figure 19 Panel A-1).

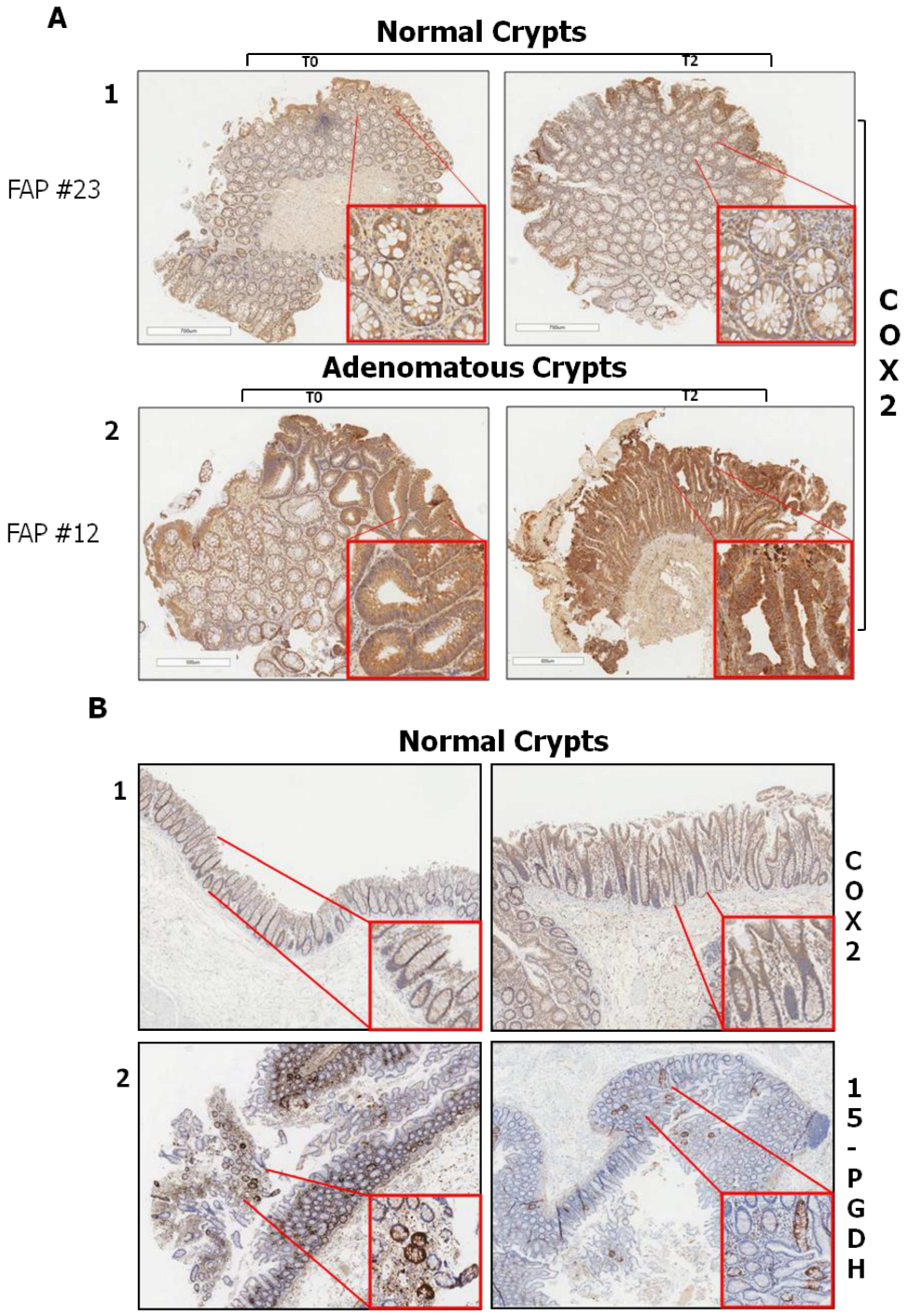
A
Normal Crypts
T0
T2
1
FAP #23
Adenomatous Crypts
T0
T2
2
FAP #12
COX2
B
Normal Crypts
1
COX2
2
15-PGDH

Figure 19: Panel A-1: COX-2 IHC performed on Normal AAP biopsies collected before the dietary intervention (T0) and after six-months of diet (T2); Panel A- 2: COX-2 IHC performed on Adenoma AAP Biopsies at both T0 and T2. Panel B-1: COX-2 IHC performed on Normal Colon Mucosa collected from surgery for sporadic colon cancer; Panel B-2: 15-PGDH IHC performed on Normal Colon Mucosa collected from surgery for sporadic colon cancer.

No significant differences in COX-2 expression were observed for any of the cell compartments analysed, in both normal tissue and adenomas (Figure 19 panel A-1, A-2). Given the role of COX-2 in the regulation of inflammation of the colonic mucosa and the numerous mechanisms that lead to its activation, the dietary intervention was not sufficient to modulate the expression of COX-2 at T2.

6.1.4 15-PGDH IHC expression

FFPE biopsies obtained from 16 patients, collected at T0 and T2, were stained and evaluated following the same procedure used for COX-2. Also, five FFPE normal colon mucosa samples of subjects not affected by AAP were analysed. At T0, AAP biopsies showed almost null levels of 15-PGDH in most healthy crypts and adenomas, except for four samples from the adenoma group, in which 15-PGDH was expressed also by the two infiltrates. This is in agreement with the high levels of COX-2 and faecal calprotectin previously described, highlighting presence of local inflammation. After the dietary intervention (T2), an increase in the number of 15-PGDH positive normal crypts in most of the cases was observed (WSR: 0.02) (Figure 20 A, Figure 20 B-1). A similar trend was also present in the adenomatous crypts, although the number of 15-PGDH positive crypts was lower and varied among patients (Figure 20 B-2). In the normal colonic mucosa control samples, 15-PGDH immunoreactive normal crypts and infiltrating the lamina propria immune cells were visible all along the mucosa (Figure 19 B-2). The simultaneous presence of COX-2 and 15-PGDH in these control samples confirmed that COX-2/15-PGDH pathway is not deregulated. No statistically significant results were observed for the remaining cell compartments analyzed.

A

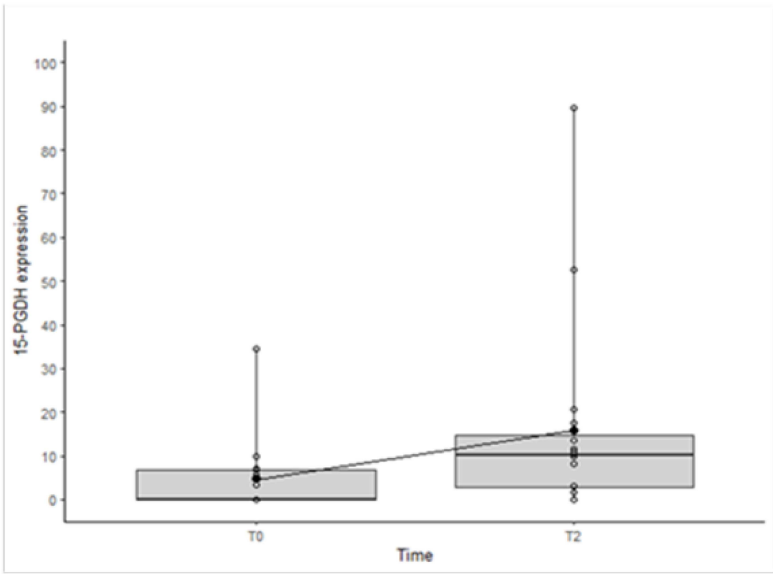
15-PGDH expression
100
90
80
70
60
50
40
30
20
10
0
T0
T2
Time

B

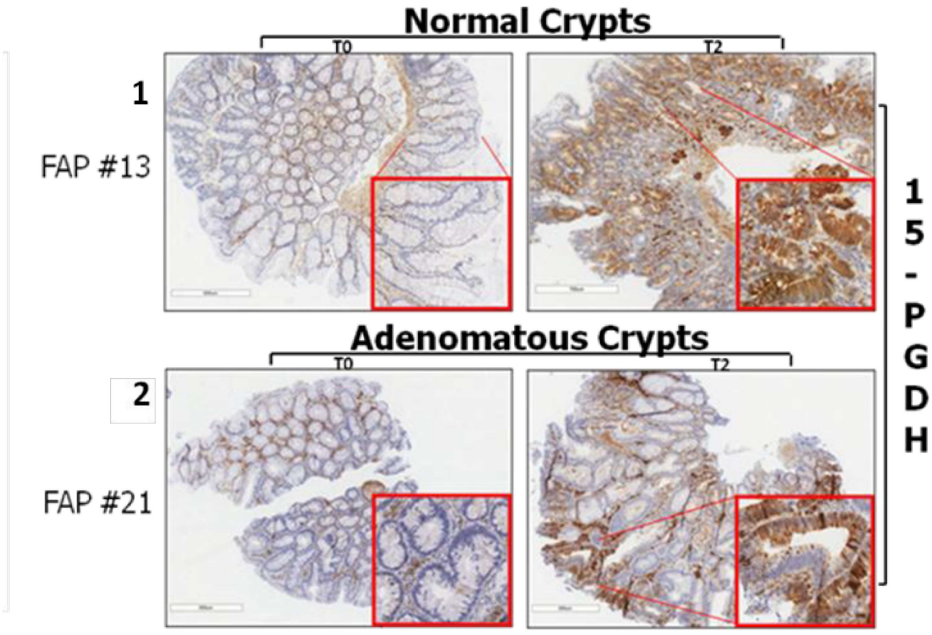
Normal Crypts
T0
T2
1
FAP #13
Adenomatous Crypts
T0
T2
2
FAP #21
15-PGDH

Figure 20: 15-PGDH expression in the Normal and Adenomatous Crypts. Boxplot reflecting the
distribution of 15-PGDH expression at baseline (T0) and six months (T2) (Panel A). Each box indicates the 25th and 75th centiles of the distribution. The horizontal line inside the box indicates the median, and the whiskers indicate the extreme measured values. Each individual value is represented by a dot. Examples of 15-PGDH IHC performed on Normal AAP biopsies at both T0 and T2 (Panel B-1) and of 15-PGDH IHC performed on Adenoma AAP Biopsies at both T0 and T2 (Panel B-2).

6.2 DEVELOMENT OF 3D MODELS OF AAP

6.2.1 FAP PDOs generation

Organoids were generated pooling two to four adenomas (depending on their size) obtained from the colon removed by colectomy from four individuals carrying germline mutations in *APC* gene. Visual inspection of the samples at the microscope showed that cells growing in Matrigel acquire shapes that mimic the complexity of the colon niches. Each culture presented specific morphologic peculiarities (Figure 21). Indeed, heterogeneity of the 3D structures is well explained in literature [121]. In particular, FAP1 and FAP2 Organoids, which harbor different *APC* germline mutations, reproduced the morphologic and phenotypic features described in literature for Organoids carrying *APC* somatic mutations. They showed some big spheroid structures closely related to well-differentiated cell aggregates who retraced a high complex epithelial-like crest. FAP3 PDOs, which harbor the same *APC* germline mutation of FAP2, showed more complex and solid cell aggregates characterized by invaginations and cell protrusions and by a greater ability to grow in adhesion. Unlike FAP1 and FAP2 PDOs that had a massive component of big spheroid structures, FAP3 PDOs displayed small spheroid structures flanked by well-differentiated cell aggregates. The fact that FAP2 and FAP3 PDOs carried the same mutation in *APC* gene, excludes the possible link between germline mutations in this gene and the observed phenotypes. FAP4 Organoids presented peculiar morphologic characteristics and were composed by both spheroid and well-differentiated structures in the same percentage (Figure 21).
Splitting rate after the first week of culture was the same for the four PDOs (1:3 every 4 days). However, FAP4 Organoids were bigger than the other three PDOs.

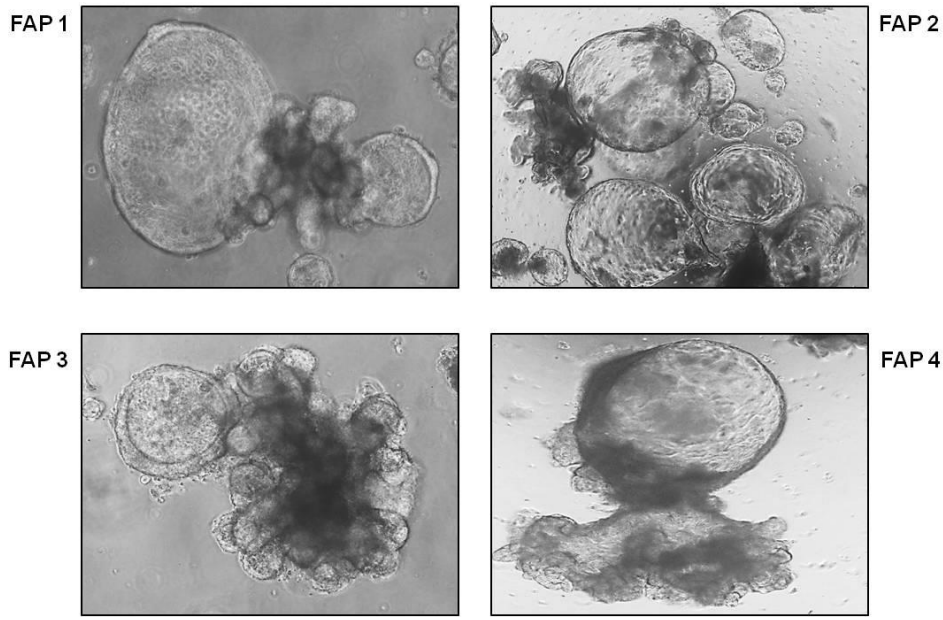

Figure 21: Microscopic visualization of FAP1-4 PDOs at 4X magnification. Organoids were seeded in Matrigel and maintained in medium 4 until the passage procedure was performed.

6.2.2 Characterization of the Organoids

In order to confirm that AAP PDOs maintained the characteristics of their tissue of origin, IHC staining was performed on FFPE Organoids sections by using the following markers of colonic epithelium: Cytokeratins (CK) AE1/AE3 that identify the glandular/epithelial differentiation of cells; CK 19 and 20 that are specific for the large intestinal tract; Caudal Type Homeobox 2 (CDX2), which is specific for the intestinal tract cells, located down from the diaphragm area. Each Organoid expressed CK AE1-AE3, -19, -20 and CDX2. According to the observed rapid growth, all PDOs had a very high Ki67 staining (Mib1) (Figure 22). FAP1 and FAP4 PDOs exhibited glandular structures lined by pseudo-stratified columnar cells, frequently observed on colonic epithelium, with central fibrinoid core and dirty necrosis along with roundish solid aggregates of nonaligned epithelial cells. These features were partially present also in FAP2 Organoids, in which glandular structures showed a more complex pattern of necrosis frame. In FAP3 PDO cells showed high positivity to all CKs and to the other markers.
Staining for LGR5, which is a strongly recognized colorectal staminal cell marker, showed different patterns among the four PDO cultures, in particular FAP1 and FAP4 PDOs displayed diffuse immunoreactivity in most

of the cells constituting the Organoids. Conversely, FAP2 and FAP3 PDOs showed less widespread LGR5 immunoreactivity, which describes a minor stem cell component within FAP2 and FAP3 PDOs. Figure 22 shows the IHC characterization of the four established Organoids.

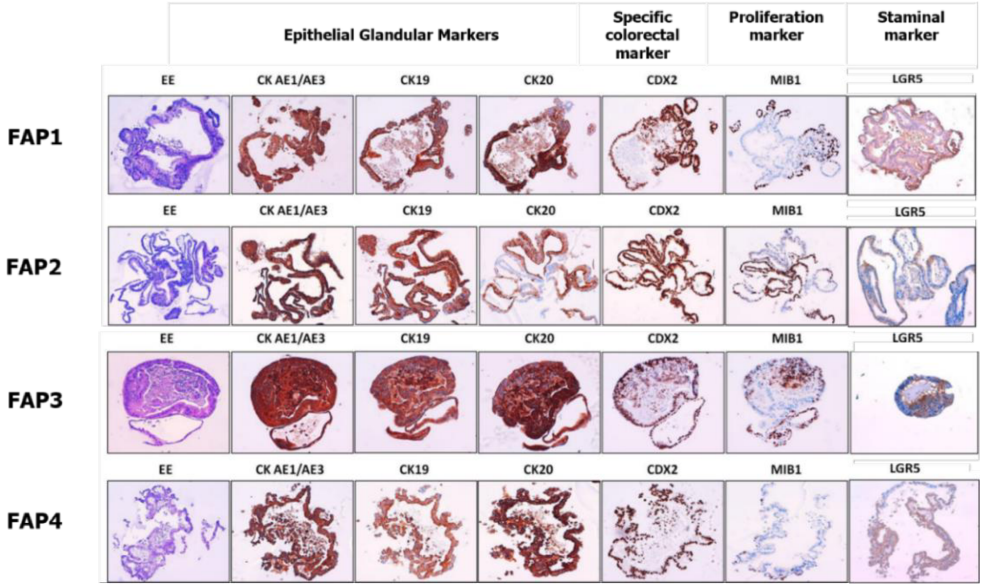

Figure 22: FAP1-4 PDOs IHC characterization. PDOs were characterized using epithelial glandular markers (from left to middle part of the panel), specific colorectal (CDX2), proliferation (mib-1) and staminal (LGR5) markers (from middle to right part of the panel).

6.2.3 Molecular characterization of Organoids

To verify if the FAP PDOs maintained the same molecular features of their tissue of origin, NGS analysis was performed on DNA extracted from both the organoids and their corresponding tissue sample, and the mutational profiles of matched pairs were compared. The NGS panel used for the analysis contained 48 different genes most frequently mutated in CRC. Comparison between DNA from Organoids and tissue of patients showed an overlapping >90%. Concordance was observed for all the mutations, with few exceptions that are showed in Table 5 and in Supplementary Table 3 and 4. In particular, FAP1 Organoids displayed a missense variant (c.4285C>T), with a Variant Allele Frequency of 8% of the *APC* gene in addition to the germline mutation. FAP2 and FAP3 PDOs had full

concordance with their tissues of origin. FAP4 PDOs gained a synonymous variant of *ATM* (c.3909C>A) and lose a synonymous variant of *PIK3CA* (c.1263A>G) respect to their tissue of origin. In addition, we found an *APC* stop-codon mutation (c.4630G>T) with a Variant Allelic Frequency of 7% in FAP4 PDO cells (Table 5).

Genomic Alteration of AAP Patients						
Sample ID	Gene Mutated	Germinal alteration	Protein alteration	Gene Mutated	Organoid Genomic alterations	Protein alteration
FAP 1	*APC*	c.2369_2372 DEL GACA	p.Arg790ThrFS*2p	*APC*	c.2369_2372 DEL GACA	p.Arg790ThrFS*2p
					c.4285C>T	p.Gln1429Ter
FAP 2	*APC*	c.3927_3931 DEL AAAGA	p.Glu1309ASPFS*	*APC*	c.3927_3931 DEL AAAGA	p.Glu1309ASPFS*
FAP 3	*APC*	c.3927_3931 DEL AAAGA	p.Glu1309ASPFS*	*APC*	c.3927_3931 DEL AAAGA	p.Glu1309ASPFS*
FAP 4	*APC*	c.3919_3937 DUP GAAATAAAAGAAAAGATTG	p.Thr1313ASNFS*Ter8	*APC*	c.3919_3937 DUP GAAATAAAAGAAAAGATTG	p.Thr1313ASNFS*Ter8
					c.4630G>T	p.Glu1544Ter

Table 5: NGS molecular characterization of *APC* gene in FAP1-4 PDOs compared to the germline AAP mutations carried by adenomas collected from patients.

6.3 STUDY OF INFLAMMATION IN AAP-PDO

6.3.1 COX-2 15-PGDH expression in 3D Organoids

COX-2 and 15-PGDH immunoreactivity we also evaluated in the four AAP PDOs. High levels of COX-2 were found in FAP1, FAP2 and FAP4 PDOs but not FAP3.
15-PGDH resulted deregulated in FAP1 and FAP2 PDOs but not in FAP3 and FAP4. To verify if COX-2/15-PGDH axis can be activated in all PDOs, 10nM/mL of synthetic PGE2 was added to the culture medium and up-regulation of 15-PGDH was observed in all PDOs (Figure 23).

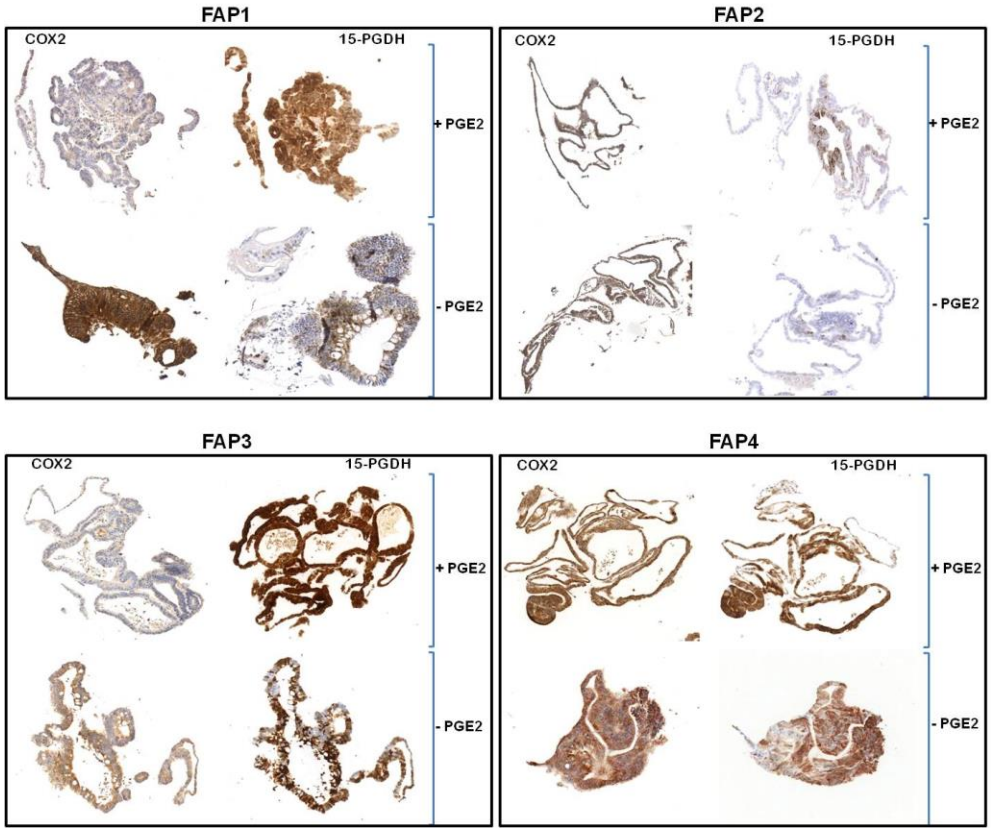

Figure 23: COX-2 (left) and 15-PGDH (right) immunoreactivity of the FAP1-4 PDOs grown with or without PGE2. The presence of PGE2 in the medium is associated with an increased immunoreactivity of 15-PGDH, conversely the absence of PGE2 is related to an increased immunoreactivity of COX-2.

These results underline that the heterogeneous cell populations of the colorectal mucosa are fundamental for the regulation of inflammatory processes. PDOs consist of colonic epithelial cells, not enough to study such a complex process. Consequently, efforts have been directed towards the development of *in vitro* models including lymphoid and / or myeloid-derived factors that could sustain inflammatory processes present in the colonic mucosa.

6.3.2 Organoids Cell Cycle Analysis under lymphoid inflammatory conditions

As a first step, inflammatory factors produced by lymphoid cells that could influence the epithelial cells of the colonic mucosa, were identified from a literature survey and added to the culture medium [122]. PDOs were supplemented with IL-17a, IL-22 and IL-6 cytokines, typical of Th17 and Th22 lymphocytes, which are involved in maintaining normal tissue homeostasis. The medium was deprived from PGE2, to obtain uniform COX-2 expression.
In order to evaluate the possible changes that inflammatory cytokines can make on the PDOs, a cell cycle analysis was performed on Organoids grown in ILs conditioned medium and with the standard medium as control. FAP1, FAP2 and FAP3 PDOs had a similar behaviour under inflammatory conditions; the percentage of cells in G1 phase was steadily increased over time, while the percentage of cells in G2/M phase decreased after 36 hours. This result suggests that the exposure of FAP1, FAP2 and FAP3 to Th17 and Th22 cytokines slows cell growth by blocking cells in the G1 phase.
FAP4 PDOs showed a completely different trend: during growth with medium containing ILs no changes were observed in the percentage of cells in G1, which were similar to that of the control sample. On the contrary, the percentage of cells in G2/M phase increased significantly over time. This finding suggests that ILs positively affected FAP4 Organoid cell growth at both 24 and 36 hours.

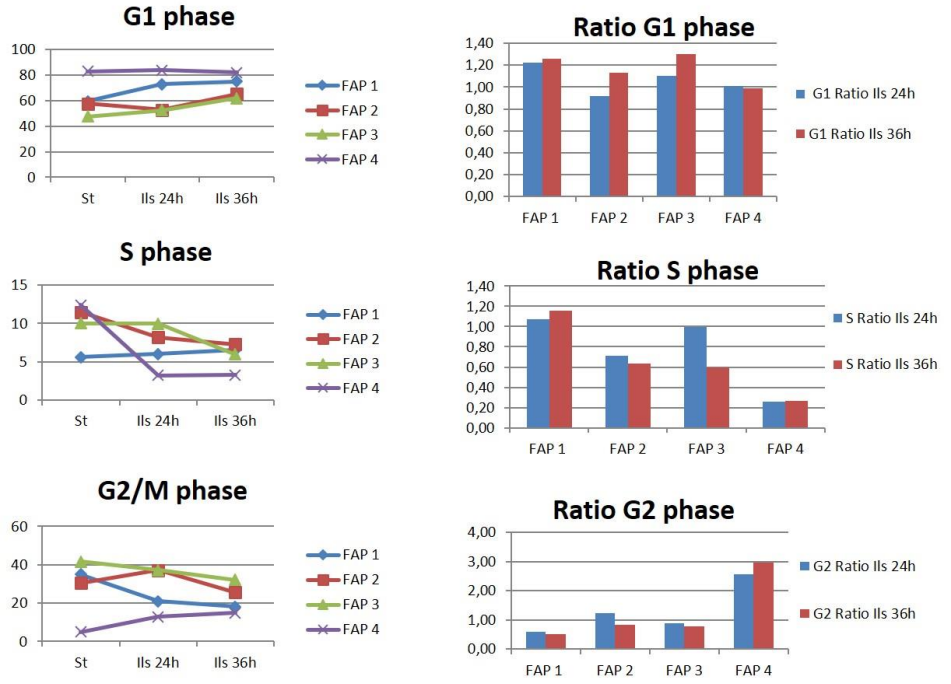

Figure 24: Cell Cycle Analysis of FAP1-4 PDOs after 24 and 36 hours of culture with the medium supplemented with 25ng/mL of Il-17, IL-22 and IL-6. Variation of G1, S and G2/M phases after 24 and 36 hours of maintenance is displayed on the left panels. On the right panels G1, S and G2/M Ratio regarding Standard vs ILs condition at both 24 and 36 hours of culture is described for each FAP PDOs.

6.3.3 Inflammatory cytokines produced by THP1 cells

Myeloid cells also play a fundamental role in maintaining the homeostasis of the colon mucosa, acting against pathogens and secreting pro-inflammatory cytokines. In this class of immune cells, macrophages are one of the most represented cell populations in the colorectal mucosa.
Evidences from literature, describe that the human acute monocytic leukemia cell line THP1 in presence of LPS is able to secrete pro-inflammatory cytokines typical of activated macrophages (M1); moreover, their stimulation over time can induce differentiation to macrophages.THP1 cells were stimulated with LPS and their secretome was assayed for presence of inflammatory cytokines expresses by the macrophages. After 8 hours of stimulation a large amount of IL-8 was secreted while small amounts of IL-6 and Chemokine 2 (CCL2), both pro-inflammatory cytokines, and also IL1β were produced. No production of Chemokine 22 (CCL22), Chemokine 3, Chemokine 4 and Chemokine 5 (CCL3-4-5) was observed.

Presence of IL-8, IL-6 CCL2 and small levels of IL-1β confirmed that stimulated THP1 can be used to induce an *in vitro* pro-inflammatory co-culture environment.

	THP1 cells		THP1 stimulated cells
Cytokine		**Cytokine**	
IL-8	39 pg/mL	**IL-8**	11800 pg/mL
IL-6	0 pg/mL	**IL-6**	3329 pg/mL
CCL2	8,4 pg/mL	**CCL2**	1800 pg/mL
IL-1β	1,7 pg/mL	**IL-1β**	350 pg/mL

Table 6: Comparison between cytokines secreted by THP1 cells in standard culture conditions and after LPS stimulation for 8 hours.

6.4 EFFECTS OF INFLAMMATORY CONDITIONS ON FAP-PDOs

6.4.1 Immune Gene Expression Profile

To investigate the effects of the different inflammatory culture conditions on PDOs, a gene expression profiling on RNA from the four PDOs, was performed using the NanoString PanCancer Immune Expression panel. PDOs grown under normal conditions, with Th17 and Th22 cytokines and co-cultured with LPS stimulated THP1 cells were analysed.

a) Th17 and Th22 inflammatory conditions: Unsupervised clustering performed on the raw data of the genes composing the panel showed almost complete separation of FAP PDOs grown under standard conditions from those grown for 36 hours with ILs conditioned medium, except for FAP4 PDOs cultured in standard conditions (figure 26). This finding confirms what observed with the morphological and cell cycle analyses.

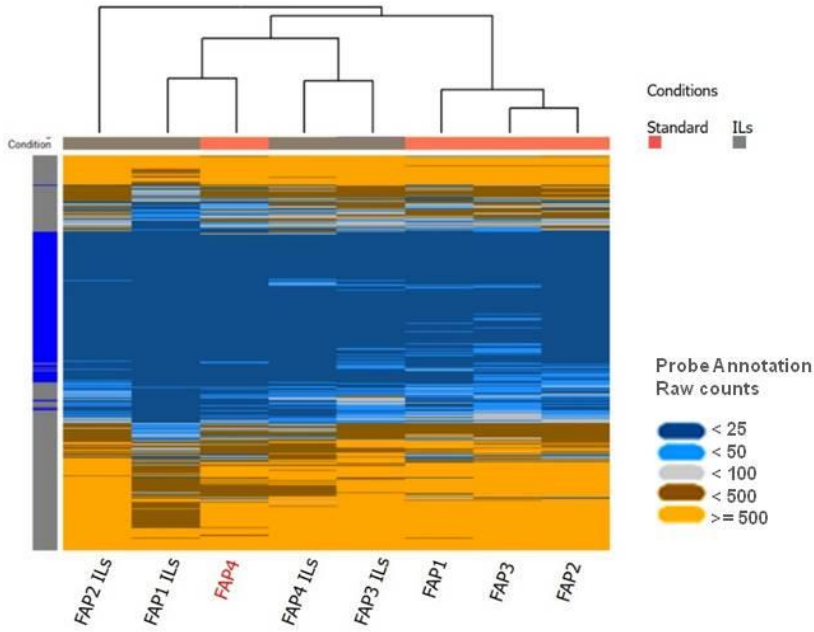

Figure 26: Unsupervised Hierarchical Clustering of NanoString Immune Profile raw data.

Unsupervised clustering on normalized data considering only the genes related to the Cell Cycle subgroup, showed that FAP4 grown in standard medium clustered closer to FAP PDOs cultured under ILs condition, while IL stimulated FAP3 PDOs were more similar to untreated PDOs (Figure 27 A).

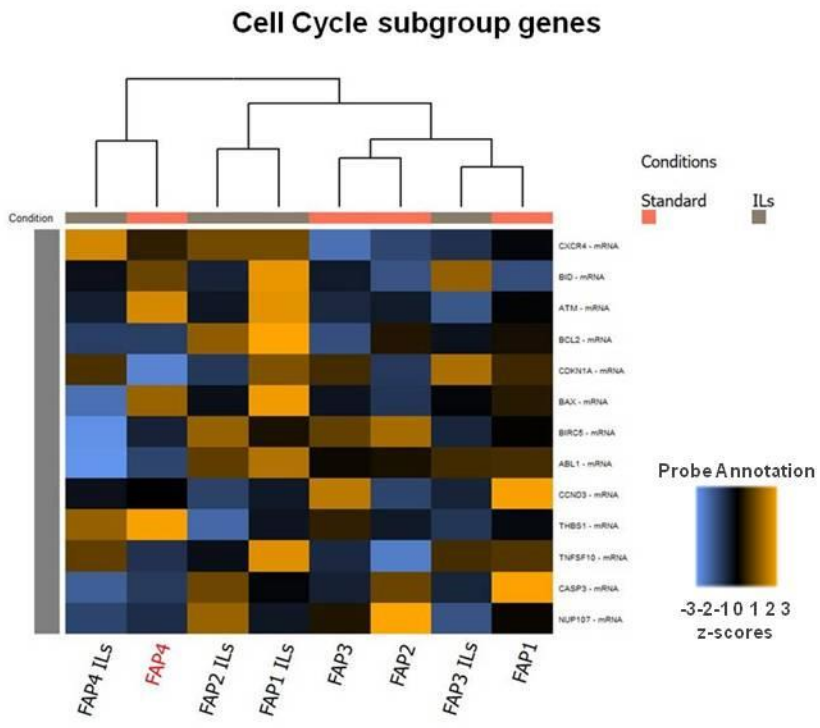

Figure 27: Panel A depicts hierarchical clustering of the cell cycle genes subgroup contained in the PanCancer Immune Profile panel.

No significant results were observed for the other gene categories included in the panel, such as those in the Cell Functions, Adhesion, Senescence or TNF subgroups.

b) THP1 Co-Culture Condition: unsupervised clustering analysis performed on raw data showed almost complete segregation of the FAP PDOs grown under standard conditions from those co-cultured with THP1 cells for 36 hours, except for FAP4 and co-cultured FAP2 (Figure 28). This result was not supported by any difference observed during the co-culture procedure, such as for example morphological or phenotypical features.

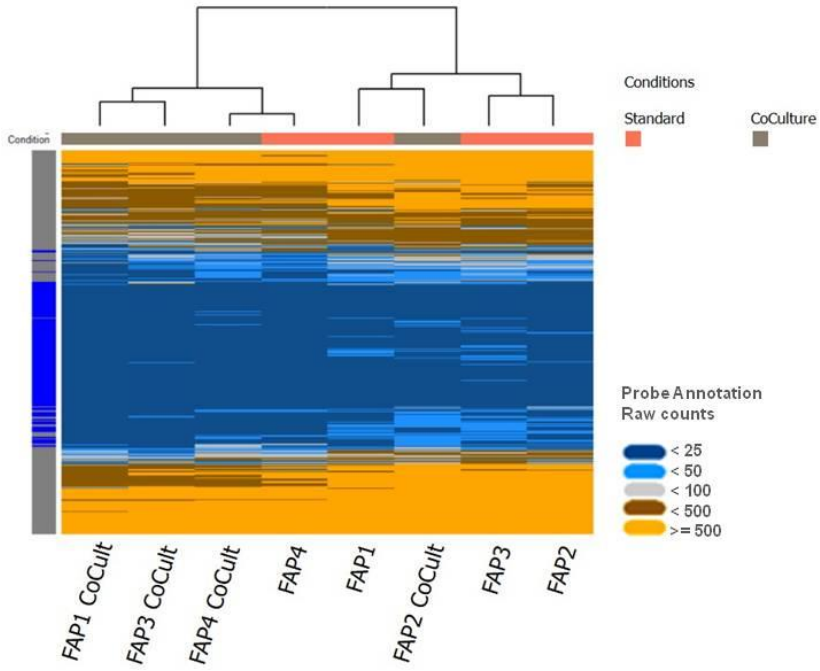

Figure 28: Unsupervised Hierarchical clustering of AAP PDOs grown under THP1 co-culture condition.

Advanced Analysis module of NanoString nSolver 4.0 did not show any significance for all the subgroups of genes included in the panel.

6.4.2 Data analysis of cancer Immune Profile through the Degust tool

After Quality Control (QC) assessment in which the relative logarithmic expression (RLE) was standardized in all samples (Figure 29), analyses were performed on the Degust platform using the edge package for R (edgeR). FAP PDOs grown under standard conditions (set as baseline) were compared with IL stimulated PDOs, or with PDOs co-cultured with THP1 stimulated cells.

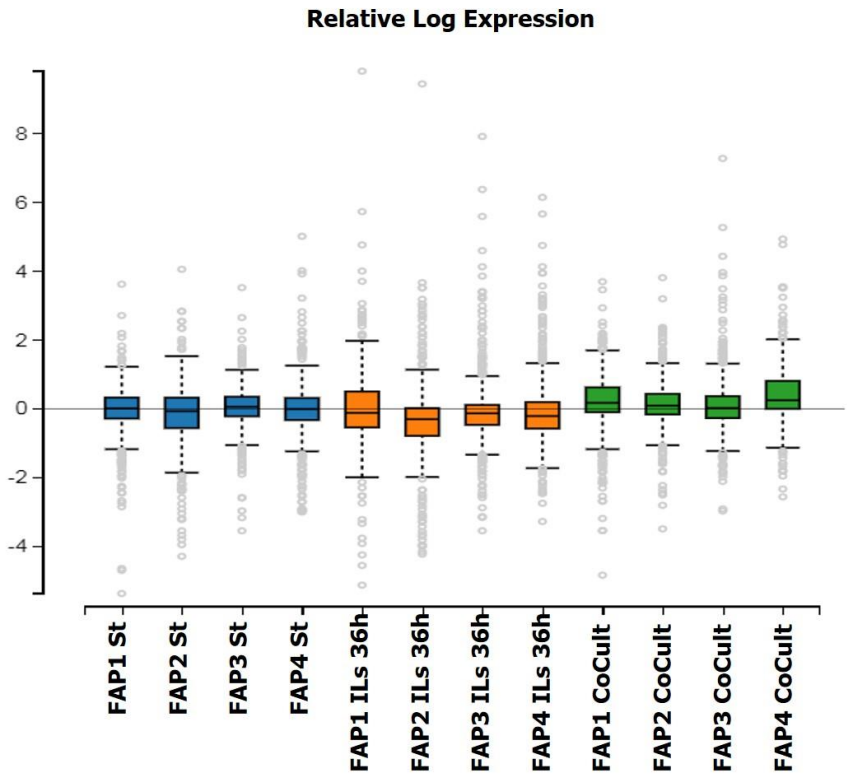

Figure 29: Relative Logarithmic expression plot of NanoString PanCancer Immune profile genes for each AAP PDOs cultured under Standard, inflammatory ILs and THP1 co-culture condition.

6.4.3 Th17 and Th22 inflammatory conditions increases *DMBT1* expression

Among the 667 genes of the panel analysed, 28 were significantly increased after comparison with the baseline (Log_2 Fold Change (log_2FC) > 2 and False Discovery Rate (FDR) cut off 0.05) (details are shown in Table 7). Within these 28 genes, the tumor suppressor gene *DMBT1*, was the most differentially expressed (Figure 30 A-1). Changes in *DMBT1* showed more than 3-fold increase in FAP3, 9-fold in FAP2, and 7.5-fold in FAP1 PDOs under ILs condition (Figure 30 A-2). Interestingly, FAP4 PDO levels of *DMBT1* were like those observed in all PDOs cultured in Standard conditions (Figure 30 B).

Genes

Showing 0..12 of 28 — Download CSV — Search:

Probe Name	Accession #	Class Name	FDR	P valu...	FAP NT rep	FAP IL rep
DMBT1	NM_007329.2	Endogenous	1.65e-15	2.44e-18	0.00	9.34
CFB	NM_001710.5	Endogenous	1.38e-13	4.07e-16	0.00	4.15
NOS2A	NM_153292.1	Endogenous	1.09e-12	4.83e-15	0.00	5.21
CCL20	NM_004591.1	Endogenous	8.84e-11	5.22e-13	0.00	4.40
SAA1	NM_199161.1	Endogenous	3.03e-9	2.24e-11	0.00	5.49
SOCS1	NM_003745.1	Endogenous	3.89e-9	3.45e-11	0.00	4.21
CFI	NM_000204.3	Endogenous	6.84e-8	7.07e-10	0.00	4.27
C4BPA	NM_000715.3	Endogenous	1.14e-7	1.35e-9	0.00	3.88
HLA-DRA	NM_019111.3	Endogenous	6.80e-7	9.04e-9	0.00	4.55
CXCL1	NM_001511.1	Endogenous	6.86e-7	1.01e-8	0.00	3.03
LCN2	NM_005564.3	Endogenous	1.33e-6	2.16e-8	0.00	3.15
CXCL2	NM_002089.3	Endogenous	2.65e-6	4.69e-8	0.00	2.99
CASP1	NM_001223.3	Endogenous	3.98e-6	7.64e-8	0.00	2.43
BLK	NM_001715.2	Endogenous	1.10e-5	2.28e-7	0.00	2.82
HLA-DPA1	NM_033554.2	Endogenous	1.19e-5	2.64e-7	0.00	3.61
C2	NM_000063.3	Endogenous	5.70e-5	1.35e-6	0.00	3.26
IL19	NM_013371.3	Endogenous	8.40e-5	2.11e-6	0.00	3.70
CXCL3	NM_002090.2	Endogenous	6.96e-4	1.95e-5	0.00	2.17
MUC1	NM_001018017.1	Endogenous	7.45e-4	2.20e-5	0.00	2.90
CD74	NM_001025159.1	Endogenous	2.11e-3	6.54e-5	0.00	2.03
HLA-DMB	NM_002118.3	Endogenous	2.97e-3	9.65e-5	0.00	3.11
S100A7	NM_002963.2	Endogenous	3.08e-3	1.05e-4	0.00	4.38
IFITM1	NM_003641.3	Endogenous	6.16e-3	2.37e-4	0.00	2.27
SEMG1	NM_003007.2	Endogenous	9.15e-3	3.65e-4	0.00	2.46
HLA-DPB1	NM_002121.4	Endogenous	0.01	4.60e-4	0.00	2.30
C3	NM_000064.2	Endogenous	0.02	1.17e-3	0.00	3.07
CXCR2	NM_001557.2	Endogenous	0.03	1.42e-3	0.00	2.39
HLA-DRB4	NM_021983.4	Endogenous	0.04	1.91e-3	0.00	2.52

Table 7: Differentially expressed gene list of ILs vs Standard culture condition. Only values with Log_2 FC >2 and FDR cut off 0.05 were considered.

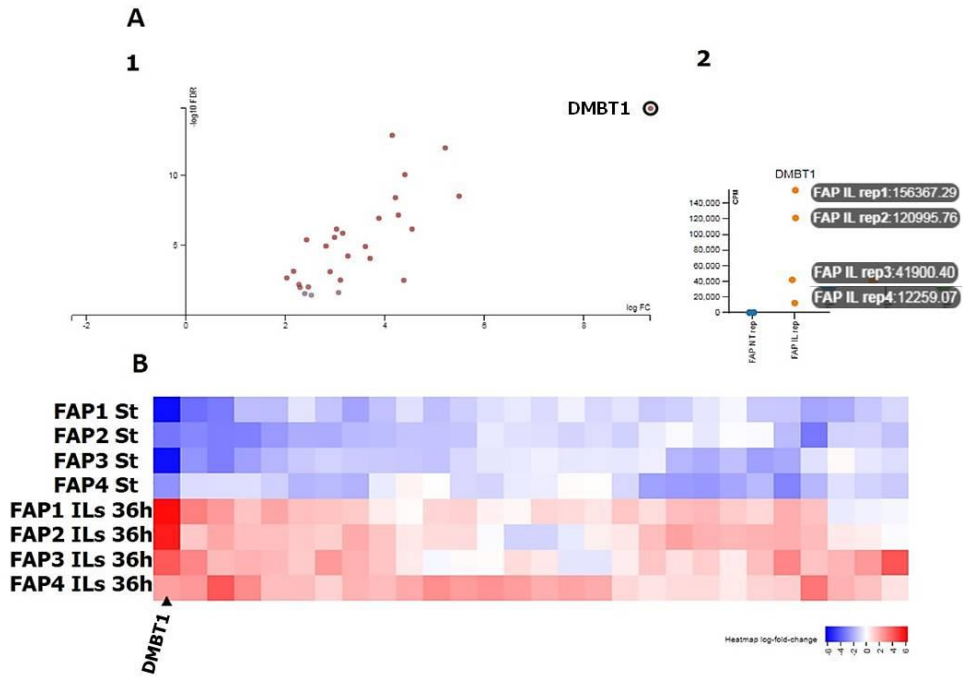

Figure 30: Panel A-1 depicts volcano plot of AAP PDOs differentially expressed genes with Log_2 FC >2 and FDR cut off 0.05. *DMBT1* dot is highlighted by a black circle. Panel A-2 depicts *DMBT1* counts for each FAP PDOs in both Standard and ILs condition. All FAP1-4 PDOs cultured under Standard condition had 0 counts for *DMBT1*, conversely FAP1-4 cultured for 36 hours with ILs displayed different counts for *DMBT1* gene. Panel B shows heatmap of differentially expressed genes for each AAP PDO.

6.4.4 Th17 and Th22 inflammatory conditions increases Human Leukocyte Antigen (*HLA*) expression in FAP4-PDOs

Comparison of ILs vs baseline profiles highlighted that up-regulation of several Human Leukocyte Antigen genes was higher in FAP4 respect to the other PDOs. In particular, class II *HLA-DRA*, *HLA-DPA1* and *HLA-DMB* levels was 3-fold higher respect the other PDOs (Figure 31 A-1 and A-2) and also from FAP1-4 PDOs cultured under Standard condition (Figure 31 B). FAP4 PDOs also displayed a slight up-regulation of *HLA-DRB4* and *HLA-DPB1* genes (Figure 31 B).

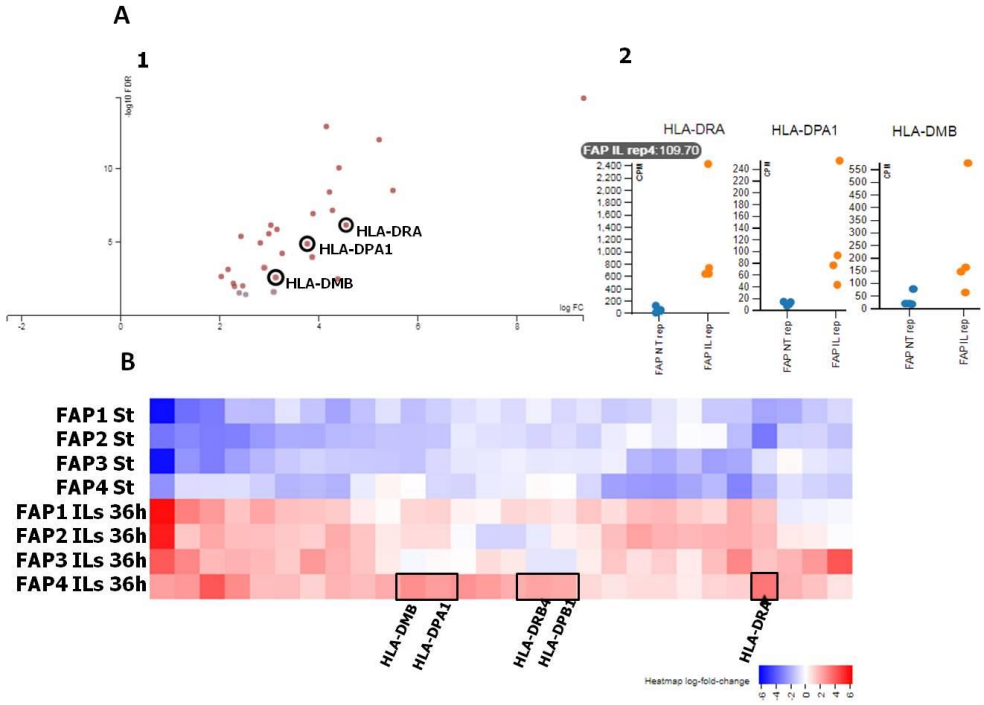

Figure 31: Panel A-1 depicts volcano plot of AAP PDOs differentially expressed genes with Log_2 FC >2 and FDR cut off 0.05. The most expressed HLA class II genes are highlighted by black circles. Panel A-2 depict *HLA-DRA*, *HLA-DPA1* and *HLA-DMB* gene counts in which FAP4 PDOs display 3-fold increase expression than AAP PDOs grown under Standard condition. Panel B shows heatmap of differentially expressed gene for AAP PDOs, black squares highlight *HLA* class II gene expressed by FAP4 PDOs under ILs condition.

6.4.5 THP1 and FAP PDOs co-culture condition

Using the same parameters adopted for ILs condition (log_2FC > 2 and FDR cut off 0.05) no differentially expressed genes were found. Looking individually at each pair of FAP PDOs cultured with the two conditions, few differences were noticed (absolute log_2FC > 1.5 and FDR 0.05). Best results were obtained for FAP3 PDOs as shown in Table 8.

Genes

Showing 0..12 of 14 Download CSV Search:

Probe Name	Accession #	Class Name	FDR	P valu...	FAP NT rep	FAP CoC rep
S100A8	NM_002964.3	Endogenous	0.39	1.35e-3	0.00	4.90
CDK1	NM_001786.4	Endogenous	0.39	0.01	0.00	-1.78
C3	NM_000064.2	Endogenous	0.39	6.04e-3	0.00	2.54
BIRC5	NM_001168.2	Endogenous	0.39	0.01	0.00	-1.57
ARG2	NM_001172.3	Endogenous	0.39	4.30e-3	0.00	2.45
PBK	NM_018492.2	Endogenous	0.39	8.48e-3	0.00	-1.95
LAMP3	NM_014398.3	Endogenous	0.39	0.01	0.00	1.52
S100A12	NM_005621.1	Endogenous	0.39	0.01	0.00	2.21
F13A1	NM_000129.3	Endogenous	0.39	5.98e-3	0.00	1.63
CCL5	NM_002985.2	Endogenous	0.39	0.01	0.00	1.84

Table 8: List of the genes differentially expressed between FAP3 PDOs co-cultured with THP1 cells vs standard culture condition. Only values with absolute Log_2 FC > 1.5 and FDR cut off 0.05 were considered.

With this analysis *S100A8* (also known as *Calgranulin A*) resulted more than 4-fold increased in THP1 co-cultured FAP3 PDOs (Figure 32 A-1 and A-2) compared to its control (Figure 32 B).
These results, conducted on a small number of PDOs are very preliminary, however set the basis for further investigations on larger sample cohorts.

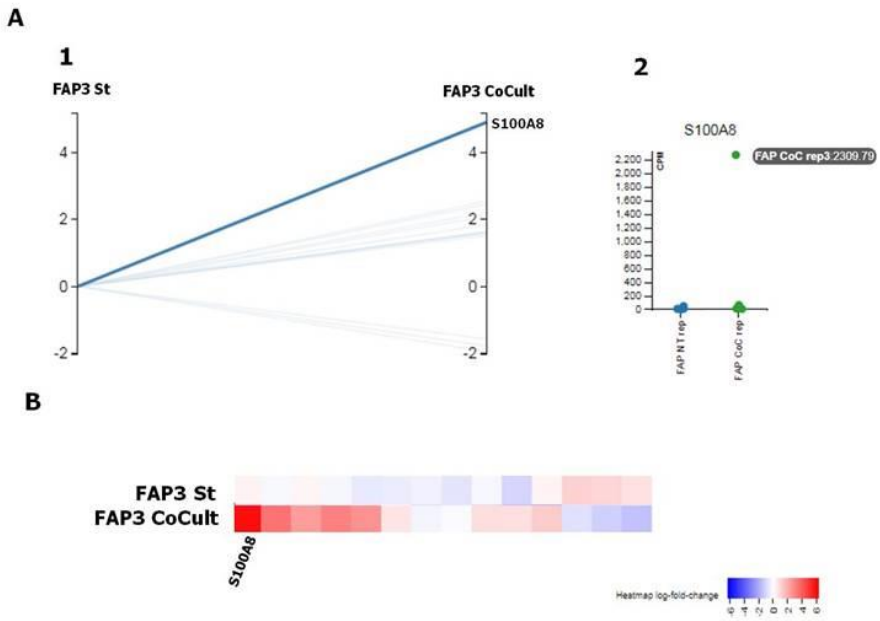

Figure 32: Panel A-1 shows parallel coordinates expression of FAP3 PDOs under Standard vs FAP3 co-culture condition ($log_2FC > 1.5$ and FDR 0.05). Panel A-2 depicts *S100A8* gene counts in which FAP3 PDOs display elevate expression than AAP PDOs grown under Standard and THP1 co-cultured condition. Panel B heatmap of upregulated genes of FAP3 PDOs in Standard and THP1 co-cultured condition.

6.4.6 NanoString miR-v3 expression analysis

Considered the role of miRNAs in inflammation, a miRNA profile of PDOs was performed using the NanoString miR-v3 panel on PDOs grown under normal conditions, with Th17 and Th22 cytokines and co-cultured with LPS stimulated THP1 cells. The hierarchical clustering of all data showed less distinct segregation of FAP PDO miRNAs than that obtained in the Immune Profile analysis. In particular, FAP PDOs co-cultured with THP1 cells showed higher number of “spiked” miRNAs expression, as well as FAP1 and FAP4 PDOs under ILs condition (left side of the dendrogram, Figure 33). Conversely, ILs FAP2 and FAP3 PDOs displayed, for the large majority of the transcripts, almost null miRNAs expression, and clustered together with FAP1-4 PDOs grown under standard condition (right side of the dendrogram, Figure 33).

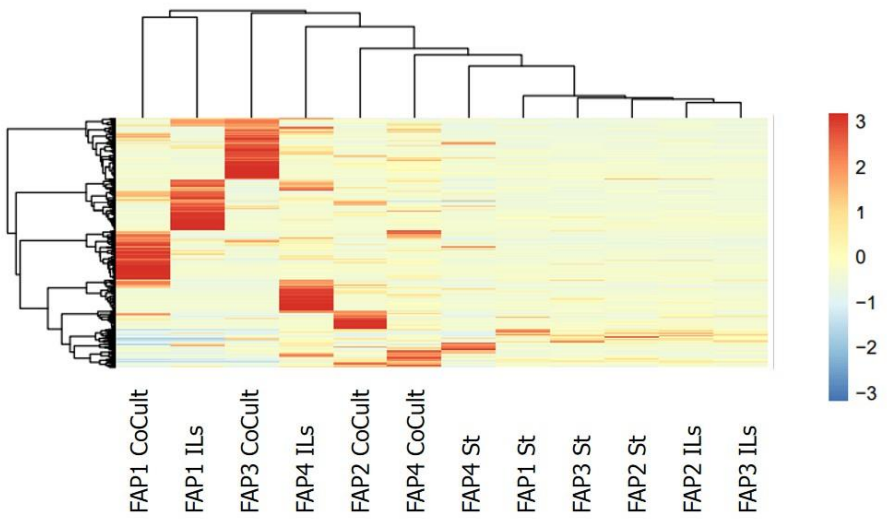

Figure 33: Dendogram of all AAP PDO miRNAs after geometric mean cartridge correction and background subtraction.

6.4.7 MiRNA Correlogram analysis

Based on the observation that FAP1-4 PDOs clustered independently from the culture condition in which they were grown, the correlation of every cultured PDOs was tested, to determine whether the biological variations in the data series (in this case miRNA expression after co-culture with THP1 or ILs condition) are casual or might be associated with any trend, either linear or constant over time. The correlogram of the data obtained by NanoString mir V3 panel showed that the variations of FAP1-4 grown under the THP1 co-culture and ILs condition were not significantly correlated and their distribution was likely accidental (Figure 34). This finding advised to avoid class comparisons between the miRNA profiles, to prevent biases that might be introduced by significant but non reproducible expression variations.

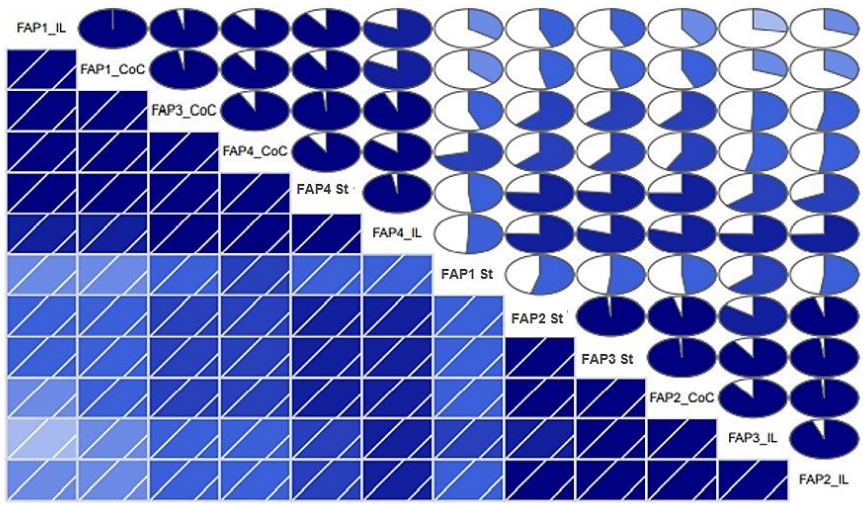

Figure 34: Correlogram of all AAP PDO miRNAs after background subtraction.

7 DISCUSSION

The role of Inflammation as “bad conditioner” of the healthy status of the colorectal mucosa has been documented for several years. As a consequence, the control of the inflammatory state of subjects predisposed to developing colorectal diseases, such as IBD and cancer has become crucial. This is true also for individuals with inherited CRC related syndromes such as AAP. Several trials conducted on patients with sporadic CRC confirmed that treatment with NSAID reduced the risk to develop colorectal adenomas and subsequently CRC [27,123]. However, long-term treatment with these drugs causes cardiological risks; there is therefore a pressing need for an alternative prevention strategy that is safe and well tolerated. A pilot study designed on AAP individuals to evaluate whether a low-inflammatory diet can reduce gastrointestinal markers of inflammation helped to better elucidate the inflammatory processes that lead to the development of adenomas in AAP subjects. After three-months of active dietary intervention, a reduction of systemic and local inflammation markers was observed.

Calprotectin decreased both in stool and serum, and a statistically significant time trend was also observed for Insulin and IGF-1. Changes in COX-2 expression were also evaluated. IHC analysis of COX-2 performed on normal colonic mucosal specimens from not-AAP patients and endoscopic biopsies of AAP patients enrolled in the pilot study collected prior to starting the diet confirmed high levels of inflammation for all AAP patients. Inflammation was present in every cell compartment analyzed (normal crypts, stromal cells of the lamina propria, adenomatous crypts, and immune cell infiltrating adenoma). The diet was not sufficient to reduce COX-2 local expression; in fact, the same diffuse immunoreactivity was observed in the biopsies collected after six months. COX-2 upregulation along the colorectal mucosa is driven by several stimuli, including environmental factors [124], dysbiosis, homeostasis alterations and inflammatory conditions mediated by IL-6 [125]. COX-2 expression is also regulated by the binding of Beta-catenin to its promoter region as reported by Araki and collaborators [126]. In AAP patients Beta-catenin is not ubiquitinated for degradation by the APC/Glycogen synthase kinase 3 beta (GSK3-β)/Axin complex. Levels of 15-PGDH were almost null in AAP individuals prior the dietary intervention, for all the four cell compartments analyzed. This finding is in agreement with what reported in the literature, where high levels of COX-2 negatively regulate 15-PGDH expression along the colorectal mucosa [63, 66]. Despite this diffuse inflammatory status, a significant increase of 15-PGDH immunoreactive normal crypts was observed in the normal colon mucosa after six months. The increase of 15-PGDH is an encouraging result to counter the neoplastic progression of aberrant crypt foci of the colon, especially in the normal mucosa, which acts to antagonize the prostaglandin generating activity of COX-2. Gravaghi and collaborators described how a diet rich in n-3 polyunsaturated fatty acids

(PUFAs) exerts an anti-inflammatory action on mice by decreasing PGE2 levels and inhibiting the incorporation of arachidonic acid (AA), the precursor of eicosanoids, including PGE2, in the phospholipid membrane [127]. Another study conducted by Fini and collaborators. demonstrated how ω3-PUFA supplementation reported a reduction in the number and size of tumors, correlated with inhibition of COX-2, reduction of nuclear translocation of Beta-catenin and increase of apoptosis in Apc (Min/+) mice [128]. Considering these results, it could be hypothesized that the ω3-PUFAs upregulate levels of 15-PGDH. However, there are no studies related to PGE2 decrease and 15-PGDH expression levels and to date there are few studies explaining how dietary habits regulate intestinal inflammation.

To investigate how inflammation influences epithelial cells of the colorectal mucosa, a 3D model was derived from adenomas of AAP patients who underwent prophylactic total colectomy at INT. Microscopic observation of the four AAP-derived PDOs analysed showed that they were able to reproduce the complexity of the colonic epithelium. All FAP-PDOs showed different peculiarities. However, each of them was characterized by two main components: a less differentiated one consisting of large spheroidal structures that grew from a solid core and expanded from the inner portion outwards and, a well-differentiated one, formed by complex structures that grew asymmetrically, with a core that was often not easily recognizable. The presence of these two components is well explained in the literature. Some studies have demonstrated that the spheroid like component of organoids is mainly made up of stem cells; vice versa, the more complex structures are formed by differentiated cells following the physiological intestinal process that guides to the renewal of the colorectal mucosa [129]. All these features are considered to be of primary importance in colorectal organoids. The PDOs exhibited similar proliferation rates, except for FAP4 which grew faster and reached larger size.
Immunophenotypical and molecular characterization of PDOs highlighted their similarity with the tissue of origin. IHC confirmed the expression of epithelial glandular markers (CKAE1/E3, CK19 and CK20), specific colorectal marker (CDX2) and colorectal staminal marker (LGR5). FAP1 and FAP4 PDOs exhibited glandular structures lined by pseudo-stratified columnar cells with central fibrinoid core and dirty necrosis along with roundish solid aggregates of nonaligned epithelial cells. These features were partially present also in FAP2 organoids, in which glandular structures showed a more complex pattern of necrosis frame. FAP3 PDO cells showed high positivity to all CKs, but LGR5 immunoreactive cells were less frequent than in other FAP PDOs, this feature highlighted that FAP3 PDO cell components were likely more differentiated than staminal. All the Organoids presented a solid core confirming the features observed in culture condition. Targeted NGS analysis of 48 genes frequently mutated in cancer confirmed that PDOs carried the same germline mutations of the AAP subjects from

which they were generated. In FAP1 (c.4285C>T) and FAP4 (c.4360G>T) a second deleterious pathogenetic *APC* alteration was also detected. Considering that the four PDOs generated showed different morphological features, mutation of additional genes that were not included in the NGS panel cannot be excluded. The two acquired mutations in FAP1 and FAP4 may have occurred during the maintenance of the cultures. Although it cannot be excluded that these mutations were already present in a sub-clonal cell population within the adenomas used to generate the Organoids. This observation, together with their LGR5 immunoreactivity, could indicate that FAP1 and FAP4 PDOs present a high stem cell component that is influenced by the molecular instability typical of cells progressing to malignancy. Therefore, the cell heterogeneity of FAP Organoids reflects the *in vivo* condition of the colon mucosa in AAP patients, where hundreds of polyps, with different mutations somatically acquired, grow simultaneously. These results demonstrate that PDOs are reliable models to study AAP disease. Moreover, the fact that FAP PDOs are able to preserve the mutational status of their tissue of origin without acquiring somatic mutation in CRC related genes such as *KRAS, BRAF* or *TP53*, for several culture passages makes them 3D models suitable for drug sensitivity studies aimed at reducing polyps growth in AAP subjects.

IHC for COX-2 and 15-PGDH showed different pattern of expression within the four PDO cultures. Contrary to what expected FAP1, FAP2 and FAP4 PDOs showed high immunoreactivity for COX-2 when maintained in medium without synthetic PGE2 addition, while FAP3 PDOs displayed low levels of COX-2.15-PGDH was absent in FAP1, FAP2 and FAP4 PDOs; after the addiction of 10µg/mL of synthetic PGE2, a consistent 15-PGDH upregulation was observed in all FAP PDOs with a significant reduction of COX-2 expression in FAP1 and FAP3.
These findings underline that even in the absence of stimuli from the microenvironment (provided by microbes and lamina propria mast cells [130]) epithelial PDOs cells produce high COX-2 levels. Moreover, AAP cells were able to deregulate 15-PGDH expression and consequently its tumor suppressor activity. Only the addition of synthetic PGE2 to the culture medium has led to the upregulation of 15-PGDH in FAP PDOs. The accumulation of Beta-catenin due to *APC* alterations in AAP patients could overcome these deficiencies by keeping the COX-2 transcription constantly active and consequently increasing inflammation.

The architecture of the normal colonic mucosa is complex. Normal crypts are surrounded by numerous different stromal and immune cells which constantly exchange signaling molecules and create network of interactions. The continuous self-renewal of the normal colonic mucosa is a process finely regulated also by stromal and inflammatory cells inside the niche which play a crucial role in the maintenance of the normal structure. Finally, inflammatory cells protect the integrity of the colonic mucosa avoiding

microbial dysbiosis by regulating the production of the mucus layer. Considering all these features it was clear that FAP-PDOs, which consist of colonic epithelial cells only, were not enough to study a complex process such as inflammation. Consequently, *in vitro* models of PDOs including lymphoid and/or myeloid-derived factors have been developed. These factors play an important role in the maintenance of tissue homeostasis and could sustain inflammatory processes present in the colonic mucosa. Specific ILs produced by the T helper CD4+ lymphocytes (IL-17a, IL-22 and IL-6) were added to the PDOs culture medium. Among the CD4+ T cell lineage, Th17 are pro-inflammatory lymphocytes that perform their function prominently at mucosal surfaces where they trigger pro-inflammatory danger signals that promote clearance of extracellular bacteria and fungi by recruiting and activating neutrophil granulocytes. Antimicrobial factors expressed by Th17 cells, play an important role in tissue homeostasis along the colorectal mucosa. Recently Th22 CD4+ lymphocyte subtype has been observed together with Th17 in the regulation of pro-inflammatory processes along the colorectal mucosa. Two independent studies [131, 132] found that the percentage of circulating and intratumoral Th17, Th22 and $CD4^+$ cells co-producing IL-17a/IL-22 was higher in advanced stages of CRC than in early stages, and that the overall Th22 subset was higher in the intratumoral region regardless of the tumor stage with respect to the peritumoral tissue. Moreover, IL-22 produced by Th22 cells can stimulate CRC proliferation through STAT-3 activation and its binding to the promoter of the Polycomb Repressor complex 2 (PRC2). The expression of PRC2 results in the inhibition of p21 and p16 and finally, the increase in the proliferation of CRC cells [133]. Th17 and Th22 cells are present also in normal colorectal mucosa, although with a different distribution. They are described to be more abundant in the healthy human cecum than in the ileum, as well asin the sigma portion [134]. These differences highlight that Th17 and Th22 can be recruited specifically in colorectal region according to factors related to the microenvironment or microbiota.

Both Th17 and Th22 secrete considerable amount of IL-6, a pro-inflammatory cytokine which is produced in response to infections and tissue injuries and contributes to host defense through the stimulation of acute phase responses, hematopoiesis, and immune reactions. Various studies have found an increased expression of IL-6 in patients with CRC, both in the serum of patients and in tumor tissue itself [135, 136]. However recent studies conducted on IL-10 -/- deficient mice showed that IL-6 inhibition exacerbates colitis and increase systemic inflammation, suggesting also a protective role of IL-6 when IL-10 is absent. Cell cycle analysis showed that only FAP4 PDOs grown for 36 hours in presence of Th17 and Th22 had a different behaviour: the percentage of cells in G1 phase did not change, while the percentage of cells in G2/M phase increased significantly. The increase of G2/M phase of FAP4 under ILs condition could be due to the stimulatory effect operated by the pro-inflammatory condition. FAP4 PDOs grew faster *in vitro* and showed high

LGR5 immunoreactivity. As reported in literature, IL-6 and IL-22 promote growth of malignant cells. Also the presence of a large duplication on the *APC* gene together with the second deleterious mutation could result in a different response of FAP4 PDO cells to the pro-inflammatory environment that could increase their proliferation. A gene expression immune profile of FAP PDOs under ILs condition highlighted a clear split between PDOs grown under standard condition and in the presence of ILs, with the exception of FAP4 PDOs, for which the two growth conditions were clustered closely, confirming that the profile of FAP4 was different from that of FAP1-3 PDOs. Analysis of the differentially expressed genes between ILs and Standard conditions showed that the most expressed gene in FAP1, FAP2 and FAP3 PDOs was the Deleted in Malignant Brain Tumor 1 (*DMBT1*) gene. Expression of *DMBT1* was very low in Standard conditions and was not induced by ILs in FAP4 PDOs. *DMBT1* is downregulated in several cancers and could be considered as a candidate tumor suppressor gene for brain, lung, esophageal, gastric, and colorectal cancers [137, 138, 139, 140]. Some studies highlighted that IL-22 treatment [141] enhances the expression of *DMBT1* through STAT3 tyrosine phosphorylation and NF-κB activation in CRC cells and that *DMBT1* may play roles in the mucosal defence system, in cellular immune defence and in the epithelial differentiation. The decrease in proliferation observed in FAP1-3 PDOs could be related to the increase in *DMBT1* expression; on the other hand, the FAP4 PDOs, which in culture showed a faster growth, could be more advanced towards neoplastic progression and be over the steps where *DMBT1* has a growth suppressor function. Furthermore, upregulation of *DMBT1* on FAP1-3 PDOs may be indicative of a protective effect of ILs on epithelial cells. The role of Th17 and Th22 lymphocytes in maintaining cellular balance within the colorectal mucosa could be attenuated in AAP colonic cells that are driven to proliferate in an uncontrolled manner. DGE analysis also highlighted that FAP4 PDOs grown in presence of ILs displayed upregulation of several Human Leukocyte Antigen genes. Class II *HLA-DRA, HLA-DPA1* and *HLA-DMB* levels were increased by 3-fold compared with FAP1-3 PDOs cultured under ILs condition and also from their relative controls. A slight upregulation of *HLA-DRB4* and *HLA-DPB1* genes was also observed in FAP4 PDOs. The main role of HLA class II cell surface proteins is to present antigens from outside of the cells to T-lymphocytes, playing a fundamental role in the regulation of the immune system. Different gene expression studies showed that *HLA-DMB* [142] and *HLA DPA1* [143] were upregulated respectively in prostate cancer of Caucasian people and ovarian cancer. Furthermore, their upregulation within the tumor tissue and the surrounding stroma was associated with good prognosis in advanced cancers. Although different studies have been conducted on the presence of HLA proteins in CRC, their role in the progression and dedifferentiation of CRC has not been clarified yet. To reproduce a myeloid inflammatory environment, a co-culture of FAP PDOs and monocytic cells was established. In recent years co-cultures between

colorectal Organoids and immune cells are increasing, especially to recreate models of ulcerative colitis and colitis-associatedcolon cancer [144]. Although interest in this topic is growing, few studies have been conducted to date, particularly on AAP Organoids. Unfortunately, the collection of peripheral blood mononuclear cells from AAP patients was not planned for this study. For this reason, co-cultures of FAP PDOs and THP1 stimulated cell lines were established. THP1 human monocytic leukemia cells can differentiate into functional M1 or M2 macrophages upon *in vitro* stimulation. Among the myeloid cells infiltrating the colorectal mucosa, macrophages represent one of the most important immune subtypes. Their role is to monitor the health of the colon mucosa by counteracting dysbiosis, a condition that can frequently occur when the colon epithelium is damaged or is in a chronic inflammatory condition. Pro inflammatory Macrophages expressing the M1 phenotype have been observed along the mucosa of patients with IBD [145]. Moreover, studies conducted on $Apc^{1638N/+}$ mice which developed spontaneously colorectal adenomas and CRC, showed that tumors and adenomas infiltrating myeloid cells displayed high number of neutrophils and macrophages compared to the small intestine.
Secretome of LPS activated THP1 cells confirmed that proinflammatory cytokines were secreted. In particular, high levels of IL-8 and IL-6 were observed as described in literature for activated macrophages, as well as of CCL2 and IL-1β inflammatory cytokines. Gene expression analysis with the PanCancer Immune profile panel used for ILs condition showed that FAP4 PDOs grown in Standard condition clustered with the co-cultured PDOs. This result was in agreement with what observed previously and with the fact that FAP4 PDOs had more advanced characteristics. FAP2 PDOs clustered in the region of PDOs grown in Standard conditions. Indeed, FAP2 and FAP3 displayed to be less advanced at both morphological and molecular level. DGE analysis showed no differentially expressed genes between co-cultured FAP PDOs and their relative controls. Looking individually at each PDO line, few differences were noticed. In particular, co-cultured FAP3 PDOs showed high levels of S100A8 compared to their control. S100A8 is a calcium- and zinc- binding protein, which, together with the S100A9, forms the Calprotectin heterodimer. The role of calprotectin on the colorectal mucosa is predominantly antimicrobial. It is mainly produced by neutrophils and its measurement is a useful surrogate for gastrointestinal inflammation. Aranda CJ and collaborators demonstrated that intrarectal administration of Calprotectin in a mice model of ulcerative colitis protected significantly mice from macroscopic and microscopic damage [146]. Considering this last feature, the upregulation of one of the Calprotectin subunits by co-cultured FAP3 PDOs reflects that they are responsive to external stimuli and that the inflammatory environment derived from stimulated THP1 can activate a defence mechanism. Finally, possible correlations between the miRNAs expressed by FAP PDOs and their inflammatory status were investigated. About 350 different miRNAs have been specifically associated to CRC. Some of them, for example miR-155

[147], enhance cell growth, survival, and proliferation (onco-miRNAs [oncomiRs]); others, such as miR-143 and miR-145 [148], suppress these activities (tumor-suppressor [TS]-miRNAs) [149]. Distinct but overlapping miRNA profiles have been observed in IBD ulcerative colitis and Crohn's disease [150]. MiRNAs perform also their oncogenic mechanism in chronic inflammation. Ye and collaborators found that TNF-α, triggers miR-122a expression, which acts on occludin, a protein involved in enterocyte permeability that is decreased in ulcerative colitis, Crohn's, and other irritable bowel disorders [151]. Moreover, not only differences in inflammation state, but also different miRNAs are expressed in different locations within the colon. In the sigmoid colon of active Crohn's patients, miR-23b, miR-106, and miR-191 were all increased. Instead, in the terminal ileum, miR-16, miR-21, miR-223, and miR-594 were increased [152]. Finally, aberrant expression of COX-2 and miRNA expression could be an important factor in connecting inflammation to cancer incidence. In addition to the APC mutation-driven mechanism leading to Beta-catenin accumulation and subsequent action on the COX-2 promoter, miR-101 and miR-101a were inversely related to COX-2 expression in colon cancer [153, 154]. *In silico* prediction studies revealed that miR-26b has a unique binding site within COX-2, and cells transfected with miR-26b after nine days formed fewer colonies than cells transfected with the non-coding vector [155].

miRNA expression profiles conducted on FAP PDOs cultured in standard conditions (control), under ILs and co-cultured with THP1 did not present specific differences related to the growth condition used. The correlation between the three conditions showed that variations of FAP1-4 grown under the THP1 co-culture and ILs were not significantly correlated and their distribution were likely accidental. Evidences in literature show that miRNAs are strictly related to the advanced state of cells. FAP4 PDOs have been shown to be the most advanced culture within the four FAP Organoids, but at the same time the expression density of miRNAs has shown that FAP4 Organoids are highly sensitive to changes of environmental conditions in which they are maintained. The same could be said for FAP1 PDOs considering that at molecular level they present a double APC mutation like the FAP4 PDOs. However, the high variability between the expressed miRNAs within different PDOs did not allow to proceed with further analysis.

8 CONCLUSIONS

Results from this study showed that a low-inflammatory diet can reduce inflammatory markers in AAP subjects both systemically and locally. At the tissue level, the diet induced upregulation of 15-PGDH in the colonic mucosa, which can counteract the inflammatory effects produced by COX-2. To confirm this data, prospective dietary intervention studies will be conducted on larger cohorts of individuals with germline *APC* alterations.

The AAP PDO models reproduced *in vitro* the specific characteristics of each patient from which they were generated, as confirmed by NGS analysis and immunophenotypical characterization.
FAP PDOs have proved to be a useful tool for studying the effects of inflammation on the proliferation of epithelial colonic cells. In fact, cell cycle analysis of FAP PDOs growth in a lymphoid inflammatory environment highlighted the possible protective role of Th17 and Th22 lymphocytes from malignant progression. PDOs arrest in G1 phase was observed, except for FAP4 PDO culture, where G2/M phase was increased. Similarly, the gene expression analysis showed that the lymphoid inflammatory environment induced upregulation of the tumor suppressor gene DMBT1, with the exception of FAP4 PDOs, confirming that this culture exhibits more aggressive characteristics than the other PDOs. This finding suggests that inflammation could worsen adenoma onset in a subset of AAP patients, also considering the large variety of *APC* mutations present in AAP subjects. Further investigations on a larger number of PDOs originated from different AAP subjects are needed to confirm the presented results.

This work has set the basis for future research aimed at exploring in depth the mechanisms underlying adenoma progression and inflammation in AAP subjects that will be investigated in the AAP PDO developed. Finally, the PDOs model will allow to screen for novel anti-inflammatory components that could help in reducing the development of adenomas in both heridatary and sporadic CRC.

9 REFERENCES

1- Bray F, Ferlay J, Soerjomataram I, Siegel RL, Torre LA, Jemal A. Global cancer statistics 2018: GLOBOCAN estimates of incidence and mortality worldwide for 36 cancers in 185 countries. CA Cancer J Clin. 2018 Nov;68(6):394-424. doi: 10.3322/caac.21492. Epub 2018 Sep 12. Erratum in: CA Cancer J Clin. 2020 Jul;70(4):313. PMID: 30207593.

2- Rawla P, Sunkara T, Barsouk A. Epidemiology of colorectal cancer: incidence, mortality, survival, and risk factors. Prz Gastroenterol. 2019;14(2):89-103. doi: 10.5114/pg.2018.81072. Epub 2019 Jan 6. PMID: 31616522; PMCID: PMC6791134.

3- Jasperson KW, Patel SG, Ahnen DJ. *APC*-Associated Polyposis Conditions. 1998 Dec 18 [updated 2017 Feb 2]. In: Adam MP, Ardinger HH, Pagon RA, Wallace SE, Bean LJH, Stephens K, Amemiya A, editors. GeneReviews® [Internet]. Seattle (WA): University of Washington, Seattle; 1993–2020. PMID: 20301519.

4- Tamura K, Kaneda M, Futagawa M, Takeshita M, Kim S, Nakama M, Kawashita N, Tatsumi-Miyajima J. Genetic and genomic basis of the mismatch repair system involved in Lynch syndrome. Int J Clin Oncol. 2019 Sep;24(9):999-1011. doi: 10.1007/s10147-019-01494-y. Epub 2019 Jul 4. Erratum in: Int J Clin Oncol. 2019 Jul 31: PMID: 31273487.

5- Samadder NJ, Baffy N, Giridhar KV, Couch FJ, Riegert-Johnson D. Hereditary Cancer Syndromes-A Primer on Diagnosis and Management, Part 2: Gastrointestinal Cancer Syndromes. Mayo Clin Proc. 2019 Jun;94(6):1099-1116. doi: 10.1016/j.mayocp.2019.01.042. PMID: 31171120.

6- Neklason DW, Thorpe BL, Ferrandez A, Tumbapura A, Boucher K, Garibotti G, Kerber RA, Solomon CH, Samowitz WS, Fang JC, Mineau GP, Leppert MF, Burt RW, Kuwada SK. Colonic adenoma risk in familial colorectal cancer--a study of six extended kindreds. Am J Gastroenterol. 2008 Oct;103(10):2577-84. doi: 10.1111/j.1572-0241.2008.02019.x. Epub 2008 Jul 30. PMID: 18671820; PMCID: PMC2922112.

7- Nielsen M, Morreau H, Vasen HF, Hes FJ. MUTYH-associated polyposis (MAP). Crit Rev Oncol Hematol. 2011 Jul;79(1):1-16. doi: 10.1016/j.critrevonc.2010.05.011. Epub 2010 Jul 21. PMID: 20663686.

8- Laurent-Puig P, Béroud C, Soussi T. APC gene: database of germline and somatic mutations in human tumors and cell lines. Nucleic Acids Res. 1998 Jan 1;26(1):269-70. doi: 10.1093/nar/26.1.269. PMID: 9399850; PMCID: PMC147178.

9- Moisio AL, Järvinen H, Peltomäki P. Genetic and clinical characterisation of familial adenomatous polyposis: a population based study. Gut. 2002 Jun;50(6):845-50. doi: 10.1136/gut.50.6.845. PMID: 12010888; PMCID: PMC1773245.

10- Michils G, Tejpar S, Thoelen R, van Cutsem E, Vermeesch JR, Fryns JP, Legius E, Matthijs G. Large deletions of the APC gene in 15% of mutation-negative patients with classical polyposis (FAP): a Belgian study. Hum Mutat. 2005 Feb;25(2):125-34. doi: 10.1002/humu.20122. PMID: 15643602.

11- Miyoshi Y, Nagase H, Ando H, Horii A, Ichii S, Nakatsuru S, Aoki T, Miki Y, Mori T, Nakamura Y. Somatic mutations of the APC gene in colorectal tumors: mutation cluster region in the APC gene. Hum Mol Genet. 1992 Jul;1(4):229-33. doi: 10.1093/hmg/1.4.229. PMID: 1338904.

12- Lamlum H, Papadopoulou A, Ilyas M, Rowan A, Gillet C, Hanby A, Talbot I, Bodmer W, Tomlinson I. APC mutations are sufficient for the growth of early colorectal adenomas. Proc Natl Acad Sci U S A. 2000 Feb 29;97(5):2225-8. doi: 10.1073/pnas.040564697. PMID: 10681434; PMCID: PMC15782.

13- Polakis P. Wnt signaling in cancer. Cold Spring Harb Perspect Biol. 2012 May 1;4(5):a008052. doi: 10.1101/cshperspect.a008052. PMID: 22438566; PMCID: PMC3331705.

14- van de Wetering M, Sancho E, Verweij C, de Lau W, Oving I, Hurlstone A, van der Horn K, Batlle E, Coudreuse D, Haramis AP, Tjon-Pon-Fong M, Moerer P, van den Born M, Soete G, Pals S, Eilers M, Medema R, Clevers H. The beta-catenin/TCF-4 complex imposes a crypt progenitor phenotype on colorectal cancer cells. Cell. 2002 Oct 18;111(2):241-50. doi: 10.1016/s0092-8674(02)01014-0. PMID: 12408868.

15- Shih IM, Wang TL, Traverso G, Romans K, Hamilton SR, Ben-Sasson S, Kinzler KW, Vogelstein B. Top-down morphogenesis of colorectal tumors. Proc Natl Acad Sci U S A. 2001 Feb 27;98(5):2640-5. doi: 10.1073/pnas.051629398. Epub 2001 Feb 20. PMID: 11226292; PMCID: PMC30191.

16- Kim PJ, Plescia J, Clevers H, Fearon ER, Altieri DC. Survivin and molecular pathogenesis of colorectal cancer. Lancet. 2003 Jul 19;362(9379):205-9. doi: 10.1016/S0140-6736(03)13910-4. PMID: 12885482.

17- Spirio LN, Samowitz W, Robertson J, Robertson M, Burt RW, Leppert M, White R. Alleles of APC modulate the frequency and classes of

mutations that lead to colon polyps. Nat Genet. 1998 Dec;20(4):385-8. doi: 10.1038/3865. PMID: 9843214.

18- Lamlum H, Ilyas M, Rowan A, Clark S, Johnson V, Bell J, Frayling I, Efstathiou J, Pack K, Payne S, Roylance R, Gorman P, Sheer D, Neale K, Phillips R, Talbot I, Bodmer W, Tomlinson I. The type of somatic mutation at APC in familial adenomatous polyposis is determined by the site of the germline mutation: a new facet to Knudson's 'two-hit' hypothesis. Nat Med. 1999 Sep;5(9):1071-5. doi: 10.1038/12511. PMID: 10470088.

19- Hankey W, Frankel WL, Groden J. Functions of the APC tumor suppressor protein dependent and independent of canonical WNT signaling: implications for therapeutic targeting. Cancer Metastasis Rev. 2018 Mar;37(1):159-172. doi: 10.1007/s10555-017-9725-6. PMID: 29318445; PMCID: PMC5803335.

20- Heitman SJ, Ronksley PE, Hilsden RJ, Manns BJ, Rostom A, Hemmelgarn BR. Prevalence of adenomas and colorectal cancer in average risk individuals: a systematic review and meta-analysis. Clin Gastroenterol Hepatol. 2009 Dec;7(12):1272-8. doi: 10.1016/j.cgh.2009.05.032. Epub 2009 Jun 10. PMID: 19523536.

21- Bersentes K, Fennerty MB, Sampliner RE, Garewal HS. Lack of spontaneous regression of tubular adenomas in two years of follow-up. Am J Gastroenterol. 1997 Jul;92(7):1117-20. PMID: 9219781.

22- Kadmon M, Tandara A, Herfarth C. Duodenal adenomatosis in familial adenomatous polyposis coli. A review of the literature and results from the Heidelberg Polyposis Register. Int J Colorectal Dis. 2001 Apr;16(2):63-75. doi: 10.1007/s003840100290. PMID: 11355321.

23- Giardiello FM, Offerhaus GJ, Lee DH, Krush AJ, Tersmette AC, Booker SV, Kelley NC, Hamilton SR. Increased risk of thyroid and pancreatic carcinoma in familial adenomatous polyposis. Gut. 1993 Oct;34(10):1394-6. doi: 10.1136/gut.34.10.1394. PMID: 8244108; PMCID: PMC1374548.

24- Cetta F, Ugolini G, Martellucci J, Gotti G. Screening for thyroid cancer in patients with familial adenomatous polyposis. Ann Surg. 2015 Jan;261(1):e13-4. doi: 10.1097/SLA.0000000000000442. PMID: 24394556.

25- Nieuwenhuis MH, Lefevre JH, Bülow S, Järvinen H, Bertario L, Kernéis S, Parc Y, Vasen HF. Family history, surgery, and APC mutation are risk factors for desmoid tumors in familial adenomatous polyposis: an international cohort study. Dis Colon Rectum. 2011 Oct;54(10):1229-34. doi: 10.1097/DCR.0b013e318227e4e8. PMID: 21904137.

26- Sinha A, Tekkis PP, Gibbons DC, Phillips RK, Clark SK. Risk factors predicting desmoid occurrence in patients with familial adenomatous polyposis: a meta-analysis. Colorectal Dis. 2011 Nov;13(11):1222-9. doi: 10.1111/j.1463-1318.2010.02345.x. Epub 2010 Jun 2. PMID: 20528895.

27- Giardiello FM, Hamilton SR, Krush AJ, Piantadosi S, Hylind LM, Celano P, Booker SV, Robinson CR, Offerhaus GJ. Treatment of colonic and rectal adenomas with sulindac in familial adenomatous polyposis. N Engl J Med. 1993 May 6;328(18):1313-6. doi: 10.1056/NEJM199305063281805. PMID: 8385741.

28- Olendzki BC, Silverstein TD, Persuitte GM, Ma Y, Baldwin KR, Cave D. An anti-inflammatory diet as treatment for inflammatory bowel disease: a case series report. Nutr J. 2014 Jan 16;13:5. doi: 10.1186/1475-2891-13-5. PMID: 24428901; PMCID: PMC3896778.

29- Marlow G, Ellett S, Ferguson IR, Zhu S, Karunasinghe N, Jesuthasan AC, Han DY, Fraser AG, Ferguson LR. Transcriptomics to study the effect of a Mediterranean-inspired diet on inflammation in Crohn's disease patients. Hum Genomics. 2013 Nov 27;7(1):24. doi: 10.1186/1479-7364-7-24. PMID: 24283712; PMCID: PMC4174666.

30- Ullman TA, Itzkowitz SH. Intestinal inflammation and cancer. Gastroenterology. 2011 May;140(6):1807-16. doi: 10.1053/j.gastro.2011.01.057. PMID: 21530747.

31- Fearon ER, Vogelstein B. A genetic model for colorectal tumorigenesis. Cell. 1990 Jun 1;61(5):759-67. doi: 10.1016/0092-8674(90)90186-i. PMID: 2188735.

32- Greenhough A, Smartt HJ, Moore AE, Roberts HR, Williams AC, Paraskeva C, Kaidi A. The COX-2/PGE2 pathway: key roles in the hallmarks of cancer and adaptation to the tumour microenvironment. Carcinogenesis. 2009 Mar;30(3):377-86. doi: 10.1093/carcin/bgp014. Epub 2009 Jan 9. PMID: 19136477.

33- Crosnier C, Stamataki D, Lewis J. Organizing cell renewal in the intestine: stem cells, signals and combinatorial control. Nat Rev Genet. 2006 May;7(5):349-59. doi: 10.1038/nrg1840. PMID: 16619050.

34- van der Flier LG, Clevers H. Stem cells, self-renewal, and differentiation in the intestinal epithelium. Annu Rev Physiol. 2009;71:241-60. doi: 10.1146/annurev.physiol.010908.163145. PMID: 18808327.

35- Wasan HS, Park HS, Liu KC, Mandir NK, Winnett A, Sasieni P, Bodmer WF, Goodlad RA, Wright NA. APC in the regulation of intestinal crypt

fission. J Pathol. 1998 Jul;185(3):246-55. doi: 10.1002/(SICI)1096-9896(199807)185:3<246::AID-PATH90>3.0.CO;2-8. PMID: 9771477.

36- Green RA, Wollman R, Kaplan KB. APC and EB1 function together in mitosis to regulate spindle dynamics and chromosome alignment. Mol Biol Cell. 2005 Oct;16(10):4609-22. doi: 10.1091/mbc.e05-03-0259. Epub 2005 Jul 19. PMID: 16030254; PMCID: PMC1237068.

37- Draviam VM, Shapiro I, Aldridge B, Sorger PK. Misorientation and reduced stretching of aligned sister kinetochores promote chromosome missegregation in EB1- or APC-depleted cells. EMBO J. 2006 Jun 21;25(12):2814-27. doi: 10.1038/sj.emboj.7601168. Epub 2006 Jun 8. PMID: 16763565; PMCID: PMC1500857.

38- Dikovskaya D, Schiffmann D, Newton IP, Oakley A, Kroboth K, Sansom O, Jamieson TJ, Meniel V, Clarke A, Näthke IS. Loss of APC induces polyploidy as a result of a combination of defects in mitosis and apoptosis. J Cell Biol. 2007 Jan 15;176(2):183-95. doi: 10.1083/jcb.200610099. Erratum in: J Cell Biol. 2007 Jan 29;176(3):369. PMID: 17227893; PMCID: PMC2063938.

39- Fleming ES, Temchin M, Wu Q, Maggio-Price L, Tirnauer JS. Spindle misorientation in tumors from APC(min/+) mice. Mol Carcinog. 2009 Jul;48(7):592-8. doi: 10.1002/mc.20506. PMID: 19123231.

40- Caldwell CM, Green RA, Kaplan KB. APC mutations lead to cytokinetic failures in vitro and tetraploid genotypes in Min mice. J Cell Biol. 2007 Sep 24;178(7):1109-20. doi: 10.1083/jcb.200703186. PMID: 17893240; PMCID: PMC2064647.

41- Quyn AJ, Appleton PL, Carey FA, Steele RJ, Barker N, Clevers H, Ridgway RA, Sansom OJ, Näthke IS. Spindle orientation bias in gut epithelial stem cell compartments is lost in precancerous tissue. Cell Stem Cell. 2010 Feb 5;6(2):175-81. doi: 10.1016/j.stem.2009.12.007. PMID: 20144789.

42- Pease JC, Tirnauer JS. Mitotic spindle misorientation in cancer--out of alignment and into the fire. J Cell Sci. 2011 Apr 1;124(Pt 7):1007-16. doi: 10.1242/jcs.081406. PMID: 21402874.

43- Cario E, Gerken G, Podolsky DK. Toll-like receptor 2 controls mucosal inflammation by regulating epithelial barrier function. Gastroenterology. 2007 Apr;132(4):1359-74. doi: 10.1053/j.gastro.2007.02.056. Epub 2007 Feb 25. PMID: 17408640.

44- Kaiko GE, Ryu SH, Koues OI, Collins PL, Solnica-Krezel L, Pearce EJ, Pearce EL, Oltz EM, Stappenbeck TS. The Colonic Crypt Protects Stem Cells from Microbiota-Derived Metabolites. Cell. 2016 Jun 16;165(7):1708-1720. doi: 10.1016/j.cell.2016.05.018. Epub 2016 Jun 2. Erratum in: Cell. 2016 Nov 3;167(4):1137. PMID: 27264604; PMCID: PMC5026192.

45- Okada T, Fukuda S, Hase K, Nishiumi S, Izumi Y, Yoshida M, Hagiwara T, Kawashima R, Yamazaki M, Oshio T, Otsubo T, Inagaki-Ohara K, Kakimoto K, Higuchi K, Kawamura YI, Ohno H, Dohi T. Microbiota-derived lactate accelerates colon epithelial cell turnover in starvation-refed mice. Nat Commun. 2013;4:1654. doi: 10.1038/ncomms2668. PMID: 23552069.

46- Vogel JD, West GA, Danese S, De La Motte C, Phillips MH, Strong SA, Willis J, Fiocchi C. CD40-mediated immune-nonimmune cell interactions induce mucosal fibroblast chemokines leading to T-cell transmigration. Gastroenterology. 2004 Jan;126(1):63-80. doi: 10.1053/j.gastro.2003.10.046. PMID: 14699489.

47- Pinchuk IV, Beswick EJ, Saada JI, Suarez G, Winston J, Mifflin RC, Di Mari JF, Powell DW, Reyes VE. Monocyte chemoattractant protein-1 production by intestinal myofibroblasts in response to staphylococcal enterotoxin a: relevance to staphylococcal enterotoxigenic disease. J Immunol. 2007 Jun 15;178(12):8097-106. doi: 10.4049/jimmunol.178.12.8097. PMID: 17548648.

48- Powell DW, Pinchuk IV, Saada JI, Chen X, Mifflin RC. Mesenchymal cells of the intestinal lamina propria. Annu Rev Physiol. 2011;73:213-37. doi: 10.1146/annurev.physiol.70.113006.100646. PMID: 21054163; PMCID: PMC3754809.

49- Nagashima R, Maeda K, Imai Y, Takahashi T. Lamina propria macrophages in the human gastrointestinal mucosa: their distribution, immunohistological phenotype, and function. J Histochem Cytochem. 1996 Jul;44(7):721-31. doi: 10.1177/44.7.8675993. PMID: 8675993.

50- Müller AJ, Kaiser P, Dittmar KE, Weber TC, Haueter S, Endt K, Songhet P, Zellweger C, Kremer M, Fehling HJ, Hardt WD. Salmonella gut invasion involves TTSS-2-dependent epithelial traversal, basolateral exit, and uptake by epithelium-sampling lamina propria phagocytes. Cell Host Microbe. 2012 Jan 19;11(1):19-32. doi: 10.1016/j.chom.2011.11.013. PMID:

51- Pull SL, Doherty JM, Mills JC, Gordon JI, Stappenbeck TS. Activated macrophages are an adaptive element of the colonic epithelial progenitor niche necessary for regenerative responses to injury. Proc Natl Acad Sci U

S A. 2005 Jan 4;102(1):99-104. doi: 10.1073/pnas.0405979102. Epub 2004 Dec 22. PMID: 15615857; PMCID: PMC544052.

52- Smythies LE, Sellers M, Clements RH, Mosteller-Barnum M, Meng G, Benjamin WH, Orenstein JM, Smith PD. Human intestinal macrophages display profound inflammatory anergy despite avid phagocytic and bacteriocidal activity. J Clin Invest. 2005 Jan;115(1):66-75. doi: 10.1172/JCI19229. PMID: 15630445; PMCID: PMC539188.

53- Malvin NP, Seno H, Stappenbeck TS. Colonic epithelial response to injury requires Myd88 signaling in myeloid cells. Mucosal Immunol. 2012 Mar;5(2):194-206. doi: 10.1038/mi.2011.65. Epub 2012 Jan 18. PMID: 22258450; PMCID: PMC3791628.

54- Bain CC, Scott CL, Uronen-Hansson H, Gudjonsson S, Jansson O, Grip O, Guilliams M, Malissen B, Agace WW, Mowat AM. Resident and pro-inflammatory macrophages in the colon represent alternative context-dependent fates of the same Ly6Chi monocyte precursors. Mucosal Immunol. 2013 May;6(3):498-510. doi: 10.1038/mi.2012.89. Epub 2012 Sep 19. PMID: 22990622; PMCID: PMC3629381.

55- Ma TY, Iwamoto GK, Hoa NT, Akotia V, Pedram A, Boivin MA, Said HM. TNF-alpha-induced increase in intestinal epithelial tight junction permeability requires NF-kappa B activation. Am J Physiol Gastrointest Liver Physiol. 2004 Mar;286(3):G367-76. doi: 10.1152/ajpgi.00173.2003. PMID: 14766535.

56- Pender SL, Quinn JJ, Sanderson IR, MacDonald TT. Butyrate upregulates stromelysin-1 production by intestinal mesenchymal cells. Am J Physiol Gastrointest Liver Physiol. 2000 Nov;279(5): G918-24. doi: 10.1152/ajpgi.2000.279.5.G918. PMID: 11052988.

57- Weaver CT, Hatton RD, Mangan PR, Harrington LE. IL-17 family cytokines and the expanding diversity of effector T cell lineages. Annu Rev Immunol. 2007; 25:821-52. doi: 10.1146/annurev.immunol.25.022106.141557. PMID: 17201677.

58- Boniface K, Bernard FX, Garcia M, Gurney AL, Lecron JC, Morel F. IL-22 inhibits epidermal differentiation and induces proinflammatory gene expression and migration of human keratinocytes. J Immunol. 2005 Mar 15;174(6):3695-702. doi: 10.4049/jimmunol.174.6.3695. PMID: 15749908.

59- Wolk K, Witte E, Wallace E, Döcke WD, Kunz S, Asadullah K, Volk HD, Sterry W, Sabat R. IL-22 regulates the expression of genes responsible for antimicrobial defense, cellular differentiation, and mobility in keratinocytes: a

potential role in psoriasis. Eur J Immunol. 2006 May;36(5):1309-23. doi: 10.1002/eji.200535503. PMID: 16619290.

60- Andoh A, Zhang Z, Inatomi O, Fujino S, Deguchi Y, Araki Y, Tsujikawa T, Kitoh K, Kim-Mitsuyama S, Takayanagi A, Shimizu N, Fujiyama Y. Interleukin-22, a member of the IL-10 subfamily, induces inflammatory responses in colonic subepithelial myofibroblasts. Gastroenterology. 2005 Sep;129(3):969-84. doi: 10.1053/j.gastro.2005.06.071. PMID: 16143135.

61- Nielsen OH, Kirman I, Rüdiger N, Hendel J, Vainer B. Upregulation of interleukin-12 and -17 in active inflammatory bowel disease. Scand J Gastroenterol. 2003 Feb;38(2):180-5. doi: 10.1080/00365520310000672. PMID: 12678335.

62- Andoh A, Zhang Z, Inatomi O, Fujino S, Deguchi Y, Araki Y, Tsujikawa T, Kitoh K, Kim-Mitsuyama S, Takayanagi A, Shimizu N, Fujiyama Y. Interleukin-22, a member of the IL-10 subfamily, induces inflammatory responses in colonic subepithelial myofibroblasts. Gastroenterology. 2005 Sep;129(3):969-84. doi: 10.1053/j.gastro.2005.06.071. PMID: 16143135.

63- Brown JR, DuBois RN. COX-2: a molecular target for colorectal cancer prevention. J Clin Oncol. 2005 Apr 20;23(12):2840-55. doi: 10.1200/JCO.2005.09.051. PMID: 15837998.

64- Phipps RP, Stein SH, Roper RL. A new view of prostaglandin E regulation of the immune response. Immunol Today. 1991 Oct;12(10):349-52. doi: 10.1016/0167-5699(91)90064-Z. PMID: 1958288.

65- Weller CL, Collington SJ, Hartnell A, Conroy DM, Kaise T, Barker JE, Wilson MS, Taylor GW, Jose PJ, Williams TJ. Chemotactic action of prostaglandin E2 on mouse mast cells acting via the PGE2 receptor 3. Proc Natl Acad Sci U S A. 2007 Jul 10;104(28):11712-7. doi: 10.1073/pnas.0701700104. Epub 2007 Jul 2. PMID: 17606905; PMCID: PMC1913869.

66- Wang MT, Honn KV, Nie D. Cyclooxygenases, prostanoids, and tumor progression. Cancer Metastasis Rev. 2007 Dec;26(3-4):525-34. doi: 10.1007/s10555-007-9096-5. PMID: 17763971.

67- Park JY, Pillinger MH, Abramson SB. Prostaglandin E2 synthesis and secretion: the role of PGE2 synthases. Clin Immunol. 2006 Jun;119(3):229-40. doi: 10.1016/j.clim.2006.01.016. Epub 2006 Mar 15. PMID: 16540375.

68- Yan M, Myung SJ, Fink SP, Lawrence E, Lutterbaugh J, Yang P, Zhou X, Liu D, Rerko RM, Willis J, Dawson D, Tai HH, Barnholtz-Sloan JS, Newman RA, Bertagnolli MM, Markowitz SD. 15-Hydroxyprostaglandin

dehydrogenase inactivation as a mechanism of resistance to celecoxib chemoprevention of colon tumors. Proc Natl Acad Sci U S A. 2009 Jun 9;106(23):9409-13. doi: 10.1073/pnas.0902367106. Epub 2009 May 22. PMID: 19470469; PMCID: PMC2695050.

69- Yan M, Rerko RM, Platzer P, Dawson D, Willis J, Tong M, Lawrence E, Lutterbaugh J, Lu S, Willson JK, Luo G, Hensold J, Tai HH, Wilson K, Markowitz SD. 15-Hydroxyprostaglandin dehydrogenase, a COX-2 oncogene antagonist, is a TGF-beta-induced suppressor of human gastrointestinal cancers. Proc Natl Acad Sci U S A. 2004 Dec 14;101(50):17468-73. doi: 10.1073/pnas.0406142101. Epub 2004 Dec 1. PMID: 15574495; PMCID: PMC536023.

70- Myung SJ, Rerko RM, Yan M, Platzer P, Guda K, Dotson A, Lawrence E, Dannenberg AJ, Lovgren AK, Luo G, Pretlow TP, Newman RA, Willis J, Dawson D, Markowitz SD. 15-Hydroxyprostaglandin dehydrogenase is an in vivo suppressor of colon tumorigenesis. Proc Natl Acad Sci U S A. 2006 Aug 8;103(32):12098-102. doi: 10.1073/pnas.0603235103. Epub 2006 Jul 31. PMID: 16880406; PMCID: PMC1567703.

71- Moore AE, Young LE, Dixon DA. MicroRNA and AU-rich element regulation of prostaglandin synthesis. Cancer Metastasis Rev. 2011 Dec;30(3-4):419-35. doi: 10.1007/s10555-011-9300-5. PMID: 22005950; PMCID: PMC3447743.

72- Myung SJ, Rerko RM, Yan M, Platzer P, Guda K, Dotson A, Lawrence E, Dannenberg AJ, Lovgren AK, Luo G, Pretlow TP, Newman RA, Willis J, Dawson D, Markowitz SD. 15-Hydroxyprostaglandin dehydrogenase is an in vivo suppressor of colon tumorigenesis. Proc Natl Acad Sci U S A. 2006 Aug 8;103(32):12098-102. doi: 10.1073/pnas.0603235103. Epub 2006 Jul 31. PMID: 16880406; PMCID: PMC1567703.

73- Monteleone NJ, Moore AE, Iacona JR, Lutz CS, Dixon DA. miR-21-mediated regulation of 15-hydroxyprostaglandin dehydrogenase in colon cancer. Sci Rep. 2019 Apr 1;9(1):5405. doi: 10.1038/s41598-019-41862-2. PMID: 30931980; PMCID: PMC6443653.

74- Yi R, O'Carroll D, Pasolli HA, Zhang Z, Dietrich FS, Tarakhovsky A, Fuchs E. Morphogenesis in skin is governed by discrete sets of differentially expressed microRNAs. Nat Genet. 2006 Mar;38(3):356-62. doi: 10.1038/ng1744. Epub 2006 Feb 5. PMID: 16462742.

75- Yang Y, Ma Y, Shi C, Chen H, Zhang H, Chen N, Zhang P, Wang F, Yang J, Yang J, Zhu Q, Liang Y, Wu W, Gao R, Yang Z, Zou Y, Qin H. Overexpression of miR-21 in patients with ulcerative colitis impairs intestinal

epithelial barrier function through targeting the Rho GTPase RhoB. Biochem Biophys Res Commun. 2013 May 17;434(4):746-52. doi: 10.1016/j.bbrc.2013.03.122. Epub 2013 Apr 10. PMID: 23583411.

76- Wu F, Zhang S, Dassopoulos T, Harris ML, Bayless TM, Meltzer SJ, Brant SR, Kwon JH. Identification of microRNAs associated with ileal and colonic Crohn's disease. Inflamm Bowel Dis. 2010 Oct;16(10):1729-38. doi: 10.1002/ibd.21267. PMID: 20848482; PMCID: PMC2946509.

77- Schaefer JS, Attumi T, Opekun AR, Abraham B, Hou J, Shelby H, Graham DY, Streckfus C, Klein JR. MicroRNA signatures differentiate Crohn's disease from ulcerative colitis. BMC Immunol. 2015 Feb 10;16:5. doi: 10.1186/s12865-015-0069-0. PMID: 25886994; PMCID: PMC4335694.

78- Dai X, Chen X, Chen Q, Shi L, Liang H, Zhou Z, Liu Q, Pang W, Hou D, Wang C, Zen K, Yuan Y, Zhang CY, Xia L. MicroRNA-193a-3p Reduces Intestinal Inflammation in Response to Microbiota via Down-regulation of Colonic PepT1. J Biol Chem. 2015 Jun 26;290(26):16099-115. doi: 10.1074/jbc.M115.659318. Epub 2015 Apr 30. PMID: 25931122; PMCID: PMC4481212.

79- Runtsch MC, Hu R, Alexander M, Wallace J, Kagele D, Petersen C, Valentine JF, Welker NC, Bronner MP, Chen X, Smith DP, Ajami NJ, Petrosino JF, Round JL, O'Connell RM. MicroRNA-146a constrains multiple parameters of intestinal immunity and increases susceptibility to DSS colitis. Oncotarget. 2015 Oct 6;6(30):28556-72. doi: 10.18632/oncotarget.5597. PMID: 26456940; PMCID: PMC4745677.

80- Yamaguchi T, Iijima T, Wakaume R, Takahashi K, Matsumoto H, Nakano D, Nakayama Y, Mori T, Horiguchi S, Miyaki M. Underexpression of miR-126 and miR-20b in hereditary and nonhereditary colorectal tumors. Oncology. 2014;87(1):58-66. doi: 10.1159/000363303. Epub 2014 Jun 28. PMID: 24994098.

81- Hubbard LL, Ballinger MN, Thomas PE, Wilke CA, Standiford TJ, Kobayashi KS, Flavell RA, Moore BB. A role for IL-1 receptor-associated kinase-M in prostaglandin E2-induced immunosuppression post-bone marrow transplantation. J Immunol. 2010 Jun 1;184(11):6299-308. doi: 10.4049/jimmunol.0902828. Epub 2010 May 3. PMID: 20439918; PMCID: PMC4040537.

82- Snijdewint FG, Kaliński P, Wierenga EA, Bos JD, Kapsenberg ML. Prostaglandin E2 differentially modulates cytokine secretion profiles of human T helper lymphocytes. J Immunol. 1993 Jun 15;150(12):5321-9. PMID: 8390534

83- Khayrullina T, Yen JH, Jing H, Ganea D. In vitro differentiation of dendritic cells in the presence of prostaglandin E2 alters the IL-12/IL-23 balance and promotes differentiation of Th17 cells. J Immunol. 2008 Jul 1;181(1):721-35. doi: 10.4049/jimmunol.181.1.721. PMID: 18566439; PMCID: PMC2835359.

84- Bergmann C, Strauss L, Zeidler R, Lang S, Whiteside TL. Expansion of human T regulatory type 1 cells in the microenvironment of cyclooxygenase 2 overexpressing head and neck squamous cell carcinoma. Cancer Res. 2007 Sep 15;67(18):8865-73. doi: 10.1158/0008-5472.CAN-07-0767. PMID: 17875728.

85- Banerjee DK, Dhodapkar MV, Matayeva E, Steinman RM, Dhodapkar KM. Expansion of FOXP3high regulatory T cells by human dendritic cells (DCs) in vitro and after injection of cytokine-matured DCs in myeloma patients. Blood. 2006 Oct 15;108(8):2655-61. doi: 10.1182/blood-2006-03-011353. Epub 2006 Jun 8. PMID: 16763205; PMCID: PMC1895594.

86- Huang M, Stolina M, Sharma S, Mao JT, Zhu L, Miller PW, Wollman J, Herschman H, Dubinett SM. Non-small cell lung cancer cyclooxygenase-2-dependent regulation of cytokine balance in lymphocytes and macrophages: up-regulation of interleukin 10 and down-regulation of interleukin 12 production. Cancer Res. 1998 Mar 15;58(6):1208-16. PMID: 9515807.

87- Ochoa AC, Zea AH, Hernandez C, Rodriguez PC. Arginase, prostaglandins, and myeloid-derived suppressor cells in renal cell carcinoma. Clin Cancer Res. 2007 Jan 15;13(2 Pt 2):721s-726s. doi: 10.1158/1078-0432.CCR-06-2197. PMID: 17255300.

88- Fujita M, Kohanbash G, Fellows-Mayle W, Hamilton RL, Komohara Y, Decker SA, Ohlfest JR, Okada H. COX-2 blockade suppresses gliomagenesis by inhibiting myeloid-derived suppressor cells. Cancer Res. 2011 Apr 1;71(7):2664-74. doi: 10.1158/0008-5472.CAN-10-3055. Epub 2011 Feb 15. PMID: 21324923; PMCID: PMC3075086.

89- Rossi G, Manfrin A, Lutolf MP. Progress and potential in organoid research. Nat Rev Genet. 2018 Nov;19(11):671-687. doi: 10.1038/s41576-018-0051-9. PMID: 30228295.

90- EHRMANN RL, GEY GO. The growth of cells on a transparent gel of reconstituted rat-tail collagen. J Natl Cancer Inst. 1956 Jun;16(6):1375-403. PMID: 13320119.

91- Orkin RW, Gehron P, McGoodwin EB, Martin GR, Valentine T, Swarm R. A murine tumor producing a matrix of basement membrane. J Exp Med.

1977 Jan 1;145(1):204-20. doi: 10.1084/jem.145.1.204. PMID: 830788; PMCID: PMC2180589.

92- Michalopoulos G, Pitot HC. Primary culture of parenchymal liver cells on collagen membranes. Morphological and biochemical observations. Exp Cell Res. 1975 Aug;94(1):70-8. doi: 10.1016/0014-4827(75)90532-7. PMID: 243.

93- Sato T, Vries RG, Snippert HJ, van de Wetering M, Barker N, Stange DE, van Es JH, Abo A, Kujala P, Peters PJ, Clevers H. Single Lgr5 stem cells build crypt-villus structures in vitro without a mesenchymal niche. Nature. 2009 May 14;459(7244):262-5. doi: 10.1038/nature07935. Epub 2009 Mar 29. PMID: 19329995.

94- Sasai Y. Cytosystems dynamics in self-organization of tissue architecture. Nature. 2013 Jan 17;493(7432):318-26. doi: 10.1038/nature11859. PMID: 23325214.

95- Sato T, van Es JH, Snippert HJ, Stange DE, Vries RG, van den Born M, Barker N, Shroyer NF, van de Wetering M, Clevers H. Paneth cells constitute the niche for Lgr5 stem cells in intestinal crypts. Nature. 2011 Jan 20;469(7330):415-8. doi: 10.1038/nature09637. Epub 2010 Nov 28. PMID: 21113151; PMCID: PMC3547360.

96- Sato T, Clevers H. Growing self-organizing mini-guts from a single intestinal stem cell: mechanism and applications. Science. 2013 Jun 7;340(6137):1190-4. doi: 10.1126/science.1234852. PMID: 23744940.

97- Lancaster MA, Renner M, Martin CA, Wenzel D, Bicknell LS, Hurles ME, Homfray T, Penninger JM, Jackson AP, Knoblich JA. Cerebral organoids model human brain development and microcephaly. Nature. 2013 Sep 19;501(7467):373-9. doi: 10.1038/nature12517. Epub 2013 Aug 28. PMID: 23995685; PMCID: PMC3817409.

98- Huch M, Gehart H, van Boxtel R, Hamer K, Blokzijl F, Verstegen MM, Ellis E, van Wenum M, Fuchs SA, de Ligt J, van de Wetering M, Sasaki N, Boers SJ, Kemperman H, de Jonge J, Ijzermans JN, Nieuwenhuis EE, Hoekstra R, Strom S, Vries RR, van der Laan LJ, Cuppen E, Clevers H. Long-term culture of genome-stable bipotent stem cells from adult human liver. Cell. 2015 Jan 15;160(1-2):299-312. doi: 10.1016/j.cell.2014.11.050. Epub 2014 Dec 18. PMID: 25533785; PMCID: PMC4313365.

99- McCracken KW, Catá EM, Crawford CM, Sinagoga KL, Schumacher M, Rockich BE, Tsai YH, Mayhew CN, Spence JR, Zavros Y, Wells JM. Modelling human development and disease in pluripotent stem-cell-derived gastric organoids. Nature. 2014 Dec 18;516(7531):400-4. doi:

10.1038/nature13863. Epub 2014 Oct 29. PMID: 25363776; PMCID: PMC4270898.

100- Bartfeld S, Bayram T, van de Wetering M, Huch M, Begthel H, Kujala P, Vries R, Peters PJ, Clevers H. In vitro expansion of human gastric epithelial stem cells and their responses to bacterial infection. Gastroenterology. 2015 Jan;148(1):126-136.e6. doi: 10.1053/j.gastro.2014.09.042. Epub 2014 Oct 13. PMID: 25307862; PMCID: PMC4274199.

101- Castellanos-Gonzalez A, Cabada MM, Nichols J, Gomez G, White AC Jr. Human primary intestinal epithelial cells as an improved in vitro model for Cryptosporidium parvum infection. Infect Immun. 2013 Jun;81(6):1996-2001. doi: 10.1128/IAI.01131-12. Epub 2013 Mar 18. PMID: 23509153; PMCID: PMC3676030.

102- Cugola FR, Fernandes IR, Russo FB, Freitas BC, Dias JL, Guimarães KP, Benazzato C, Almeida N, Pignatari GC, Romero S, Polonio CM, Cunha I, Freitas CL, Brandão WN, Rossato C, Andrade DG, Faria Dde P, Garcez AT, Buchpigel CA, Braconi CT, Mendes E, Sall AA, Zanotto PM, Peron JP, Muotri AR, Beltrão-Braga PC. The Brazilian Zika virus strain causes birth defects in experimental models. Nature. 2016 Jun 9;534(7606):267-71. doi: 10.1038/nature18296. Epub 2016 May 11. PMID: 27279226; PMCID: PMC4902174.

103- Zhou T, Tan L, Cederquist GY, Fan Y, Hartley BJ, Mukherjee S, Tomishima M, Brennand KJ, Zhang Q, Schwartz RE, Evans T, Studer L, Chen S. High-Content Screening in hPSC-Neural Progenitors Identifies Drug Candidates that Inhibit Zika Virus Infection in Fetal-like Organoids and Adult Brain. Cell Stem Cell. 2017 Aug 3;21(2):274-283.e5. doi: 10.1016/j.stem.2017.06.017. Epub 2017 Jul 20. PMID: 28736217; PMCID: PMC5553280.

104- Cutting GR. Modifier genetics: cystic fibrosis. Annu Rev Genomics Hum Genet. 2005;6:237-60. doi: 10.1146/annurev.genom.6.080604.162254. PMID: 16124861.

105- Sachs N, de Ligt J, Kopper O, Gogola E, Bounova G, Weeber F, Balgobind AV, Wind K, Gracanin A, Begthel H, Korving J, van Boxtel R, Duarte AA, Lelieveld D, van Hoeck A, Ernst RF, Blokzijl F, Nijman IJ, Hoogstraat M, van de Ven M, Egan DA, Zinzalla V, Moll J, Boj SF, Voest EE, Wessels L, van Diest PJ, Rottenberg S, Vries RGJ, Cuppen E, Clevers H. A Living Biobank of Breast Cancer Organoids Captures Disease Heterogeneity. Cell. 2018 Jan 11;172(1-2):373-386.e10. doi: 10.1016/j.cell.2017.11.010. Epub 2017 Dec 7. PMID: 29224780.

106- Broutier L, Andersson-Rolf A, Hindley CJ, Boj SF, Clevers H, Koo BK, Huch M. Culture and establishment of self-renewing human and mouse adult liver and pancreas 3D organoids and their genetic manipulation. Nat Protoc. 2016 Sep;11(9):1724-43. doi: 10.1038/nprot.2016.097. Epub 2016 Aug 25. PMID: 27560176.

107- Prior N, Inacio P, Huch M. Liver organoids: from basic research to therapeutic applications. Gut. 2019 Dec;68(12):2228-2237. doi: 10.1136/gutjnl-2019-319256. Epub 2019 Jul 12. PMID: 31300517; PMCID: PMC6872443.

108- Little MH, Combes AN. Kidney organoids: accurate models or fortunate accidents. Genes Dev. 2019 Oct 1;33(19-20):1319-1345. doi: 10.1101/gad.329573.119. PMID: 31575677; PMCID: PMC6771389.

109- Qian X, Song H, Ming GL. Brain organoids: advances, applications and challenges. Development. 2019 Apr 16;146(8):dev166074. doi: 10.1242/dev.166074. PMID: 30992274; PMCID: PMC6503989.

110- Sato T, Stange DE, Ferrante M, Vries RG, Van Es JH, Van den Brink S, Van Houdt WJ, Pronk A, Van Gorp J, Siersema PD, Clevers H. Long-term expansion of epithelial organoids from human colon, adenoma, adenocarcinoma, and Barrett's epithelium. Gastroenterology. 2011 Nov;141(5):1762-72. doi: 10.1053/j.gastro.2011.07.050. Epub 2011 Sep 2. PMID: 21889923.

111- Crespo M, Vilar E, Tsai SY, Chang K, Amin S, Srinivasan T, Zhang T, Pipalia NH, Chen HJ, Witherspoon M, Gordillo M, Xiang JZ, Maxfield FR, Lipkin S, Evans T, Chen S. Colonic organoids derived from human induced pluripotent stem cells for modeling colorectal cancer and drug testing. Nat Med. 2017 Jul;23(7):878-884. doi: 10.1038/nm.4355. Epub 2017 Jun 19. Erratum in: Nat Med. 2018 Apr 10;24(4):526. PMID: 28628110; PMCID: PMC6055224.

112- Fernández-Ballart JD, Piñol JL, Zazpe I, Corella D, Carrasco P, Toledo E, Perez-Bauer M, Martínez-González MA, Salas-Salvadó J, Martín-Moreno JM. Relative validity of a semi-quantitative food-frequency questionnaire in an elderly Mediterranean population of Spain. Br J Nutr. 2010 Jun;103(12):1808-16. doi: 10.1017/S0007114509993837. Epub 2010 Jan 27. PMID: 20102675.

113- Pasanisi P, Gariboldi M, Verderio P, Signoroni S, Mancini A, Rivoltini L, Milione M, Masci E, Ciniselli CM, Bruno E, Macciotta A, Belfiore A, Ricci MT, Gargano G, Morelli D, Apolone G, Vitellaro M. A Pilot Low-Inflammatory Dietary Intervention to Reduce Inflammation and Improve Quality of Life in

Patients With Familial Adenomatous Polyposis: Protocol Description and Preliminary Results. Integr Cancer Ther. 2019 Jan-Dec;18:1534735419846400. doi: 10.1177/1534735419846400. PMID: 31055940; PMCID: PMC6505234.

114- De Simone V, Franzè E, Ronchetti G, Colantoni A, Fantini MC, Di Fusco D, Sica GS, Sileri P, MacDonald TT, Pallone F, Monteleone G, Stolfi C. Th17-type cytokines, IL-6 and TNF-α synergistically activate STAT3 and NF-kB to promote colorectal cancer cell growth. Oncogene. 2015 Jul;34(27):3493-503. doi: 10.1038/onc.2014.286. Epub 2014 Sep 1. PMID: 25174402; PMCID: PMC4493653.

115- Bosshart H, Heinzelmann M. THP-1 cells as a model for human monocytes. Ann Transl Med. 2016 Nov;4(21):438. doi: 10.21037/atm.2016.08.53. PMID: 27942529; PMCID: PMC5124613.

116- https://www.r-project.org/

117- Powell D. R. Degust v3.2.0. Zenodo https://doi.org/10.5281/zenodo.3258933 (2015)

118- Cheasley D, Wakefield MJ, Ryland GL, Allan PE, Alsop K, Amarasinghe KC, Ananda S, Anglesio MS, Au-Yeung G, Böhm M, Bowtell DDL, Brand A, Chenevix-Trench G, Christie M, Chiew YE, Churchman M, DeFazio A, Demeo R, Dudley R, Fairweather N, Fedele CG, Fereday S, Fox SB, Gilks CB, Gourley C, Hacker NF, Hadley AM, Hendley J, Ho GY, Hughes S, Hunstman DG, Hunter SM, Jobling TW, Kalli KR, Kaufmann SH, Kennedy CJ, Köbel M, Le Page C, Li J, Lupat R, McNally OM, McAlpine JN, Mes-Masson AM, Mileshkin L, Provencher DM, Pyman J, Rahimi K, Rowley SM, Salazar C, Samimi G, Saunders H, Semple T, Sharma R, Sharpe AJ, Stephens AN, Thio N, Torres MC, Traficante N, Xing Z, Zethoven M, Antill YC, Scott CL, Campbell IG, Gorringe KL. The molecular origin and taxonomy of mucinous ovarian carcinoma. Nat Commun. 2019 Sep 2;10(1):3935. doi: 10.1038/s41467-019-11862-x. PMID: 31477716; PMCID: PMC6718426.

119- Chen, Y., Lun, A. T., McCarthy, D. J., Ritchie, M. E., Phipson, B., Hu, Y., ... & Smyth, G. K. edgeR-package: Empirical analysis of digital gene expression data in R.

120- Yan M, Rerko RM, Platzer P, Dawson D, Willis J, Tong M, Lawrence E, Lutterbaugh J, Lu S, Willson JK, Luo G, Hensold J, Tai HH, Wilson K, Markowitz SD. 15-Hydroxyprostaglandin dehydrogenase, a COX-2 oncogene antagonist, is a TGF-beta-induced suppressor of human gastrointestinal cancers. Proc Natl Acad Sci U S A. 2004 Dec

14;101(50):17468-73. doi: 10.1073/pnas.0406142101. Epub 2004 Dec 1. PMID: 15574495; PMCID: PMC536023.

121- Costales-Carrera A, Fernández-Barral A, Bustamante-Madrid P, Domínguez O, Guerra-Pastrián L, Cantero R, Del Peso L, Burgos A, Barbáchano A, Muñoz A. Comparative Study of Organoids from Patient-Derived Normal and Tumor Colon and Rectal Tissue. Cancers (Basel). 2020 Aug 15;12(8):2302. doi: 10.3390/cancers12082302. PMID: 32824266; PMCID: PMC7465167.

122- De Simone V, Franzè E, Ronchetti G, Colantoni A, Fantini MC, Di Fusco D, Sica GS, Sileri P, MacDonald TT, Pallone F, Monteleone G, Stolfi C. Th17-type cytokines, IL-6 and TNF-α synergistically activate STAT3 and NF-kB to promote colorectal cancer cell growth. Oncogene. 2015 Jul;34(27):3493-503. doi: 10.1038/onc.2014.286. Epub 2014 Sep 1. PMID: 25174402; PMCID: PMC4493653.

114- Chan E, Lafleur B, Rothenberg ML, Merchant N, Lockhart AC, Trivedi B, Chung CH, Coffey RJ, Berlin JD. Dual blockade of the EGFR and COX-2 pathways: a phase II trial of cetuximab and celecoxib in patients with chemotherapy refractory metastatic colorectal cancer. Am J Clin Oncol. 2011 Dec;34(6):581-6. doi: 10.1097/COC.0b013e3181fe46a1. PMID: 21217396; PMCID: PMC3133812.

115- Hashemi Goradel N, Najafi M, Salehi E, Farhood B, Mortezaee K. Cyclooxygenase-2 in cancer: A review. J Cell Physiol. 2019 May;234(5):5683-5699. doi: 10.1002/jcp.27411. Epub 2018 Oct 20. PMID: 30341914.

116- Wang J, Zou K, Feng X, Chen M, Li C, Tang R, Xuan Y, Luo M, Chen W, Qiu H, Qin G, Li Y, Zhang C, Xiao B, Kang L, Kang T, Huang W, Yu X, Wu X, Deng W. Downregulation of NMI promotes tumor growth and predicts poor prognosis in human lung adenocarcinomas. Mol Cancer. 2017 Oct 12;16(1):158. doi: 10.1186/s12943-017-0705-9. PMID: 29025423; PMCID: PMC5639741.

117- Araki Y, Okamura S, Hussain SP, Nagashima M, He P, Shiseki M, Miura K, Harris CC. Regulation of cyclooxygenase-2 expression by the Wnt and ras pathways. Cancer Res. 2003 Feb 1;63(3):728-34. PMID: 12566320.

118- Kawahara K, Hohjoh H, Inazumi T, Tsuchiya S, Sugimoto Y. Prostaglandin E2-induced inflammation: Relevance of prostaglandin E receptors. Biochim Biophys Acta. 2015 Apr;1851(4):414-21. doi: 10.1016/j.bbalip.2014.07.008. Epub 2014 Jul 17. PMID: 25038274.

119- Gravaghi C, La Perle KM, Ogrodwski P, Kang JX, Quimby F, Lipkin M, Lamprecht SA. Cox-2 expression, PGE(2) and cytokines production are inhibited by endogenously synthesized n-3 PUFAs in inflamed colon of fat-1 mice. J Nutr Biochem. 2011 Apr;22(4):360-5. doi: 10.1016/j.jnutbio.2010.03.003. Epub 2010 Jul 23. PMID: 20655721.

120- Fini L, Piazzi G, Ceccarelli C, Daoud Y, Belluzzi A, Munarini A, Graziani G, Fogliano V, Selgrad M, Garcia M, Gasbarrini A, Genta RM, Boland CR, Ricciardiello L. Highly purified eicosapentaenoic acid as free fatty acids strongly suppresses polyps in Apc(Min/+) mice. Clin Cancer Res. 2010 Dec 1;16(23):5703-11. doi: 10.1158/1078-0432.CCR-10-1990. Epub 2010 Oct 28. PMID: 21030497; PMCID: PMC3795521.

121- Mustata RC, Vasile G, Fernandez-Vallone V, Strollo S, Lefort A, Libert F, Monteyne D, Pérez-Morga D, Vassart G, Garcia MI. Identification of Lgr5-independent spheroid-generating progenitors of the mouse fetal intestinal epithelium. Cell Rep. 2013 Oct 31;5(2):421-32. doi: 10.1016/j.celrep.2013.09.005. Epub 2013 Oct 17. PMID: 24139799.

122- Cremon C, Carini G, Wang B, Vasina V, Cogliandro RF, De Giorgio R, Stanghellini V, Grundy D, Tonini M, De Ponti F, Corinaldesi R, Barbara G. Intestinal serotonin release, sensory neuron activation, and abdominal pain in irritable bowel syndrome. Am J Gastroenterol. 2011 Jul;106(7):1290-8. doi: 10.1038/ajg.2011.86. Epub 2011 Mar 22. PMID: 21427712.

123- Sun D, Lin Y, Hong J, Chen H, Nagarsheth N, Peng D, Wei S, Huang E, Fang J, Kryczek I, Zou W. Th22 cells control colon tumorigenesis through STAT3 and Polycomb Repression complex 2 signaling. Oncoimmunology. 2015 Sep 2;5(8):e1082704. doi: 10.1080/2162402X.2015.1082704. PMID: 27622053; PMCID: PMC5007968.

124- Doulabi H, Rastin M, Shabahangh H, Maddah G, Abdollahi A, Nosratabadi R, Esmaeili SA, Mahmoudi M. Analysis of Th22, Th17 and $CD4^+$cells co-producing IL-17/IL-22 at different stages of human colon cancer. Biomed Pharmacother. 2018 Jul;103:1101-1106. doi: 10.1016/j.biopha.2018.04.147. Epub 2018 Apr 26. PMID: 29710675.

125- Sun D, Lin Y, Hong J, Chen H, Nagarsheth N, Peng D, Wei S, Huang E, Fang J, Kryczek I, Zou W. Th22 cells control colon tumorigenesis through STAT3 and Polycomb Repression complex 2 signaling. Oncoimmunology. 2015 Sep 2;5(8):e1082704. doi: 10.1080/2162402X.2015.1082704. PMID: 27622053; PMCID: PMC5007968.

126- Wolff MJ, Leung JM, Davenport M, Poles MA, Cho I, Loke P. TH17, TH22 and Treg cells are enriched in the healthy human cecum. PLoS One.

2012;7(7):e41373. doi: 10.1371/journal.pone.0041373. Epub 2012 Jul 19. PMID: 22829946; PMCID: PMC3400627.

127- Komoda H, Tanaka Y, Honda M, Matsuo Y, Hazama K, Takao T. Interleukin-6 levels in colorectal cancer tissues. World J Surg. 1998 Aug;22(8):895-8. doi: 10.1007/s002689900489. PMID: 9673566.

128- Chung YC, Chang YF. Serum interleukin-6 levels reflect the disease status of colorectal cancer. J Surg Oncol. 2003 Aug;83(4):222-6. doi: 10.1002/jso.10269. PMID: 12884234.

129- Ma N, Zhao Y. DMBT1 suppresses cell proliferation, migration and invasion in ovarian cancer and enhances sensitivity to cisplatin through galectin-3/PI3k/Akt pathway. Cell Biochem Funct. 2020 Aug;38(6):801-809. doi: 10.1002/cbf.3549. Epub 2020 May 19. PMID: 32424818.

130- Du J, Guan M, Fan J, Jiang H. Loss of DMBT1 expression in human prostate cancer and its correlation with clinical progressive features. Urology. 2011 Feb;77(2):509.e9-13. doi: 10.1016/j.urology.2010.09.023. Epub 2010 Dec 16. PMID: 21167560.

131- Schulten HJ, Bangash M, Karim S, Dallol A, Hussein D, Merdad A, Al-Thoubaity FK, Al-Maghrabi J, Jamal A, Al-Ghamdi F, Choudhry H, Baeesa SS, Chaudhary AG, Al-Qahtani MH. Comprehensive molecular biomarker identification in breast cancer brain metastases. J Transl Med. 2017 Dec 29;15(1):269. doi: 10.1186/s12967-017-1370-x. PMID: 29287594; PMCID: PMC5747948.

132- Park HS, Kim BC, Yeo HY, Kim KH, Yoo BC, Park JW, Chang HJ. Deleted in malignant brain tumor 1 is a novel prognostic marker in colorectal cancer. Oncol Rep. 2018 May;39(5):2279-2287. doi: 10.3892/or.2018.6287. Epub 2018 Mar 1. PMID: 29498404.

133- Fukui H, Sekikawa A, Tanaka H, Fujimori Y, Katake Y, Fujii S, Ichikawa K, Tomita S, Imura J, Chiba T, Fujimori T. DMBT1 is a novel gene induced by IL-22 in ulcerative colitis. Inflamm Bowel Dis. 2011 May;17(5):1177-88. doi: 10.1002/ibd.21473. Epub 2010 Sep 7. PMID: 20824812.

134- Kinseth MA, Jia Z, Rahmatpanah F, Sawyers A, Sutton M, Wang-Rodriguez J, Mercola D, McGuire KL. Expression differences between African American and Caucasian prostate cancer tissue reveals that stroma is the site of aggressive changes. Int J Cancer. 2014 Jan 1;134(1):81-91. doi: 10.1002/ijc.28326. Epub 2013 Jul 13. PMID: 23754304; PMCID: PMC3800217.

135- Callahan MJ, Nagymanyoki Z, Bonome T, Johnson ME, Litkouhi B, Sullivan EH, Hirsch MS, Matulonis UA, Liu J, Birrer MJ, Berkowitz RS, Mok SC. Increased HLA-DMB expression in the tumor epithelium is associated with increased CTL infiltration and improved prognosis in advanced-stage serous ovarian cancer. Clin Cancer Res. 2008 Dec 1;14(23):7667-73. doi: 10.1158/1078-0432.CCR-08-0479. PMID: 19047092; PMCID: PMC3000165.

136- Kvorjak M, Ahmed Y, Miller ML, Sriram R, Coronnello C, Hashash JG, Hartman DJ, Telmer CA, Miskov-Zivanov N, Finn OJ, Cascio S. Cross-talk between Colon Cells and Macrophages Increases ST6GALNAC1 and MUC1-sTn Expression in Ulcerative Colitis and Colitis-Associated Colon Cancer. Cancer Immunol Res. 2020 Feb;8(2):167-178. doi: 10.1158/2326-6066.CIR-19-0514. Epub 2019 Dec 12. PMID: 31831633; PMCID: PMC7002239.

137- Tamoutounour S, Henri S, Lelouard H, de Bovis B, de Haar C, van der Woude CJ, Woltman AM, Reyal Y, Bonnet D, Sichien D, Bain CC, Mowat AM, Reis e Sousa C, Poulin LF, Malissen B, Guilliams M. CD64 distinguishes macrophages from dendritic cells in the gut and reveals the Th1-inducing role of mesenteric lymph node macrophages during colitis. Eur J Immunol. 2012 Dec;42(12):3150-66. doi: 10.1002/eji.201242847. Epub 2012 Oct 17. PMID: 22936024.

138- Aranda CJ, Ocón B, Arredondo-Amador M, Suárez MD, Zarzuelo A, Chazin WJ, Martínez-Augustin O, Sánchez de Medina F. Calprotectin protects against experimental colonic inflammation in mice. Br J Pharmacol. 2018 Oct;175(19):3797-3812. doi: 10.1111/bph.14449. Epub 2018 Sep 2. PMID: 30007036; PMCID: PMC6135788.

139- Mattiske S, Suetani RJ, Neilsen PM, Callen DF. The oncogenic role of miR-155 in breast cancer. Cancer Epidemiol Biomarkers Prev. 2012 Aug;21(8):1236-43. doi: 10.1158/1055-9965.EPI-12-0173. Epub 2012 Jun 26. PMID: 22736789.

140- Akao Y, Nakagawa Y, Naoe T. MicroRNAs 143 and 145 are possible common onco-microRNAs in human cancers. Oncol Rep. 2006 Oct;16(4):845-50. PMID: 16969504.

141- Hutchison J, Cohen Z, Onyeagucha BC, Funk J, Nelson MA. How microRNAs influence both hereditary and inflammatory-mediated colon cancers. Cancer Genet. 2013 Sep-Oct;206(9-10):309-16. doi: 10.1016/j.cancergen.2013.06.005. Epub 2013 Sep 14. PMID: 24042167; PMCID: PMC3893936.

142- Fasseu M, Tréton X, Guichard C, Pedruzzi E, Cazals-Hatem D, Richard C, Aparicio T, Daniel F, Soulé JC, Moreau R, Bouhnik Y, Laburthe M, Groyer A, Ogier-Denis E. Identification of restricted subsets of mature microRNA abnormally expressed in inactive colonic mucosa of patients with inflammatory bowel disease. PLoS One. 2010 Oct 5;5(10):e13160. doi: 10.1371/journal.pone.0013160. PMID: 20957151; PMCID: PMC2950152.

143- Ye D, Guo S, Al-Sadi R, Ma TY. MicroRNA regulation of intestinal epithelial tight junction permeability. Gastroenterology. 2011 Oct;141(4):1323-33. doi: 10.1053/j.gastro.2011.07.005. Epub 2011 Jul 18. PMID: 21763238; PMCID: PMC3724217.

144- Wu F, Zikusoka M, Trindade A, Dassopoulos T, Harris ML, Bayless TM, Brant SR, Chakravarti S, Kwon JH. MicroRNAs are differentially expressed in ulcerative colitis and alter expression of macrophage inflammatory peptide-2 alpha. Gastroenterology. 2008 Nov;135(5):1624-1635.e24. doi: 10.1053/j.gastro.2008.07.068. Epub 2008 Aug 3. PMID: 18835392.

145- Strillacci A, Griffoni C, Sansone P, Paterini P, Piazzi G, Lazzarini G, Spisni E, Pantaleo MA, Biasco G, Tomasi V. MiR-101 downregulation is involved in cyclooxygenase-2 overexpression in human colon cancer cells. Exp Cell Res. 2009 May 1;315(8):1439-47. doi: 10.1016/j.yexcr.2008.12.010. Epub 2008 Dec 24. PMID: 19133256.

146- Ji Y, He Y, Liu L, Chong X. Corrigendum to "MiRNA-26b regulates the expression of cyclooxygenase-2 in desferrioxamine-treated CNE cells" [FEBS Lett. 584 (5) (2010) 961-967]. FEBS Lett. 2015 Jan 16;589(2):277. doi: 10.1016/j.febslet.2014.12.001. Erratum for: FEBS Lett. 2010 Mar 5;584(5):961-7. PMID: 26874650.

10 ACKNOWLEDGEMENTS

There is a long list of people who contributed to the realization of this thesis, and the gratitude towards them is even greater.

Difficulties have arises during the last three years of PhD when even finishing an experiment seemed like a mission impossible. However, most of the times when problems have occurred, Dr. Manuela Gariboldi has found solutions to continue this study. My deepest and most heartfelt thanks go to her, because, beyond the teachings and advices she has given me, the patience and dedication she has used over the years, will be an example for me in the years to come.
Another special thank goes to Professor Nadia Ranzani, without whom I could never have reached this goal. Three years ago, after admission to the PhD course she told me that I would be one of her last PhD students, given the admiration I have for her, I have worked hard to ensure that the opportunity that was given to me was deserved.

A huge thanks goes to all the staff of the Department of Pathology and Laboratory Medicine of the IRCCS Istituto Nazionale Tumori of Milan, where I carried out the entire study. In particular I would like to thank the head of the department, Prof. Giancarlo Pruneri who allowed me to carry out my PhD by giving me the opportunity to dedicate myself to this study. I am honored to be part of his staff.
Within the department I cannot fail to thank my colleagues ”I ragazzi di CRAB” of the Clinical Research lABoratory, in particular:
Andrea Vingiani, our coordinator and friend, the one who endured all my speculations on organoids, colorectal adenomas, cytokines and many other sometimes senseless things, always finding the time to listen and advise me.
Silvia Brich, the colleague I have known for the longest time and the one who, when I was the "new-comer" in the lab, explained to me how to do my first Western Blot.
Alessia Bertolotti, the person who always knows how to give good advices.
Giovanni Centonze, who patiently helped me when I fist approached R environment.
Vincenzo Lagano, who has been putting up with my daily complaints for the past few months.
Also, I would like to thank all the Molecular Laboratory staff of our Department, in particular Dr Elena Tamborini and Federica Perrone, Adele Busico, Elena Conca and Iolanda Capone for the NGS analysis. Luca Agnelli, who introduced me even just below of the surface of bioinformatics and whose experience helped me to figure out the meaning of my data.

Dr Fabio Bozzi, the “master” of cell cultures and Luca Varinelli, with whom I started the Organoids generation.
Cristina Borzì and Massimiliano Moro, who helped me in cell cycle analysis.
A special thank goes also to Dr Marco Vitellaro, head of the Unit of Hereditary Digestive Tract Tumors of Fondazione IRCCS Istituto Nazionale dei Tumori of Milan. He designed the pilot dietary intervention study conducted on AAP patients together with Dr Stefano Signoroni and Dr Patrizia Pasanisi of the Unit of Epidemiology and Prevention.
I would also like to thank Dr Paolo Verderio and Dr Chiara Ciniselli of the Unit of Bioinformatics and Biostatistics who helped me with statistical analysis of data presented in the study. Dr Licia Rivoltini and Elena Daveri of the Unit of Immunotherapy of Human Tumors who helped me with THP1 cells.
Finally, I would like to thank Dr Massimo Milione, head of the First Pathology Division, who helped me in the interpretation of IHC data and introduced me to the analysis of the histological and morphological features of normal and adenomatous colorectal mucosa.

In conclusion I dedicate this thesis and the efforts of these years to people I love the most: Sonia, my mother, Massimo and Maria Laura, because when fatigue and difficulties arise along the way of life, only those who love you can give you the strength to continue.

11 SUPPLEMENTARY MATERIAL

Supplementary Table 1. Category Summary

Categories	# of Genes
Chemokines	25
Cytokines	22
Cell Functions	82
B-Cell Functions	13
Antigen Processing	155
Regulation	99
Cytotoxicity	15
NK Cell Functions	56
Transporter Functions	10
Pathogen Defense	38
Cell Cycle	6
Leukocyte Functions	6
T-Cell Functions	5
Adhesion	17
Complement	12
Senescence	154
Interleukins	12
Macrophage Functions	82
TLR	11
Microglial Functions	30
TNF Superfamily	22

Supplementary Table 1: Summary of the immune response categories included in the NanoString PanCancer Immune profile panel. Credits Nanostring Technology

Supplementary Table 2 - Primary Annotation Summary

Primary Annotations	# of Genes
Acute-phase response	8
Adaptive immune response	109
Adhesion	25
Antigen processing and presentation	21
Anti-inflammatory cytokines	10
Autophagic vacuole formation	1
Autophagy induction by intracellular pathogens	1
Basic cell functions	61
B-cell activation	8
B-cell differentiation	5
B-cell proliferation	1
B-cell receptor signaling pathway	3
CD molecules	238
CD8-positive	2
Cell cycle arrest	1
Cell cycle checkpoint and cell cycle arrest	2
Cell Type specific	109
Chemokines and receptors	88
Chronic inflammatory response	6
Chronic inflammatory response to antigenic stimulus	1
Complement pathway	15
Co-Regulators of autophagy and apoptosis/cell cycle	6
Cytokines and receptors	62
Cytotoxicity	10
Defense response to bacterium	2
Defense response to fungus	2
Defense response to tumor cell	1
Defense response to virus	10
DNA damage checkpoint	1
G1/S transition of mitotic cell cycle	1
G2 phase and G2/M transition	1
Genes linking autophagosome to lysosome	1
Genes responsible for protein transport	3
Humoral immune response	41
Immune response to tumor cell	1
Immunosuppression	3

Induction of apoptosis	1
Inflammatory response	29
Inflammatory response to antigenic stimulus	5
Innate immune response	200
Interleukins	42
Leukocyte activation	2
Leukocyte migration	5
Lipid transporter activity	1
M phase of mitotic cell cycle	1
Macrophage activation	6
Microglial cell activation	5
Negative regulation of antigen processing	1
Negative regulation of cell cycle	1
Negative regulation of immune response	9
NK cell activation	2
NK cell functions	15
Phagocytosis	3
Phagocytosis recognition and engulfment	4
Phagosome processing	1
Phagyocytosis signal transduction	2
Positive regulation of B-cell proliferation	1
Positive regulation of immune response	10
Positive regulation of macrophages	1
Protein ubiquitination	1
Receptors involved in phagocytosis	7
Regulation of cell cycle	3
Regulation of immune response	63
Regulation of inflammatory response	25
Regulators of T-cell activation	9
Regulators of Th1 and Th2 development	6
Response to drug	4
S phase and DNA replication	1
Senescence initiators	3
Senescence initiators interferon related	4
Senescence pathway	6
T-cell activation	12
T-cell anergy	2
T-cell differentiation	15
T-cell mediated immunity	1

T-cell polarization	12
T-cell proliferation	11
T-cell receptor signaling pathway	1
T-cell regulators	4
Th1 & Th2 differentiation	6
Th1 orientation	16
Th2 orientation	9
TNF superfamily members and their receptors	30
Toll-like receptor	11
Transcription factors	20
Transcriptional regulators	15

Supplementary Table 2: Summary of pathway annotations included in the NanoString PanCancer Immune profile panel. Credits Nanostring Technology.

FAP1 Tissue

Location	Consequence	Symbol	Exon	HGVSc	HGVSp	Codons	Clinical Significance
2:212812097-212812097	intron_variant	*ERBB4*	/	c.421+58A>G	/	/	/
4:1807894-1807894	synonymous variant	*FGFR3*	14/18	c.1959G>A	p.Thr653=	ACG/ACA	benign, likely_benign
4:55141055-55141055	synonymous variant	*PDGFRA*	13/23	c.1701A>G	p.Pro567=	CCA/CCG	benign
4:55593481-55593481	synonymous variant	*KIT*	10/21	c.1638A>G	p.Lys546=	AAA/AAG	likely_benign
4:55946354-55946354	intron_variant	*KDR*	/	c.3849-24C>A	/	/	/
5:112837963-112837965	deletion, frameshift_variant	*APC*	16/16	c.2369_2372delinsGACA	p.Arg790ThrFS*2P	/	/
5:112175770-112175770	synonymous variant	*APC*	16/16	c.4479G>A	p.Thr1493=	ACG/ACA	other, benign
5:149433596-149433597	3_prime_UTR_variant	*CSF1R*	22/22	c.*35_*36delins TC	/	/	/
7:55249063-55249063	synonymous variant	*EGFR*	20/28	c.2361G>A	p.Gln787=	CAG/CAA	likely_benign
10:43613843-43613843	synonymous variant	*RET*	13/20	c.2307G>T	p.Leu769=	CTG/CTT	benign
11:534242-534242	synonymous variant	*HRAS*	2/5	c.81T>C	p.His27=	CAT/CAC	uncertain_significance, benign
13:28602292-28602292	intron_varint	*FLT3*	/	c.2053+23A>G	/	/	/
13:28610183-28610183	splice_region_variant intron_variant	*FLT3*	/	c.1310-3T>C	/	/	/
17:7579472-7579472	missense_variant	*TP53*	4/11	c.215C>G	p.Pro72Arg	CCC/CGC	benisgn, drug_response
19:1220311-1220321	intron_variant	*SYTK11*	c.465-51delinsC	/	/	/	/

FAP1 Organoids

Location	Consequence	Symbol	Exon	HGVSc	HGVSp	Codons	Clinical Significance
2:212812097-212812097	intron_variant	*ERBB4*	/	c.421+58A>G	/	/	/
4:1807894-1807894	synonymous variant	*FGFR3*	14/18	c.1959G>A	p.Thr653=	ACG/ACA	benign, likely_benign
4:55141055-55141055	synonymous variant	*PDGFRA*	13/23	c.1701A>G	p.Pro567=	CCA/CCG	benign
4:55593481-55593481	synonymous variant	*KIT*	10/21	c.1638A>G	p.Lys546=	AAA/AAG	likely_benign
4:55946354-55946354	intron_variant	*KDR*	/	c.3849-24C>A	/	/	/
5:112837963-112837965	deletion, frameshift_variant	*APC*	16/16	c.2369_2372delinsGACA	p.Arg790ThrFS*2P	/	/
5:112175576-112175576	stop_gained, frameshift_variant	*APC*	16/16	c.4285delinsTA	p.Gln1429Ter	CAA/TAAA	/
5:112175770-112175770	synonymous variant	*APC*	16/16	c.4479G>A	p.Thr1493=	ACG/ACA	other, benign
5:149433596-149433597	3_prime_UTR_variant	*CSF1R*	22/22	c.*35_*36delins TC	/	/	/
7:55249063-55249063	synonymous variant	*EGFR*	20/28	c.2361G>A	p.Gln787=	CAG/CAA	likely_benign
10:43613843-43613843	synonymous variant	*RET*	13/20	c.2307G>T	p.Leu769=	CTG/CTT	benign
11:534242-534242	synonymous variant	*HRAS*	2/5	c.81T>C	p.His27=	CAT/CAC	uncertain_significance, benign
13:28602292-28602292	intron_varint	*FLT3*	/	c.2053+23A>G	/	/	/
13:28610183-28610183	splice_region_variant intron_variant	*FLT3*	/	c.1310-3T>C	/	/	/
17:7579472-7579472	missense_variant	*TP53*	4/11	c.215C>G	p.Pro72Arg	CCC/CGC	benisgn, drug_response
19:1220311-1220321	intron_variant	*SYTK11*	c.465-51delinsC	/	/	/	/

FAP2 Tissue

Location	Consequence	Symbol	Exon	HGVSc	HGVSp	Codons	Clinical Significance
2:212812097-212812097	intron_variant	*ERBB4*	/	c.421+58A>G	/	/	/
3:37067306-37067306	frameshift_variant	*MLH1*	12/19	c1217_1218insC	p.Gln407SerfsTer10	AGT/AGCT	/
4:1807894-1807897	frameshift_variant	*FGFR3*	14/18	c.1959_1962delinsAACCA	p.Asn655LysfsTer12	ACGACC/ACAACCA	/
4:55593481-55593481	synonymous variant	*KIT*	10/21	c.1638A>G	p.Lys546=	AAA/AAG	likely_benign
5:112175211-112175216	frameshift_variant	*APC*	16/16	c.3927_3931del	p.Glu1309AspfsTer4	ATAAAAGAA/ATAA	/
5:112175770-112175770	synonymous variant	*APC*	16/16	c.4479G>A	p.Thr1493=	ACG/ACA	other, benign
5:149433596-149433601	3_prime_UTR_variant	*CSF1R*	22/22	c.*31_*36delins TCCTC	/	/	/
7:55249063-55249063	synonymous variant	*EGFR*	20/28	c.2361G>A	p.Gln787=	CAG/CAA	likely_benign
10:43613843-43613843	synonymous variant	*RET*	13/20	c.2307G>T	p.Leu769=	CTG/CTT	benign
10:43615633-43615633	synonymous variant	*RET*	15/20	c.2712C>G	p.Ser904=	TCC/TCG	likely_benign
17:7579472-7579472	missense_variant	*TP53*	4/11	c.215C>G	p.Pro72Arg	CCC/CGC	benisgn, drug_response
18:48586344-48586344	intron_variant	*SMAD4*	/	c.955+58C>T	/	/	/

FAP2 Organoids

Location	Consequence	Symbol	Exon	HGVSc	HGVSp	Codons	Clinical Significance
2:212812097-212812097	intron_variant	*ERBB4*	/	c.421+58A>G	/	/	/
3:37067306-37067306	frameshift_variant	*MLH1*	12/19	c1217_1218insC	p.Gln407SerfsTer10	AGT/AGCT	/
4:1807894-1807897	frameshift_variant	*FGFR3*	14/18	c.1959_1962delinsAACCA	p.Asn655LysfsTer12	ACGACC/ACAACCA	/
4:55593481-55593481	synonymous variant	*KIT*	10/21	c.1638A>G	p.Lys546=	AAA/AAG	likely_benign
5:112175211-112175216	frameshift_variant	*APC*	16/16	c.3927_3931del	p.Glu1309AspfsTer4	ATAAAAGAA/ATAA	/
5:112175770-112175770	synonymous variant	*APC*	16/16	c.4479G>A	p.Thr1493=	ACG/ACA	other, benign
5:149433596-149433601	3_prime_UTR_variant	*CSF1R*	22/22	c.*31_*36delins TCCTC	/	/	/
7:55249063-55249063	synonymous variant	*EGFR*	20/28	c.2361G>A	p.Gln787=	CAG/CAA	likely_benign
10:43613843-43613843	synonymous variant	*RET*	13/20	c.2307G>T	p.Leu769=	CTG/CTT	benign
10:43615633-43615633	synonymous variant	*RET*	15/20	c.2712C>G	p.Ser904=	TCC/TCG	likely_benign
17:7579472-7579472	missense_variant	*TP53*	4/11	c.215C>G	p.Pro72Arg	CCC/CGC	benisgn, drug_response
18:48586344-48586344	intron_variant	*SMAD4*	/	c.955+58C>T	/	/	/

Supplementary Table 3: NGS analysis report of FAP1-2 Tissue and PDOs alterations.

FAP3 Tissue

Location	Consequence	Symbol	Exon	HGVSc	HGVSp	Codons	Clinical Significance
2:212812097-212812097	intron_variant	*ERBB4*	/	c.421+58A>G	/	/	/
4:1807894-1807894	synonymous variant	*FGFR3*	14/18	c.1959G>A	p.Thr653=	ACG/ACA	benign, likely_benign
4:55946354-55946354	intron_variant	*KDR*	/	c.3849-24C>A	/	/	/
4:55593481-55593481	synonymous variant	*KIT*	10/21	c.1638A>G	p.Lys546=	AAA/AAG	likely_benign
5:112175211-112175216	frameshift_variant	*APC*	16/16	c.3927_3931del	p.Glu1309AspfsTer4	ATAAAAGAA/ATAA	/
5:149433596-149433601	3_prime_UTR_variant	*CSF1R*	22/22	c.*31_*36delins TCCTC	/	/	/
10:43613843-43613843	synonymous variant	*RET*	13/20	c.2307G>T	p.Leu769=	CTG/CTT	benign
17:7579472-7579472	missense_variant	*TP53*	4/11	c.215C>G	p.Pro72Arg	CCC/CGC	benisgn, drug_response

FAP3 Organoids

Location	Consequence	Symbol	Exon	HGVSc	HGVSp	Codons	Clinical Significance
2:212812097-212812097	intron_variant	*ERBB4*	/	c.421+58A>G	/	/	/
4:1807894-1807894	synonymous variant	*FGFR3*	14/18	c.1959G>A	p.Thr653=	ACG/ACA	benign, likely_benign
4:55946354-55946354	intron_variant	*KDR*	/	c.3849-24C>A	/	/	/
4:55593481-55593481	synonymous variant	*KIT*	10/21	c.1638A>G	p.Lys546=	AAA/AAG	likely_benign
5:112175211-112175216	frameshift_variant	*APC*	16/16	c.3927_3931del	p.Glu1309AspfsTer4	ATAAAAGAA/ATAA	/
5:149433596-149433601	3_prime_UTR_variant	*CSF1R*	22/22	c.*31_*36delins TCCTC	/	/	/
10:43613843-43613843	synonymous variant	*RET*	13/20	c.2307G>T	p.Leu769=	CTG/CTT	benign
17:7579472-7579472	missense_variant	*TP53*	4/11	c.215C>G	p.Pro72Arg	CCC/CGC	benisgn, drug_response

FAP4 Tissue

Location	Consequence	Symbol	Exon	HGVSc	HGVSp	Codons	Clinical Significance
3:178917005-17917005	intron_variant	*PIK3CA*	/	c.352+40A>G	/	/	/
3:178927410-178927410	missense_variant	*PIK3CA*	7/21	c.1173A>G	p.Ile391Met	ATA/ATG	benign
3:178927985-178927985	synonymous variant	*PIK3CA*	8/21	c.1263A>G	p.Pro421=	CCA/CCG	benign
4:1807894-1807894	synonymous variant	*FGFR3*	14/18	c.1959G>A	/	/	benign
4:1807922-1807922	intron_variant	*FGFR3*	/	c.1965+22G>A	/	/	benign
4:55141055-55141055	synonymous variant	*PGFRA*	12/23	c.1701 A>G	p.Pro567=	CCA/CCG	benign
4:55593464-55593464	missense_variant	*KIT*	10/21	c.1621 A>C	p.Met541Leu	ATG/CTG	not provided, likely_benign
4:55980239-55980239	intron_variant	*KDR*	/	c.798+54G>A	/	/	/
5:112175206-112175206	frameshift_variant	*APC*	16/16	c.3919_3937dup	p.Thr1313AsnfsTer8	-/GAAATAAAAGAAAAGATTG	/
5:112175207-112175207	frameshift_variant	*APC*	16/16	c.3919_3937dup	p.Thr1313AsnfsTer8	GAA/GAAATAAAAGAAAAGATTGGAA	/
5:112175770-112175770	synonymous variant	*APC*	16/16	C.4479G>A	p.Thr1493=	ACG/ACA	benign
5:149433596-149433601	3_prime_UTR_variant	*CSF1R*	22/22	c.*31_*36delins TCCTC	/	/	/
10:43613843-43613843	synonymous variant	*RET*	13/20	c.2307G>T	p.Leu769=	CTG/CTT	benign
11:534242-534242	synonymous variant	*HRAS*	2/5	c.81T>C	p.His27=	CAT/CAC	uncertain_significance, benign
13:28610183-28610183	splice_region_variant intron_variant	*FLT3*	/	c.1310-3T>C	/	/	/
17:7579472-7579472	missense_variant	*TP53*	4/11	c.215C>G	p.Pro72Arg	CCC/CGC	benisgn, drug_response
19:1220311-1220321	intron_variant	*SYTK11*	c.465-51delinsC	/	/	/	/

FAP4 Organoids

Location	Consequence	Symbol	Exon	HGVSc	HGVSp	Codons	Clinical Significance
3:178917005-17917005	intron_variant	*PIK3CA*	/	c.352+40A>G	/	/	/
3:178927410-178927410	missense_variant	*PIK3CA*	7/21	c.1173A>G	p.Ile391Met	ATA/ATG	benign
4:1807894-1807894	synonymous variant	*FGFR3*	14/18	c.1959G>A	/	/	benign
4:1807922-1807922	intron_variant	*FGFR3*	/	c.1965+22G>A	/	/	benign
4:55141055-55141055	synonymous variant	*PGFRA*	12/23	c.1701 A>G	p.Pro567=	CCA/CCG	benign
4:55593464-55593464	missense_variant	*KIT*	10/21	c.1621 A>C	p.Met541Leu	ATG/CTG	not provided, likely_benign
4:55980239-55980239	intron_variant	*KDR*	/	c.798+54G>A	/	/	/
5:112175206-112175206	frameshift_variant	*APC*	16/16	c.3919_3937dup	p.Thr1313AsnfsTer8	-/GAAATAAAAGAAAAGATTG	/
5:112175207-112175207	frameshift_variant	*APC*	16/16	c.3919_3937dup	p.Thr1313AsnfsTer8	GAA/GAAATAAAAGAAAAGATTGGAA	/
5:112175770-112175770	synonymous variant	*APC*	16/16	c.4479G>A	p.Thr1493=	ACG/ACA	benign
5:112175921-112175921	stop_gained	*APC*	16/16	c.4630G>T	p.Glu1544Ter	GAA/TAA	/
5:149433596-149433601	3_prime_UTR_variant	*CSF1R*	22/22	c.*31_*36delins TCCTC	/	/	/
10:43613843-43613843	synonymous variant	*RET*	13/20	c.2307G>T	p.Leu769=	CTG/CTT	benign
11:108155116-108155116	synonymous variant	*ATM*	26/63	c.3909C>A	p.Thr1303=	ACC/ACA	
11:534242-534242	synonymous variant	*HRAS*	2/5	c.81T>C	p.His27=	CAT/CAC	uncertain_significance, benign
13:28610183-28610183	splice_region_variant intron_variant	*FLT3*	/	c.1310-3T>C	/	/	/
17:7579472-7579472	missense_variant	*TP53*	4/11	c.215C>G	p.Pro72Arg	CCC/CGC	benisgn, drug_response
19:1220311-1220321	intron_variant	*SYTK11*	c.465-51delinsC	/	/	/	/

Supplementary Table 4: NGS analysis report of FAP3-4 Tissue and PDOs alterations.